

PHARMACOKINETICS AND PHARMACODYNAMICS OF INTRAVENTRICULARLY ADMINISTERED ETOPOSIDE IN BRAIN TUMOUR PATIENTS

Dissertation
zur
Erlangung des Doktorgrades (Dr. rer. nat.)
der
Mathematisch-Naturwissenschaftlichen Fakultät
der
Rheinischen Friedrich-Wilhelms-Universität Bonn

vorgelegt von
CHULEEKORN SIRISANGTRAGUL
aus
KhonKaen, Thailand

Bonn 2006

Angefertigt mit Genehmigung der Mathematisch-Naturwissenschaftlichen
Fakultät der Rheinischen Friedrich-Wilhelms-Universität Bonn

- 1. Referent: Prof. Dr. U. Jaehde
- 2. Referent: Prof. Dr. R. Süverkrüp

Diese Dissertation ist auf dem Hochschulschriftenserver der ULB Bonn

http://hss.ulb.uni-bonn.de/diss_online elektronisch publiziert

Erscheinungsjahr: 2007

Contents

List of abbreviations.....	I
List of tables	III
List of figures.....	V
1. Introduction.....	1
1.1 Podophyllotoxin	1
1.2 Etoposide	2
1.2.1 Mechanism of action.....	3
1.2.2 Pharmacodynamics	4
1.2.3 Clinical use	5
1.3 Childhood brain tumours and therapy	6
1.4 Intraventricular administration of chemotherapy	8
1.4.1 Preclinical study.....	10
1.4.2 Clinical studies	10
2. Aims of this investigation	13
3. Materials and Methods.....	14
3.1 Pharmacokinetic study.....	14
3.1.1 Materials.....	14
3.1.2 Equipment	15
3.1.3 HPLC analysis for the determination of etoposide in CSF....	16
3.1.4 Assay validation.....	18
3.1.5 Clinical study design and patient characteristics	22
3.1.6 Drug formulation, administration and dosage.....	24
3.1.7 Sample collection.....	25
3.1.8 Non-compartmental pharmacokinetic data analysis	26
3.1.9 Compartmental pharmacokinetic data analysis	26
3.1.10 Statistical analysis.....	31
3.2 In vitro study	35
3.2.1 Materials.....	35
3.2.2 Equipment	37
3.2.3 Cell medium, buffer and solutions	38
3.2.4 HPLC analysis for the determination of etoposide in cell culture medium	39
3.2.5 Cell line	41

3.2.6	MTT Assay	41
3.2.7	Colony forming assay	43
4.	Results	47
4.1	HPLC analysis of etoposide in CSF	47
4.1.1	Selectivity	47
4.1.2	Linearity	50
4.1.3	Accuracy	50
4.1.4	Precision	52
4.2	Pharmacokinetics of etoposide in CSF after intraventricular administration	53
4.2.1	Concentration-time profiles	53
4.2.2	General of population parameters	57
4.2.3	Individual Bayesian curve fitting	58
4.2.4	Pharmacokinetic parameters in CSF	60
4.2.5	Effect of dosage regimen on pharmacokinetic parameter	60
4.2.6	Case report of a patient with hydrocephalus	69
4.2.7	Distribution of etoposide inside the CSF	70
4.3	Stability of etoposide in cell culture medium	72
4.4	Cytotoxic activity of etoposide in medulloblastoma cells	73
4.5	Antiproliferative activity of etoposide in medulloblastoma cells	75
4.5.1	Effect of concentration and duration of exposure	75
4.5.2	Effect of dosage regimen	76
5.	Discussion	82
5.1	Intraventricular administration of etoposide	82
5.2	Pharmacokinetics of etoposide in CSF after ivc administration	83
5.2.1	Peak and trough concentrations	83
5.2.2	Distribution of etoposide in the CSF	84
5.2.3	Elimination of etoposide from the CSF	85
5.2.4	Effect of disease state	85
5.2.5	Comparison with other intra-CSF administered agents	86
5.2.6	Clinical consequences	88
5.3	In vitro pharmacodynamics of etoposide in Medulloblastoma cells	88

Contents

5.3.1	Suitability of the colony forming assay.....	89
5.3.2	Effect of concentration and duration of exposure on antiproliferative activity	89
5.3.3	Effect of dosage regimen	90
6.	Summary	92
7.	References.....	94
8.	Appendix.....	105

List of abbreviations

AIC	Akaike Information Criterion
AUC	Area under the concentration-time curve
$AUC_{0-\infty}$	Area under the concentration-time curve from zero to infinity
AUC_{0-t}	Area under the concentration-time curve from zero to t hours
$AUMC_{0-\infty}$	Area under the first moment concentration-time curve from zero to infinity
AUC_{total}	Total area under the concentration-time curve in one cycle ($AUC_{0-\infty}$ x number of administrations)
BBB	Blood-brain barrier
B-CSFB	Blood-cerebrospinal fluid barrier
C x T	Concentration times time
CL	Clearance
C_{max}	Maximum concentration
C_{min}	Minimum concentration
CNS	Central nervous system
Conc.	Concentration
CSF-BB	Cerebrospinal fluid-brain barrier
CV	Coefficient of variation
D	Dose
DE	Total drug exposure (duration times concentration)
AUC_{50}	Total drug exposure (duration times concentration) required to inhibit colony formation by 50 %
DMEM	Dulbecco's Modified Eagle Medium
DNA	Deoxyribonucleic acid
EC_{50}	Drug concentration required to inhibit cell growth by 50 %
HPLC	High performance liquid chromatography
ivc	Intraventricular
λ_1	Elimination rate constant of the first phase
λ_z	Terminal elimination rate constant
OMR	Ommaya reservoir

LP	Lumbar puncture
PBS	Phosphate buffer saline solution
PCNSL	Primary central nervous system lymphoma
PNET	Primitive neuroectodermal tumours
r_c	Ratio of concentrations in SipharWin™
RE	Relative error
s.	See
SD	Standard deviation
SS	Sum of squared deviations
$t_{1/2\lambda_1}$	Elimination half-life of the first phase
$t_{1/2z}$	Terminal elimination half-life
t_{max}	Time to reach maximum concentration
V	Volume of distribution
V_c	Volume of distribution of the central compartment
V_{ss}	Volume of distribution at steady-state
W	Weighting factor
WHO	World Health Organisation
WSS	Weighted sum of squared deviations

List of tables

Table 1. Classification of paediatric brain tumours modified according to location and histological appearance.....	7
Table 2. Concentration ranges of etoposide for each sensitivity	20
Table 3. Control samples of each calibration curve for the determination of accuracy and precision	21
Table 4. Patient characteristics.....	23
Table 5. Coefficients of correlation of calibration curves at different sensitivities	50
Table 6. Within-day accuracy of etoposide.....	51
Table 7. Between-day accuracy of etoposide.....	51
Table 8. Within-day precision of etoposide	52
Table 9. Between-day precision of etoposide	53
Table 10. Individual model parameters for Bayesian curve fitting	57
Table 11. Comparison of parameters between the two dosage regimens (etoposide 0.5 mg/24 h and 1.0 mg/24 h) by using the Mann-Whitney U test	57
Table 12. Population parameters used for Bayesian curve fitting	58
Table 13. Individual pharmacokinetic parameters of etoposide in CSF (intraindividual mean \pm SD) after ivc administration of 0.25 mg/12 h	61
Table 14. Individual pharmacokinetic parameters of etoposide in CSF (intraindividual mean \pm SD) after ivc administration of 0.5 mg/24 h	62
Table 15. Individual pharmacokinetic parameters of etoposide in CSF (intraindividual mean \pm SD) after ivc administration of 1.0 mg/24 h	64
Table 16. Mean \pm SD pharmacokinetic parameters of etoposide in CSF after intraventricular administration of three different dosage regimens	67
Table 17. Pharmacokinetic parameters of one patient with hydrocephalus during ivc administration of etoposide 0.25 mg/12 h	70
Table 18. Etoposide concentrations in CSF samples drawn from an OMR and by lumbar puncture (LP) four hours after etoposide ivc administration via OMR	71

Table 19. Etoposide stability under cell incubator conditions	73
Table 20. EC_{50} and AUC_{50} of etoposide in medulloblastoma cells (D-425med) determined by using the colony forming assay.....	75
Table 21. Mean concentration-time profiles of etoposide 0.25 mg/12 h and 0.5 mg/24 h obtained from the clinical study.....	77
Table 22. Simulated concentration-time profile after 10 administrations of etoposide 0.25 mg/12 h	78
Table 23. Simulated concentration-time profile after 5 administrations of etoposide 0.5 mg/12 h	78
Table 24. AUC_{total} values of actually used etoposide concentration-time profiles	79
Table 25. Remaining colonies of D-425med cells after exposure to the twice daily dosage regimen for five days	80
Table 26. Remaining colonies of D-425med cells after exposure to the once daily dosage regimen for five days.....	80
Table 27. Pharmacokinetic parameters of anticancer agents in CSF after intra-CSF administration.....	87

List of figures

Figure 1. <i>Podophyllum peltatum</i> L.	1
Figure 2. Chemical structures of podophyllotoxin (A) and etoposide (B)	3
Figure 3. Drug delivery via an Ommaya reservoir (OMR)	9
Figure 4. Schematic presentation of a two-compartment model.....	26
Figure 5. Box plot.....	33
Figure 6. Reaction of MTT in mitochondria of living cells.....	42
Figure 7. Representative blank HPLC chromatogram of pooled CSF without etoposide.....	48
Figure 8. Representative blank HPLC chromatogram of 0.02 M phosphate buffer mixed with 0.9% NaCl	48
Figure 9. Representative HPLC chromatogram of spiked etoposide 0.80 µg/mL in 0.02 M phosphate buffer mixed with 0.9% NaCl	49
Figure 10. Representative HPLC chromatogram of etoposide in patient's CSF (determined concentration 1.18 µg/mL)	49
Figure 11. Mean CSF concentration-time profile following ivc administration of etoposide 0.25 mg/12 h on five consecutive days	54
Figure 12. CSF concentration-time profile (mean ± SD) following ivc administration of etoposide 0.50 mg/24 h on five consecutive days	54
Figure 13. CSF concentration-time profile (mean ± SD) following ivc administration of etoposide 1.0 mg/24 h on five consecutive days	55
Figure 14. Mean concentration-time profiles of etoposide in CSF after ivc administration of three different dosage regimens	56
Figure 15. CSF concentration-time profile of a representative patient who received etoposide 0.25 mg/12 h obtained by Bayesian curve fitting	58
Figure 16. CSF concentration-time profile of a representative patient who received etoposide 0.50 mg/24 h obtained by Bayesian curve fitting	59
Figure 17. CSF concentration-time profile of a representative patient who received etoposide 1.0 mg/24 h obtained by Bayesian curve fitting	59
Figure 18. Box plot of elimination half-lives after three different dosage regimens of ivc etoposide	68
Figure 19. Box plot of volumes of distribution after three different dosage	

regimens of ivc etoposide	68
Figure 20. Box plot of clearances after three different dosage regimens of ivc etoposide.....	69
Figure 21. Comparison of etoposide concentrations in CSF samples drawn from an OMR and by lumbar puncture (LP) four hours after ivc administration via an OMR	72
Figure 22. Concentration-effect relationship of etoposide in D-425med cells determined by using the MTT assay	74
Figure 23. Effect of etoposide exposure on growth rate of medulloblastoma cells (D-425med) by using the colony forming assay	76
Figure 24. Antiproliferative activity of etoposide on D-425med cells after incubation with a once daily and twice daily regimen over five days	81

1. Introduction

1.1 Podophyllotoxin

Podophyllotoxin has been used as folk medicine for centuries. The source of podophyllotoxin is the resin of *Podophyllum* rhizome, especially the resin extracted from *Podophyllum peltatum* (May apple or American mandrake) and *Podophyllum hexandrum* (syn. *P. emodi*). Both of them are the plant species currently used for the extraction of podophyllotoxin. *Podophyllum peltatum* L. (Fig. 1) is indigenous to the eastern part of the United States of America and Canada. *Podophyllum hexandrum* is found in the higher parts of the Himalayan Mountains and is also referred to as the Indian *Podophyllum*. North American Indians and inhabitants of the Himalayas used the extracts of the plants *Podophyllum peltatum* and *Podophyllum hexandrum* as an emetic, cathartic, mortal poison, antidote for snake venom, anthelmintic, cholagogue and expectorant. In 1942, podophyllotoxin was reported in pharmacopoeia as a topical application for genital warts. Podophyllotoxin is most notable among the tubulin binding ligands and acts as an inhibitor of microtubules. Its action takes place by inhibiting the polymerisation of tubulin and stopping cell division at the beginning of the metaphase. Podophyllotoxin is an important lead compound for synthetic cytotoxic agents with lower toxicity but higher efficacy¹.



Figure 1. *Podophyllum peltatum* L.

1.2 Etoposide

Etoposide, a potent antineoplastic drug, was one of several podophyllotoxin derivatives that were first synthesised in the 1960s and were then introduced into cancer clinical trials in the early 1970s. It is a semisynthetic glucosidic derivative of podophyllotoxin, which is a natural product compound extracted from *Podophyllum peltatum* and *Podophyllum hexandrum* belonging to the family of Berberidaceae. Its chemical structure is shown in Fig. 2. Etoposide provides superior pharmacological profiles and broader therapeutic potential compared to podophyllotoxin. The chemical formula of etoposide is $C_{29}H_{32}O_{13}$ with a molecular weight of 588.56 g/mol. The melting point of etoposide is 236 - 251 °C. Etoposide is highly soluble in methanol and chloroform, slightly soluble in ethanol but only sparingly soluble in water. Thus, drug formulations for intravenous administration contain organic co-solvents such as benzyl alcohol, polyethylene glycol, and ethanol¹⁻⁶.

Synonyms of etoposide are

- Demethylepipodophyllotoxin-ethylidene-glucopyranoside
- EPEG
- EPE
- Epipodophyllotoxin
- 4 α -Demethylepipodophyllotoxin-9-(4,6-O-ethylidene- β -D-glucopyranoside)
- 4 α -Demethylepipodophyllotoxin ethylidene- β -D-glucoside
- (-)-Etoposide
- *trans*-Etoposide
- VP 16
- VP 16-123
- VP 16-213

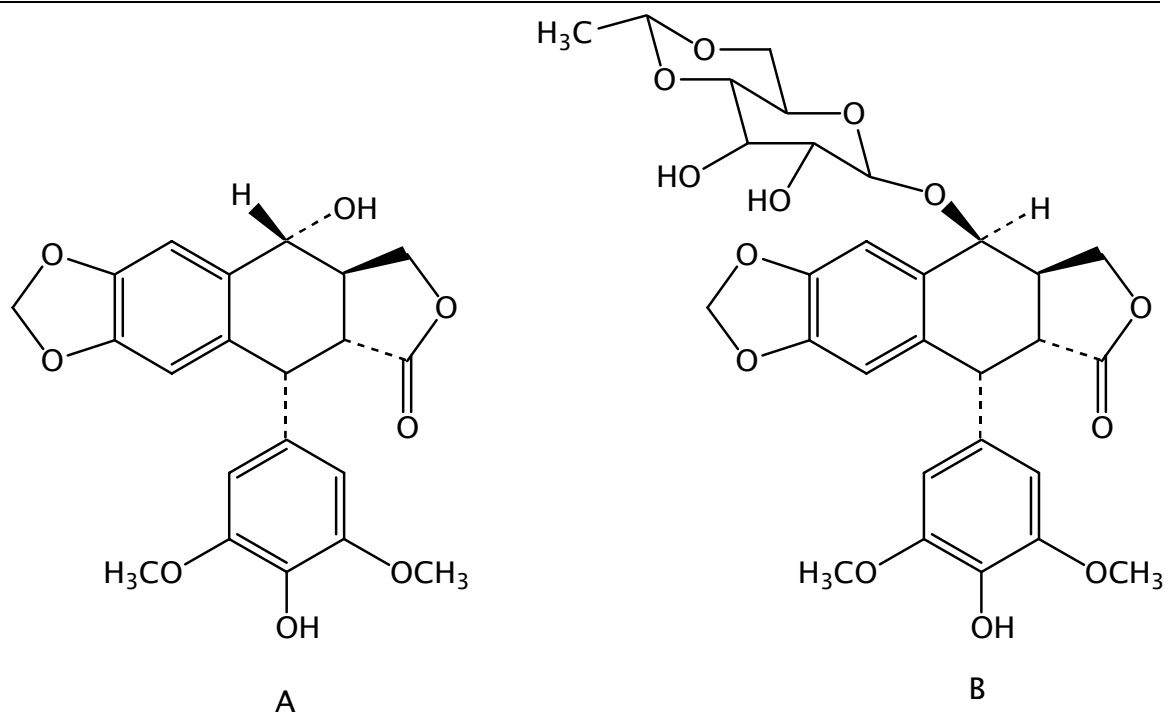


Figure 2. Chemical structures of podophyllotoxin (A) and etoposide (B)

1.2.1 Mechanism of action

Deoxyribonucleic acid (DNA) topoisomerases are nuclear enzymes inducing transient breaks in the DNA allowing DNA strands or double helices to pass through each other. DNA topoisomerases are classified into two groups: topoisomerase I enzymes that induce single stranded cuts into DNA and topoisomerase II enzymes that cut and pass double stranded DNA⁷. The major mechanism of action of etoposide is mainly explained by the interaction with topoisomerase II. By binding to topoisomerase II, etoposide stabilises the cleavable complexes which results in double strand and single strand breaks in the DNA. Unlike podophyllotoxin, etoposide does not arrest cell division at the mitotic phase by binding to microtubules, but induces a premitotic block prevalent in the late S or early G₂ period both *in vitro* and *in vivo*. Cells that are duplicating their DNA for the mitosis are very sensitive for this mechanism. The inability of etoposide to inhibit microtubule assembly is due to the glucoside moiety which sterically blocks the interaction with tubulin. Breaks in the DNA are caused by either an interaction with DNA topoisomerase II or the formation

of free radicals. Until now, it is still not clear how stabilisation of the DNA topoisomerase II-etoposide complex ultimately leads to cell death and etoposide may also have other mechanisms of cytotoxicity^{2,4,8-10}.

1.2.2 Pharmacodynamics

Etoposide has demonstrated cytotoxic activity against a variety of different tumours including adenocarcinoma lung cell lines, anaplastic bronchogenic carcinoma cell lines, human T cell lymphoma cell lines, leukaemic cell lines, lymphoid (T1) cell lines, human diploid embryo lung fibroblast cell lines, choriocarcinoma cell lines, cell lines derived from acute nonlymphoblastic leukaemia, cell lines derived from B- and T-lymphomas, cell lines derived from Hodgkin's disease, small cell lung carcinoma cell lines, haematopoietic cell lines, medulloblastoma cell lines and neuroblastoma cell lines^{2,11,12}. Etoposide demonstrates a remarkable schedule-dependence as shown in *in vitro* studies and suggested by clinical trials. The cytotoxicity of etoposide is both concentration- and time-dependent. In *in vitro* studies, leukaemia cells were incubated with etoposide at different concentrations (25 nM – 400 nM) and various exposure times (2 – 8 days) but the total drug exposure was kept constant. At the same total drug exposure, significantly greater cytotoxicity was achieved in schedules involving longer exposure times compared to those with short exposure times¹³. T-cell lymphoma (MOLT) and human anaplastic bronchogenic carcinoma cells (9812) were incubated with etoposide at a concentration range from 0.01 – 10.0 µg/mL. Each etoposide concentration was exposed to the cells with exposure durations of 1, 3, 18 and 30 h. Etoposide cytotoxicity increased with etoposide dose and duration of exposure¹⁴.

The schedule-dependence of etoposide activity was also confirmed in clinical studies¹⁵. Clinical response was compared in small cell lung cancer patients who received etoposide as 500 mg/m² continuous infusion over 24 h and patients who received 100 mg/m² etoposide as two hourly infusion for five consecutive days. The response rate of etoposide

500 mg/m² continuous infusion over 24 h (10 %) was significantly lower than that after etoposide 100 mg/m² two hourly infusion for five consecutive days (89 %)¹⁶.

The schedule-dependence of efficacy and toxicity of etoposide was also evaluated after an oral administration in small cell lung cancer patients. Etoposide was given orally in 78 patients in three different dosage regimens: 50 mg twice daily for 14 days every three weeks, 50 mg once daily for 21 days every four weeks and etoposide 50 mg twice daily for ten days every three weeks. Partial responses were observed in 76 %, 52 % and 70 % of the patients, respectively. This study demonstrated that a twice-daily regimen is preferable¹⁷.

So far, the concentration- and schedule-dependent cytotoxicity of etoposide has been reported from both *in vitro* studies and *in vivo* studies^{13,14,16-23}. However, there is sparse information about the concentration- and schedule-dependent effect of etoposide on CNS tumour cell lines especially medulloblastoma and PNET. Furthermore, there is still a lack of information on etoposide cytotoxicity from *in vitro* studies which simulate drug exposure conditions as those encountered in the patient. The time of exposure to etoposide from most *in vitro* studies was up to 24 h, whereas in the clinical situation etoposide is often administered intravenously over 3 - 5 consecutive days or orally over 14 - 21 consecutive days^{16,17,23}.

1.2.3 Clinical use

Etoposide is a highly effective and widely used agent for both the curative and palliative treatment of many neoplastic diseases including germ cell tumours, Kaposi's sarcoma associated with AIDS, Hodgkin's disease, Non-Hodgkin's lymphoma, mycosis fungoides, acute myeloblastic leukaemia, neuroblastoma, Ewing's sarcoma, paediatric rhabdomyosarcoma, ovarian carcinoma, small cell lung cancers, non-small cell lung cancers, gastric cancer and hepatoma. Etoposide is also used in the preparatory chemotherapeutic regimens given prior to bone marrow transplantation in

patients with advanced haematological malignancies. Major adverse effects of etoposide include hair loss, nausea, anorexia, diarrhoea, leucopenia and thrombocytopenia. Etoposide is known to cause fetal damage and birth defects^{2,5,6,8,24-26}.

1.3 Childhood brain tumours and therapy

Brain tumours are the most common solid tumour types in paediatric patients. They are the leading cause of cancer-related morbidity and mortality secondary to childhood malignancies. Childhood brain tumours differ from primary central nervous system (CNS) tumours occurring in adults with regard to their relative incidences, histological features, sites of origin and responsiveness to therapy. The types of paediatric brain tumours are classified according to location and histological appearance^{27,28} (Tab. 1). The causes of paediatric brain tumours remain unknown. The most common forms of childhood brain tumours are primitive neuroectodermal tumours (PNET) including medulloblastomas. Symptoms of paediatric brain tumours comprise of repeated, frequent headaches and nausea or vomiting²⁹. Currently the principle management strategies of brain tumours consist of surgical therapy, radiotherapy and chemotherapy. The type of tumours, the age of the patient and the likelihood of treatment-induced nervous system damage must be considered in order to find the optimal treatment strategy for each individual patient. Basically both surgical therapy and radiation improve the chance of cure and prolong survival time³⁰. However, there are some complications to the CNS after surgical therapy or radiation. After treatment with surgery, patients have a higher risk of permanent cranial-nerve and long tract deficits, transient pseudobulba symptoms and mutism. Moreover after cranial or craniospinal radiation significant adverse neuroendocrine and neurologic deficits, as well as impairment of intellectual function were observed especially in children younger than three years of age^{29,31}.

Chemotherapy is one approach which was introduced in order to reduce

the degree of neurocognitive sequelae resulting from surgical therapy or radiotherapy. Chemotherapy can be used to reduce the tumour size in order to decrease the risk associated with surgical therapy^{29,31}. Duffner et al. demonstrated that postoperative chemotherapy can delay radiotherapy in children younger than three years³². Overall survival rates were comparable between patients who received full-dose radiation therapy alone and patients who received reduced-dose radiotherapy plus chemotherapy^{31,33-35}. Moreover, chemotherapy has also shown to increase survival rates in childhood medulloblastoma and PNET patients who received chemotherapy with radiotherapy compared with those children receiving radiotherapy alone³⁶⁻³⁸. These studies indicated that the dose of radiation therapy can be reduced when chemotherapy is administered resulting in a lower incidence of neurocognitive sequelae which is the major adverse effect after radiation. Therefore, chemotherapy has gained an increasing role in paediatric brain tumour therapy.

Table 1. Classification of paediatric brain tumours modified according to location and histological appearance (derived from Pollack²⁸).

Location and type of tumour	Percentage of all brain tumours
Infratentorial	
Primitive neuroectodermal tumour (Medulloblastoma)	20 - 25
Low-grade astrocytoma, cerebellar	12 - 18
Ependymoma	4 - 8
Malignant glioma, brain stem	3 - 9
Low-grade astrocytoma, brain stem	3 - 6
Other	2 - 5
Total	45 - 60
Supratentorial hemispheric	
Low grade glioma	8 - 20
High grade glioma	6 - 12

Ependymoma	2 - 5
Mixed glioma	1 - 5
Ganglioglioma	1 - 5
Oligodendroglioma	1 - 2
Choroid-plexus tumour	1 - 2
Primitive neuroectodermal tumour	1 - 2
Meningioma	0.5 - 2
Other	1 - 3
Total	25 - 40
Supratentorial midline	
Suprasellar	
Craniopharyngioma	6 - 9
Low-grade glioma, chiasmatic	4 - 8
hypothalamic	1 - 2
Germ-cell tumour	0.5 - 2.5
Pituitary adenoma	
Pineal region	1 - 2
Low-grade glioma	0.5 - 2
Germ-cell tumour	0.5 - 2
Pineal parenchymal tumour	15 - 20
Total	

1.4 Intraventricular administration of chemotherapy

Chemotherapy can prolong survival of brain tumour patients, especially in patients with anaplastic gliomas, oligodendrogliomas, medulloblastoma, PNET, germ cell tumours and primary CNS lymphoma (PCNSL). At present, chemotherapy is used as primary therapy or an additional therapy following surgery and/or radiation therapy³⁹. However, the major problem in treating CNS tumours is the limited passage of cytotoxic drugs across the blood-brain barrier (BBB), the blood-cerebrospinal fluid barrier (B-CSFB)

and the cerebrospinal fluid-brain barrier (CSF-BB)⁴⁰. In an attempt to circumvent systemic toxicity and obtain higher CSF concentrations of etoposide the intraventricular (ivc) administration was introduced. Using this route of administration high drug concentrations are obtained in the CSF after relatively low doses. The drug can be infused intraventricularly by using an Ommaya reservoir (OMR). An OMR is a dome-shaped reservoir. It measures 3.4 cm in diameter and is placed subcutaneously in the scalp and connected to the ventricles within the brain via an outlet catheter as shown in Fig. 3. The drug is injected into the implanted reservoir and delivered to the ventricles by manual compression. Most common complications of reservoir implantation are infections, failures in placement, reservoir or catheter obstruction or dysfunction^{41,42}.

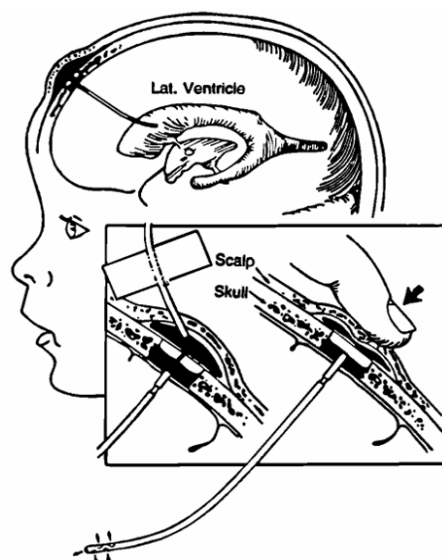


Figure 3. Drug delivery via an Ommaya reservoir (OMR)⁴³.

Direct ivc administration of chemotherapy through an indwelling subcutaneously implanted OMR has an advantage over intralumbar administration because the drug is delivered in the same direction as the CSF bulk flow. Thus, the ivc injection results in a wider distribution of the drug throughout the CSF compartment. Moreover, there is remarkably less patient discomfort since the ivc administration is not painful in contrast to the lumbar puncture (LP). Furthermore, the most meaningful advantage of the ivc route is the possibility of administration of repeated low doses of a drug over a relatively short period of time. This is also called the

‘concentration times time’ ($C \times T$) approach. By using this strategy a prolonged duration of CSF exposure to cytotoxic drug concentrations is obtained, excessively high peak concentrations are avoided and the total drug dose is reduced^{44,45}.

Until now, effective treatment of CNS tumours has still been limited by the paucity of cytotoxic agents that can be administered by the ivc route. At present, methotrexate, cytarabine and thiotepa are widely used for intra-CSF therapy. Methotrexate and cytarabine are antimetabolites and highly effective in treating CNS leukaemia. However, methotrexate can cause leucoencephalopathy in patients who received cranial radiation^{46,47} and cytarabine alone shows weak activity in malignant brain tumours⁴⁷. Thiotepa diffuses out of the CSF rapidly and furthermore, after intrathecal administration of thiotepa the active metabolite TEPA is not formed^{48,49}. To enhance the success of brain tumour therapy with ivc administration, many other chemotherapeutic agents such as etoposide, mafosfamide, fluorouracil, topotecan, diaziquone, temozolomide, sustained release cytarabine, monoclonal antiganglioside antibody have been studied in clinical trials⁴⁹⁻⁶⁰.

1.4.1 Preclinical study

Eight beagle dogs received [3H] etoposide at 2 mg/kg by intrathecal or intravenous administration. Plasma, urine, bile, cerebrospinal fluid, brain tissue and tissue of major organs were collected to analyse the etoposide concentrations. The intrathecal group exhibited higher etoposide concentrations in CSF and brain tissues compared with the intravenous group. No acute neurologic toxicity and no histopathologic changes were reported. The intrathecal administration was well tolerated at the dosage used^{61,62}.

1.4.2 Clinical studies

The ability of etoposide to pass across the BBB and the B-CSFB into the CSF is extremely poor, even after high-dose systemic intravenous or oral

administration. In 16 patients, the peak concentration of etoposide in CSF ranged only from 0.04 - 0.11 $\mu\text{g/mL}$ after oral administration (50 - 150 mg/day) or intravenous infusion over one hour (55 - 65 mg/m^2)⁶³. After intravenous infusion over two hours (300 mg/m^2) or oral administration for 21 days (50 and 25 $\text{mg/m}^2/\text{day}$) in 20 patients, the median etoposide concentrations in CSF were 0.103 $\mu\text{g/mL}$, 6.47×10^{-3} $\mu\text{g/mL}$ and 4.12×10^{-3} $\mu\text{g/mL}$, respectively⁶⁴. Even when high doses (400 - 800 $\text{mg/m}^2/\text{day}$) over two or three hours were given intravenously, the concentrations of etoposide in the CSF ranged from 0.1 - 1.4 $\mu\text{g/mL}$ or 1.8 ± 1.7 % of simultaneously measured plasma concentrations⁶⁵. Posmus et al. reported that after extremely high intravenous doses (900 - 2500 mg/m^2) over one hour every 12 h for three consecutive days, the CSF concentrations of etoposide were only up to 0.54 $\mu\text{g/mL}$ ⁶⁶. The poor distribution of etoposide into the CSF despite its lipophilic properties is thought to be due to the high binding affinity of the drug to proteins in the blood circulation^{67,68}.

In order to circumvent this problem, the ivc administration of etoposide was attempted. In 1992, van der Gaast et al. published the administration of intraventricular etoposide in two patients. An etoposide dose of 0.5 mg was given ivc once daily for five consecutive days. Three weeks later 0.5 mg were administered every 12 h for five consecutive days. The etoposide concentrations in the CSF obtained at 2 - 2.30 h after ivc administration ranged from 3.6 - 5.2 $\mu\text{g/mL}$ and at 22 - 24 h from 0.2 - 0.6 $\mu\text{g/mL}$ ⁶⁹. No treatment-related adverse effects in two patients were reported in these patients. Cytological examination showed that the CSF was free of leukaemic cells following the treatment⁶⁹.

In 2001, our group reported that intraventricularly administered etoposide 0.5 mg/day for five consecutive days repeated every 2 - 5 weeks over a period of 0 up to 11 months was well tolerated in 14 patients. The CSF peak concentrations exceeded more than 100-fold those obtained after intravenous infusion. The pharmacokinetic parameters were estimated by using a two-compartment model. The AUC (area under the concentration-time curve), CL (clearance), V_{ss} (volume of distribution at steady-state) and

$t_{1/2z}$ (terminal elimination half-life) of the treatment group without systemic etoposide were $21.9 \pm 10.3 \mu\text{g} \times \text{h/mL}$, $0.56 \pm 0.48 \text{ mL/min}$, $0.20 \pm 0.18 \text{ L}$ and $7.65 \pm 1.24 \text{ h}$, respectively. Interindividual variability of the pharmacokinetic parameters was three times higher than the intraindividual variability⁷⁰. Toxicity of intraventricularly administered etoposide was evaluated in the same patients (59 courses). Mild transient headache was found in 2 of 59 courses. Meningitis was found in 2 of 59 courses. 5 of 14 patients showed an improvement in neurological symptoms or pain reduction. 6 patients of 14 patients showed no changes. 3 patients had progressive symptoms⁷⁰. Slavic et al. reported that etoposide did not cause any discomfort in 11 patients following etoposide ivc administration of 0.5 mg daily for five consecutive days, repeated every 3 - 6 weeks for a total of 122 courses⁵¹. However, the effectiveness of intraventricularly administered etoposide alone cannot be determined from these studies because the patients received systemic chemotherapy simultaneously and also irradiation.

2. Aims of this investigation

Up to now, there is still a lack of pharmacokinetic data of etoposide after ivc administration. To optimise the dosage of intraventricularly administered etoposide, the pharmacokinetic disposition in the CSF was investigated after three different dosage regimens; 0.25 mg/12 h, 0.5 mg/24 h and 1 mg/24 h. Additionally, CSF samples were drawn simultaneously from the OMR and by lumbar puncture (LP) in order to elucidate the distribution of etoposide within the CSF compartment. Moreover, the effect of the dosage regimen on the antiproliferative effect of etoposide in medulloblastoma cells was studied by using the colony forming assay. The *in vitro* dilution model was used to simulate concentration-time profiles similar to those encountered *in vivo*.

The following objectives were defined:

- To estimate the pharmacokinetic parameters of etoposide in the CSF after ivc administration of three different dosage regimens (0.25 mg/12 h, 0.50 mg/24 h and 1 mg/24 h).
- To evaluate the distribution of etoposide after ivc administration through an OMR.
- To generate a CSF pharmacokinetic model for simulation of other regimens.
- To evaluate the effect of etoposide concentration and area under the concentration-time curve (AUC) on the growth of medulloblastoma cells.
- To evaluate the antiproliferative effect of two different concentration-time profiles similar to those encountered *in vivo* (0.25 mg/12 h and 0.50 mg/24 h).

3. Materials and Methods

3.1 Pharmacokinetic study

3.1.1 Materials

Chemicals

Methanol HPLC grade	Merck, Darmstadt, Germany J.T. Baker, Deventer, Netherlands
Sodium chloride, pure	Merck, Darmstadt, Germany
Disodiumhydrogen phosphate	Merck, Darmstadt, Germany
Phosphoric acid 85 % (V/V)	Riedel-de-Häen, Seelze, Germany
Purified water Purelab™ plus	USF, Ransbach-Baumbach, Germany
Vepesid-J™	Bristol-Myers Squibb, Munich, Germany

Consumption materials

Sample microvial (100 µL and 250 µL)	CS-Chromatographie Service Ltd., Germany
Sample vials	Labomedic, Bonn, Germany
Polytetrafluoroethylene gasket for sample vial	CS-Chromatographie Service Ltd., Germany
Metal springs	Labomedic, Bonn, Germany
Polypropylene tubes (15 mL)	Greiner Bio-one, Frickenhausen, Germany
Reaction vial Safe-Lock™ 0.5 mL, 1.5 mL	Eppendorf Hamburg, Germany

Pipette Tips 200 µL, 1000 µL	Greiner Bio-one, Frickenhausen, Germany
Membrane filter NL17 (0.45 µm, Ø 47 mm)	Schleicher & Schuell, Dassel, Germany
Sterile membrane filter 0.22 µm, cellulose acetate	Merck, Darmstadt, Germany
Graphite filter	ESA Inc. Chelmsford, USA
Parafilm™	Peckiney Plastic Packing, Neenah, USA

3.1.2 Equipment

System Gold™ HPLC Instrumentation	Beckman Coulter, Fullerton, USA
Coulochem™ II Detector system	ESA Inc., Chelmsford, USA
HPLC column, Nucleosil™ 100-5 C18	Macherey-Nagel, Düren, Germany
Heraeus HERAsafe™, laminar airflow HSP12	Kendro Laboratory Products, Germany
Single pan precision balance 770	Kern, Albstadt, Germany
pH-Meter inoLab™ 2P	WTW, Weilheim, Germany
Sonicator Sonorex™ super RK 103 H	Bandelin, Berlin, Germany
Vortex mixture L46	GLW, Würzburg, Germany
Vacuum membrane pump ME 4 C	Vacuubrand, Wertheim, Germany
Fisherbrand™ pipette (10 - 100 µL)	Fisher Scientific, Schwerte, Germany
Volu™Mate pipette (20 - 200 µL/100 - 1000 µL)	Mettler Toledo, Giessen, Germany
Purelab™ plus water purification system	USF, Ransbach-Baumbach, Germany

3.1.3 HPLC analysis for the determination of etoposide in CSF

HPLC system components

Pump	HPLC pump 125	Beckman Coulter, Fullerton, USA
Sample operation system	Autosampler 507 with 100 μ L sample loop	Beckman Coulter, Fullerton, USA
Column	Nucleosil™ 100-5 RP- C18, 5 μ m, 150 x 4.6 mm	Macherey-Nagel, Germany
Electrochemical detector	ESA Coulochem™ II with Guard cell 5020 Analytical cell 5010	ESA Inc., Chelmsford, USA
Interface	Analogue Interface Module 406	Beckman Coulter, Fullerton, USA
Integration software	Gold™ 32 Karat, version 3.0	Beckman Coulter, Fullerton, USA

Chromatographic conditions

Chromatographic separations of etoposide in CSF were performed on a Nucleosil™ 100-5 C-18 (150 x 4.6 mm, 5 μ m) analytical column under isocratic condition. The mobile phase consisted of methanol/ 0.01 M disodiumhydrogen phosphate (Na_2HPO_4) in a ratio of 52:48 (V/V) and was adjusted with 85 % (V/V) phosphoric acid (H_3PO_4) to pH 6.0. The mobile phase was degassed by using helium prior to use. Flow rate was set at 0.7 mL/min. Etoposide was quantified by electrochemical detection using a dual electrode at the potentials $E_1 = 100$ mV and $E_2 = 500$ mV. The guard cell was set at 550 mV.

Buffers and solutions

0.9 % sodium chloride: 4.5 g sodium chloride were transferred to a 500 mL volumetric flask and dissolved with purified water. The solution was filtered by using a 0.22 μm membrane filter. 0.9 % NaCl solution was used as matrix for calibration instead of CSF.

0.01 M disodiumhydrogen phosphate (pH 6.0): 1.4196 g disodiumhydrogen phosphate were dissolved in purified water and adjusted to a volume of 1000 mL. The solution was mixed with methanol for use as mobile phase and adjusted with 85 % (V/V) phosphoric acid to pH 6.0. The mobile phase was filtered by using a 0.45 μm membrane filter.

0.02 M disodiumhydrogen phosphate (pH 5.3): 0.2839 g disodiumhydrogen phosphate were added to purified water and the volume was adjusted to 100 mL. The pH was adjusted to 5.3 by using 85 % (V/V) phosphoric acid. The solution was filtered by using a 0.22 μm membrane filter. The solution was used to mix with CSF samples in order to prevent isomerisation of etoposide during analysis.

Suitability of 0.9 % NaCl as matrix for calibration

As it is difficult to obtain enough blank CSF for calibration, the suitability of 0.9 % NaCl was investigated by Henke⁷¹. Recovery of spiked etoposide in blank CSF was compared to 0.9 % NaCl at etoposide concentrations of 0.2 $\mu\text{g/mL}$, 1 $\mu\text{g/mL}$ and 5 $\mu\text{g/mL}$ and ranged from 96.5 - 106.6 %. The results showed that saline solution spiked with etoposide provided similar peak heights as blank CSF spiked with etoposide. Therefore, saline solution was used as matrix for the preparation of calibrators and quality control samples.

Preparation of calibrator solutions

A 5 mL vial of VepesidTM containing 100 mg etoposide in a mixture of 150 mg benzyl alcohol, 3250 mg macrogol 300, 1210 mg absolute ethanol, citric acid and polysorbate 80 was used for preparing etoposide stock solutions. The stock solutions were prepared by dilution with 0.9 %

NaCl and stored at a temperature $\leq 20\text{ }^{\circ}\text{C}$ until use. The concentrations of etoposide stock solutions were 100, 10 and 1 $\mu\text{g/mL}$. Etoposide concentrations in CSF samples were determined by using five different calibration curves at five different sensitivity range sets (50 nA, 2 μA , 5 μA , 10 μA and 20 μA) of the detector. Calibrator solutions were prepared by dilution of the stock solutions with 0.9 % NaCl. Each calibration curve contained at least six concentrations of etoposide (s. Tab. 2).

Sample preparation

CSF samples of patients were kept at temperature $-80\text{ }^{\circ}\text{C}$ until analysis. The samples were left at room temperature to defrost. Because only low protein concentrations are found in the CSF, protein precipitation is not required. 80 μL of CSF were mixed with 40 μL of 0.02 M Na_2HPO_4 (pH = 5.3) in order to prevent isomerisation of etoposide during sample processing and analysis. A 40 μL aliquot of the prepared sample was injected onto the HPLC system. The temperature of the autosampler tray was set at $18\text{ }^{\circ}\text{C}$.

3.1.4 Assay validation

Method validation is the process which shows that an analytical method is acceptable for its intended purpose. In general, a bioanalytical method must be validated with regard to specificity, linearity, accuracy, precision, recovery, limit of detection, and limit of quantification. For the determination of etoposide in CSF, a method of Reif et al.^{72,73} was modified. Hence the HPLC assay in this work was only partially validated regarding selectivity, linearity, accuracy and precision according to international recommendations^{74,75}.

Selectivity

Selectivity is used to confirm that the procedure is measuring only the compound of interest and that the quantification is not affected by the sample matrix components. The selectivity of the HPLC method was assessed by comparison of chromatograms of buffer and CSF samples

containing etoposide with chromatograms obtained after injection CSF of the respective blank matrix.

Linearity and calibration

Linearity means that assay response increases proportionally with increasing concentration. The calibration curve should consist of six to eight calibrator samples. In this study, at least six calibrators were used to check linearity. Calibrator samples were prepared independently, to make it easier to discover an error in any of the samples compared to preparation by serial dilution. The range of etoposide concentrations for the calibration curves at different sensitivity ranges are shown in Tab. 2. The calibration curves were prepared daily for each concentration range. By using the Software "Method Validation in Analytics" (MVA), Version 2.0 (Novia GmbH, Saabrücken, Germany), the peak heights were plotted against nominal (theoretical value) etoposide concentrations to construct the calibration curve using 1/X weighting. If the measured response has a linear relationship with the concentration, it can be described with the linear equation as shown below:

$$Y_i = aX_i + b \quad (\text{eq. 1})$$

Where:

- Y_i = Measured response
- a = Slope
- X_i = Concentration of the analyte
- b = Intercept

Table 2. Concentration ranges of etoposide for each sensitivity

Sensitivity of detector	Concentration range of calibration curve [$\mu\text{g/mL}$]
20 μA	30, 40, 50, 60, 80, 100
10 μA	15, 20, 25, 30, 32.5, 35
5 μA	6.25, 7.5, 8.75, 10, 15, 17.5
2 μA	2, 2.5, 3.125, 4.375, 5, 6.875
50 nA	0.05, 0.075, 0.125, 0.15, 0.175, 0.20

Accuracy

The accuracy of an analytical method quantifies how close the concentrations obtained by the method are to the nominal concentrations of the analyte. Accuracy is determined by replicate analysis of samples containing known amounts of analyte. Accuracy can be divided into two categories: within-day accuracy and between-day accuracy. For within-day accuracy, control samples of each calibration curve were measured six times on the same day. For between-day accuracy, control samples of each calibration curve were measured once per day on six different days. Ten control samples of etoposide were analysed six times each (two concentrations for each sensitivity) as shown in Tab. 3. The accuracy was reported as percentage relative error (RE) as shown in equation 2. The percentage RE value should be within $\pm 15\%$ of the nominal value except at the lower limit of quantification, where it should not deviate by more than $\pm 20\%$.

$$RE [\%] = \left(\frac{C_{cal} - C_{nom}}{C_{nom}} \right) \cdot 100 \quad (\text{eq. 2})$$

Where:

RE [%] = Percentage relative error

C_{cal} = Measured concentration

C_{nom} = Nominal concentration

Table 3. Control samples of each calibration curve for the determination of accuracy and precision (n = 6)

Sensitivity range of the EC detector	Conc. range of calibration curve [$\mu\text{g/mL}$]	Conc. of control samples [$\mu\text{g/mL}$]
20 μA	30.0 - 100.0	40.0
		80.0
10 μA	15.0 - 35.0	20.0
		32.5
5 μA	6.25 - 17.5	7.5
		10.0
2 μA	2.0 - 6.875	2.5
		5.0
50 nA	0.05 - 0.2	0.10
		0.18

Precision

The precision of an analytical procedure expresses the degree of scatter in a series of individual measurements when the analytical procedure is applied repeatedly to multiple aliquots of the same sample. The precision of an analytical method is usually expressed as percentage coefficient of variation (% CV) as shown in equation 3. The % CV should not exceed 15 % except for the lower limit of quantification, where it should not exceed 20 %. The precision is subdivided into within-day precision and between-day precision. For within-day precision, control samples of each calibration curve were measured six times on the same day. For between-day precision, control samples of each calibration curve were measured once per day on six different days. Ten control samples of etoposide were analysed six times each (two concentrations for each calibration curve, s. Tab. 3.)

$$\% CV = \frac{\left(\sqrt{\frac{\sum_{i=1}^n (X_i - \bar{X})^2}{n-1}} \right)}{\bar{X}} \cdot 100 \quad (\text{eq. 3})$$

Where:

- % CV = Percentage coefficient of variation
- \bar{X} = Mean value from n measurements
- X_i = Measured individual values
- n = Number of measurements

3.1.5 Clinical study design and patient characteristics

The study was designed as an open prospective clinical and pharmacological trial in an individual curing framework⁷⁶.

Patient with an age between three months to 30 years and a refractory or relapsed metastatic malignant brain tumour, i.e. spinal, ventricular and/or parenchymatous metastases and/or meningeosis, were eligible.

The following patients were excluded:

- Patients who had severe or life-threatening neurological symptoms and/or therapy-resistant seizures (WHO scale 4)⁷⁷.
- Patients who had severe non-haematological insufficiencies (e.g., renal, cardiac, pulmonary or hepatic) (WHO scale 4) and life-threatening infections (WHO scale 3 or 4)⁷⁷.
- Patients who had hydrocephalus occlusus or malresorptivus which disturb CSF circulation or CSF resorption and need ventriculosystemic shunt.
- Patients who had a proximal CSF flow obstruction.

The patient characteristics are summarised in Tab. 4 and more detailed in Appendix A1.

Table 4. Patient characteristics

Gender		
Male		12
Female		10
Age (years)		
Median		11.20
Range		3.50 – 32.40
Weight (kg)		
Median		34.80
Range		10.30 – 77.00
Height (cm)		
Median		141.00
Range		88.90 – 179.50
BSA (m ²)		
Median		1.18
Range		0.50 – 1.95
Diagnosis		
Non-CNS tumour with brain metastases		
Acute lymphoblastic leukaemia		1
CNS tumour		
Medulloblastoma / PNET		16
Ependymoma		2
Pineoblastoma		1
Intraspinal tumour		1
Plexuscarcinoma		1

The study protocol was approved by the local ethics committee of the University of Bonn. Before entering the study, all patients and their parents were informed of the investigational nature of the study and the potential risks of these regimens as well as of the poor prognosis of relapsed metastatic brain tumours. Their consent to treatment was obtained.

The treatment of the patients followed the HIT-REZ-97-Study-Protocol which comprised surgical excision, irradiation and local/systemic therapy of anticancer agents⁶². Antiemetics and analgesics were used as supportive medication.

3.1.6 Drug formulation, administration and dosage

There are three market brands of etoposide: VepesidTM (Bristol-Myers Squibb, Germany), ETO-GRYTM (GRY-Pharma-Ltd., Germany) and ETO-CSTM (Pharmacia Ltd., Germany) which were used in this study. Benzyl alcohol which is a component in VepesidTM was reported as neurotoxic substance⁷⁸⁻⁸⁰. Therefore, since 4 April 2002, VepesidTM was not used in the study anymore. From that day onwards, the patients obtained etoposide in the form of ETO-GRYTM and ETO-CSTM which do not contain benzyl alcohol as solvent. A 5 mL vial of ETO-GRYTM and ETO-CSTM contains 100 mg etoposide and macrogol 300, citric acid, polysorbate 80 and ethanol 100 % as solvent. Etoposide was administered to all patients by ivc administration via an indwelling Ommaya or Rickham reservoir^{3,81,82}. The commercial solution was diluted in the following steps to yield the final concentration of 0.2 mg/mL (1:100, V/V):

- In the first step 0.5 mL of the commercial solution (20 mg/mL) were diluted with preservative-free, pyrogen-free saline (0.9 % NaCl) 9.5 mL to obtain etoposide 1 mg/mL.
- This solution was further diluted with preservative-free, pyrogen-free saline (0.9 % NaCl) to 0.2 mg/mL as shown below:

$$\begin{array}{lcl} \text{Etoposide 0.25 mg} & = & 0.25 \text{ mL etoposide 1 mg/mL} \\ & & + 1 \text{ mL 0.9 \% NaCl} \end{array}$$

Etoposide 0.50 mg	=	0.50 mL etoposide 1 mg/mL + 2 mL 0.9 % NaCl
Etoposide 1.0 mg	=	1.00 mL etoposide 1 mg/mL + 4 mL 0.9 % NaCl

The reservoir was punctured under sterile conditions with a 27-gauge butterfly needle. 2 mL CSF were discarded or removed for culturing. 5-10 mL CSF were removed for diagnosis (chemical, pathology and pharmacokinetics) and 2 mL were removed for flushing after drug administration. Following the administration the reservoir was pumped five times to ensure adequate mixing throughout the ventricular CSF. Etoposide was given to patients in three different dosage regimens; 0.25 mg/12 h, 0.50 mg/24 h and 1.0 mg/24 h. Each dosage regimen was given for five consecutive days which was one cycle and repeated every two to five weeks.

3.1.7 Sample collection

Samples collected for measuring etoposide concentrations were obtained from cycles without any interference from etoposide systemic administration. CSF samples following etoposide 0.25 mg/12 h were collected at 0 and 0.25, 1, 2, 4 and 12 h on day 1 and at 0.25 and 12 h on day 2 to day 5. The CSF samples following etoposide 0.5 mg/24 h and 1 mg/24 h were collected at 0 and 0.25, 1, 2, 4, 8, 12 and 24 h on day 1 and at 0.25 and 24 h on day 2 to day 5. Four hours after administration one CSF sample was drawn by lumbar puncture in order to investigate the distribution of etoposide within the CSF.

The CSF samples were collected in heparinised tubes, rapidly centrifuged at 10000 rpm for two minutes and the supernatant was frozen at -80 °C until analysis.

3.1.8 Non-compartmental pharmacokinetic data analysis

Etoposide pharmacokinetic parameters in CSF such as maximum concentration (C_{\max}), minimum concentration (C_{\min}) and time to reach maximum concentration (t_{\max}) were estimated without the assumption of a specific model. They were directly taken from the observed concentration-time curve^{83,84}.

3.1.9 Compartmental pharmacokinetic data analysis

The pharmacokinetic parameters such as area under the curve (AUC), volume of distribution at steady-state (V_{ss}), clearance (CL), elimination half-life of the first phase ($t_{1/2\lambda_1}$) and terminal elimination half-life ($t_{1/2\lambda_2}$) were estimated by using compartmental analysis assuming a two-compartment model. Due to the limited number of samples, Bayesian curve fitting was applied by means of the software SipharWin™ (release 1.14, Simed, Créteil, France).

Compartmental model of etoposide in CSF

Etoposide pharmacokinetic parameters in CSF were estimated by using a two-compartment model with first-order elimination from the central compartment as shown in Fig. 4.

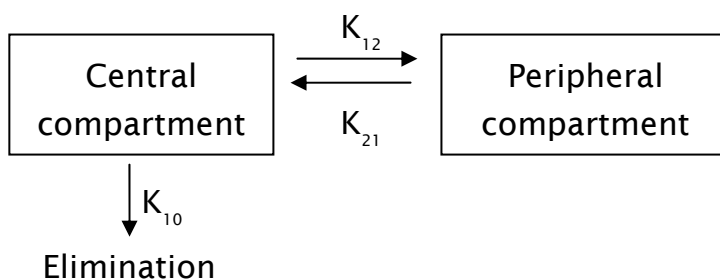


Figure 4. Schematic presentation of a two-compartment model

Where:

- | | |
|-------------------------------|---|
| \longrightarrow
K_{12} | = Direction of mass flow
= Rate constant for the transfer from the central compartment to the peripheral compartment |
|-------------------------------|---|

K_{21}	= Rate constant for the transfer from the peripheral compartment to the central compartment
K_{10}	= Elimination rate constant

The CSF etoposide concentration-time profile after ivc administration was described by a two exponential equation as shown below.

$$C_t = C_1 \cdot e^{\lambda_1 \cdot t} + C_z \cdot e^{\lambda_z \cdot t} \quad (\text{eq.4})$$

Where:

C_t	= Concentration at time t
C_1	= Intercept after extrapolation of the first phase back to the y-axis
C_z	= Intercept after extrapolation of the terminal phase back to the y-axis
λ_z	= Terminal elimination rate constant
λ_1	= Elimination rate constant of the first phase
t	= Time

Model parameters

Volume of distribution of the central compartment (V_c), ratio of concentrations in SipharWin™ (r_c), elimination rate constant of the first phase (λ_1) and terminal elimination rate constant (λ_z) were used as model parameters. V_c and r_c were calculated as shown in equation 5 and 6, respectively.

$$V_c = \frac{D}{C_1 + C_z} \quad (\text{eq.5})$$

$$r_c = \frac{C_1}{C_1 + C_z} \quad (\text{eq.6})$$

Estimation of population parameters

The population values for the model parameters were estimated from data of seven patients (three patients following 1 mg/24 h and four patients following 0.5 mg/24 h) undergoing full sampling. In the first step, initial parameters were estimated using curve peeling. These initial parameters were needed for the nonlinear regression procedure. In the next step, the selected model (two-compartment model) was fitted to the observed data applying a numerical algorithm based on the Powell method and minimising the weighted sum of squared deviations (WSS):

$$WSS = \sum_{i=1}^n W_i (C_i - \hat{C}_i)^2 \quad (\text{eq.7})$$

Where:

- W_i = Weighting factor at time i
- n = Number of measured concentrations
- C_i = Observed concentration at time i
- \hat{C}_i = Estimated concentration at time i

The individual model parameters obtained from the best fitted curve are shown in Tab. 10 in the result section. Since the model parameters were obtained from seven patients after administration of two different dosage regimens, it was tested, whether the model parameters differed between the two groups by using the Mann-Whitney U test. The results of the test are shown in Tab. 11 in the result section. No differences were found between the model parameters of the two groups. Therefore, mean values and standard deviations were calculated from the individual model

parameters of the seven patients. These parameters were used as population parameters as shown in Tab. 12 in the result section.

Estimation of individual parameters by Bayesian curve fitting

The two-compartment model was fitted to the experimental data applying a numerical algorithm based on the Powell method including the mean values and variances of the population parameters. Weighted least-squares or extended least-squares methods were used to minimise the Bayesian objective function ($OBJ_{Bayes.}$) as equation 8.

$$OBJ_{Bayes.} = \sum_{i=1}^n W_i \cdot (C_i - \hat{C}_i)^2 + \sum_{j=1}^k \frac{(P_j - \hat{P}_j)^2}{\sigma_j^2} \quad (\text{eq.8})$$

Where:

- $OBJ_{Bayes.}$ = Bayesian objective function
- W_i = Weighting factor at time i
- n = Number of observations
- k = Number of model parameters
- C_i = Measured CSF concentration at time i
- \hat{C}_i = Estimated CSF concentration at time i
- P_j = Population mean value of the j^{th} model parameter
- \hat{P}_j = Estimated value for the j^{th} model parameter
- σ_j = Population standard deviation for the j^{th} model parameter

Calculation of pharmacokinetic parameters

The following pharmacokinetic parameters were calculated:

Area under the curve ($AUC_{0-\infty}$)

$$AUC_{0-\infty} = \frac{C_1}{\lambda_1} + \frac{C_z}{\lambda_z} \quad (\text{eq.9})$$

Area under the first moment curve ($AUMC_{0-\infty}$)

$$AUMC_{0-\infty} = \frac{C_1}{\lambda_1^2} + \frac{C_z}{\lambda_z^2} \quad (\text{eq.10})$$

Clearance (CL)

$$CL = \frac{D}{AUC_{0-\infty}} \quad (\text{eq.11})$$

Volume of distribution at steady-state (V_{ss})

$$V_{ss} = \frac{D \cdot AUMC_{0-\infty}}{(AUC_{0-\infty})^2} \quad (\text{eq.12})$$

Terminal elimination half-life ($t_{1/2z}$)

$$t_{1/2z} = \frac{\ln 2}{\lambda_z} \quad (\text{eq.13})$$

Elimination half-life of the first phase ($t_{1/2\lambda_1}$)

$$t_{1/2\lambda_1} = \frac{\ln 2}{\lambda_1} \quad (\text{eq.14})$$

Simulation of concentration-time profiles

Etoposide concentration-time profiles after multiple bolus injection were simulated using the following equation⁸⁵:

$$C_t = C_1 e^{-\lambda_1 \cdot t} \cdot \frac{(1 - e^{-n \cdot \lambda_1 \cdot \tau})}{(1 - e^{-\lambda_1 \cdot \tau})} + C_z e^{-\lambda_z \cdot t} \cdot \frac{(1 - e^{-n \cdot \lambda_z \cdot \tau})}{(1 - e^{-\lambda_z \cdot \tau})} \quad (\text{eq.15})$$

Where:

- τ = Dosing interval [h]
- n = Number of administration

3.1.10 Statistical analysis

Statistical calculations were performed with SPSS™ software package, version 12.0 (SPSS Inc., Chicago, USA).

Descriptive statistics

The descriptive statistics such as median (\tilde{X}), mean (\bar{X}), standard deviation (SD), range, coefficient of variation (CV) and box plots were used to describe the basic features of the data in this study.

Median (\tilde{X}) is the score found at the exact middle of the ordered data set. Half of the scores are above the median and half are below. When there is an odd number of numbers, the median is the middle number. When there

is an even number of numbers, the median is the mean of the two middle numbers.

Mean (\bar{X}) is the average value of the data set:

$$\bar{X} = \frac{\sum_{i=1}^n X_i}{n} \quad (\text{eq.16})$$

where:

$$\begin{aligned} X_i &= \text{Individual value} \\ n &= \text{Number of observations} \end{aligned}$$

Range is the difference between the largest and the smallest observed value of the data set.

Standard deviation (SD) is a measure of the spread or dispersion of a set of data:

$$SD = \sqrt{\frac{\sum_{i=1}^n (X_i - \bar{X})^2}{n-1}} \quad (\text{eq.17})$$

Coefficient of variation is used to measure the spread of a set of data as in relation to its mean. It is often showed as a percentage and calculated as the ratio of the sample standard deviation to the sample mean:

$$CV[\%] = \frac{SD}{\bar{X}} \cdot 100 \quad (\text{eq.18})$$

Box plots

The data were graphically presented by means of box plots. The box plot as shown in Fig. 5 provides a visual summary of median, upper and lower

quartile as well as maximum and minimum values of the data set. The box itself contains the middle 50 % of the data. The box stretches from the lower hinge (Q1) which was defined as the 25th percentile to the upper hinge (Q3) which was defined as the 75th percentile. The difference of two quartiles (Q3-Q1) is known as the inter-quartile range. The median is shown as a line across the box. The vertical lines extend from the top or bottom of the box to the maximum and minimum value, respectively. Outliers are marked with a circle (O), when the values are above (Q3) or below (Q1) 1.5 times of the inter-quartile range as shown in equations 19 and 20. The extreme values are marked with an asterisk (*), when the values are above (Q3) or below (Q1) 3 times of the inter-quartile range as shown in equations 21 and 22.

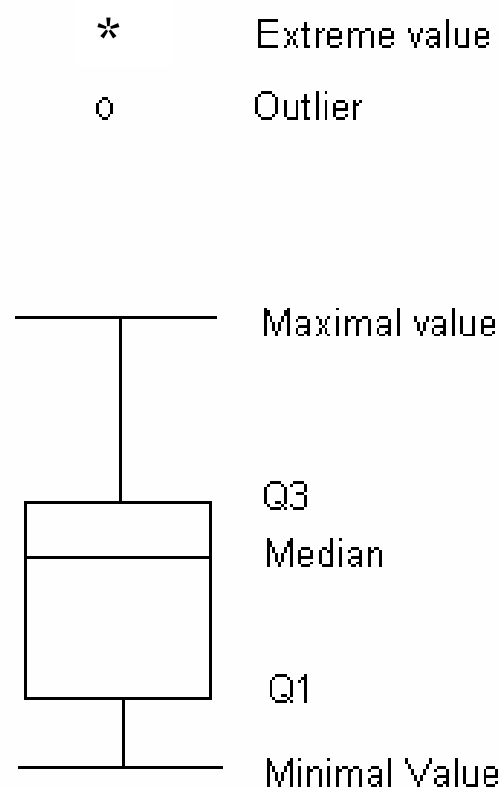


Figure 5. Box plot

$$O \leq Q1 - 1.5 \times (Q3 - Q1) \quad (\text{eq.19})$$

$$O \geq Q3 + 1.5 \times (Q3 - Q1) \quad (\text{eq.20})$$

$$* \leq Q1 - 3 \times (Q3 - Q1) \quad (\text{eq.21})$$

$$* \geq Q3 + 3 \times (Q3 - Q1) \quad (\text{eq.22})$$

Inferential statistics

Inferential statistics was used to make inferences about a population on the basis of the collected data. The null hypothesis is stated as no difference of the data between two or more populations. On the other hand, the alternative hypothesis is stated as the opposite to the null hypothesis. In this study, the null hypothesis was rejected when the level of significance (p value) was ≤ 0.05 .

The following statistical tests were used:

- The Shapiro-Wilk-test was used to assess whether data were normally distributed.
- The Mann-Whitney U test was used to assess whether the model parameters obtained from the patients undergoing full sampling following etoposide 1 mg/24 h and those obtained from the patients following etoposide 0.5 mg/24 h were different.
- The Kruskal-Wallis test was used to assess whether the pharmacokinetic parameters from three different dosage regimens were different.
- The paired t-test was used to compare the etoposide concentrations which were obtained from an Ommaya reservoir and those after lumbar puncture.

3.2 In vitro study

3.2.1 Materials

Chemicals

Methanol HPLC grade	Merck, Darmstadt, Germany and J.T. Baker, Deventer Netherlands
Methanol analytical grade	J.T. Baker, Deventer Netherlands
Disodiumhydrogen phosphate	Merck, Darmstadt, Germany
Sodium chloride	Merck, Darmstadt, Germany
Potassiumdihydrogen phosphate	Merck, Darmstadt, Germany
Potassium chloride	Merck, Darmstadt, Germany
Phosphoric acid 85 % (V/V)	Riedel-de-Häen, Seelze, Germany
Purified water (Purelab™ plus)	USF, Ransbach-Baumbach, Germany
Vepesid-J™	Bristol-Myers Squibb, Munich, Germany
Acetonitrile HPLC Grade	LCG Promochem GmbH, Wesel, Germany
Dulbecco's Modified Eagle Medium (DMEM™) with GlutaMax™	Invitrogen Gibco, Karlsruhe, Germany
Fetal calf serum	Sigma-Aldrich Chemie, Steinheim, Germany
L-Glutamine (200 mM)	Sigma-Aldrich Chemie, Steinheim, Germany
Penicillin-streptomycin solution Conc. penicillin: 10000 I.E./mL Conc. streptomycin: 10 mg/mL	Sigma-Aldrich Chemie, Steinheim, Germany

Dimethylsulfoxide (DMSO)	Promochem GmbH, Wesel, Germany
MTT [3-(4,5-dimethylthiazol-2-yl)-2,5- diphenyltetrazolium bromide]	Sigma-Aldrich Chemie, Steinheim, Germany
Isopropanol 100 %	Merck, Darmstadt, Germany
HCl 0.1 M	Grüssing, Filsum, Germany
Casy TM ton, isotonic solution	Schärfe System, Reutlingen, Germany
Giemsa colour	Sigma-Aldrich Chemie, Steinheim, Germany
Crystal violet	Sigma-Aldrich Chemie, Steinheim, Germany
Glycerine	Merck, Darmstadt, Germany
Ethanol 96 - 100 % analytical grade	Merck, Darmstadt, Germany

Consumption Materials

Sample microvial (100 µL and 250 µL)	CS-Chromatographie Service Ltd., Germany
Sample vials	Labomedic, Bonn, Germany
Polytetrafluoroethylene gasket for sample vial	CS-Chromatographie Service Ltd., Germany
Metal springs	Labomedic, Bonn, Germany
Polypropylene tubes (15 mL, 50 mL)	Greiner Bio-one, Frickenhausen, Germany
Reaction vial safe-lock TM 0.5 mL, 1.5 mL	Eppendorf Hamburg, Germany
Pipette tips 200 µL, 1000 µL	Greiner Bio-one, Frickenhausen, Germany
Membrane filter NL17 (0.45 µm, Ø 47 mm)	Schleicher & Schuell Dassel, Germany

Sterile membrane filter 0.22 μ M, cellulose acetate	Merck, Darmstadt, Germany
Parafilm™	Peckiney Plastic Packing, Neenah USA
Cell culture T-flask 25 cm ² , 75 cm ² , 175 cm ²	Greiner Bio-one, Frickenhausen, Germany
6-wells Petri-dish	Greiner Bio-one, Frickenhausen, Germany
96-wells Petri-dish	Greiner Bio-one, Frickenhausen, Germany
Disposable Plastic Pipette 10 mL	Braun, Melsungen, Germany
Glass Pipette 10 mL, 20 mL	Brand, Wertheim, Germany
Pasteur Pipette	Brand, Wertheim, Germany
Sterile glass bottle	Schott Duran, Germany

3.2.2 Equipment

System Gold™ HPLC Instrumentation	Beckman Coulter, Fullerton, USA
HPLC column, Nucleosil™ 100-5 C18	Macherey-Nagel, Düren, Germany
Heraeus HERAsafe™, laminar airflow HSP12	Kendro Laboratory Products, Germany
Single pan precision balance 770	Kern, Albstadt, Germany
pH-Meter inoLab™ 2P	WTW, Weilheim, Germany
Sonicator Sonorex™ super RK 103 H	Bandelin, Berlin, Germany
Vortex mixture L46	GLW, Würzburg, Germany
Vacuum membrane pump ME 4 C	Vacuubrand, Wertheim, Germany
Fisherbrand™ pipette (10 - 100 μ L)	Fisher Scientific, Schwerte, Germany

Volu TM Mate pipette (20 - 200 µL/100 - 1000 µL)	Mettler Toledo, Giessen, Germany
Transferpette TM -12 multi-canal pipette 20 - 200 µL	Brand, Wertheim, Germany
Aspirator pour pipette Accu-jet TM	Brand, Wertheim, Germany
Beckman Microfuge TM Lite (centrifuge)	Beckman Coulter, Munich, Germany
Centrifuge Allegra TM 21R	Beckman Coulter, Munich, Germany
Speed Vac TM SC 110	Savant Instruments INC. Holbrook, USA
Polarstar TM -Galaxy photometer	BMG-Lab-Technologies, Offenburg, Germany
Casy TM 1 Cell counter	Schärfe System, Reutlingen, Germany
Vacuum pump type model DOA-U155-BN	Benton Harbor Mich, USA
Cell culture incubator WTC Binder	WTC Labortechnik, Truttlingen, Germany
Water bath	Büchi, Switzerland
Invert microscope Axiovert TM 25	Carl Zeiss AG, Oberkochen, Germany

3.2.3 Cell medium, buffer and solutions

Cell medium: 500 mL of cell culture medium (DMEMTM with GlutaMaxTM) were supplemented with 50 mL fetal bovine serum (FBS), 7.5 mL L-Glutamine (200 mM) and 5 mL penicillin/streptomycin solution (penicillin: 10000 I.E./mL/ streptomycin: 10 mg/mL) and kept in the refrigerator. The medium was warmed in the water bath at 37 °C about 15 min before use.

PBS (Phosphate buffer saline solution): 8 g sodium chloride, 1.4 g disodiumhydrogen phosphate, 0.2 g of potassiumdihydrogen phosphate and 0.2 g potassium chloride were transferred to a 1000 mL volumetric

flask and dissolved with purified water. The pH was adjusted to 7.4 with 1 M sodium hydroxide. The solution was sterilized before use.

0.01 M disodiumhydrogen phosphate (pH 6.0): 1.4196 g disodiumhydrogen phosphate were dissolved in purified water and adjusted to a volume of 1000 mL. The solution was mixed with methanol for use as mobile phase and adjusted with 85 % (V/V) phosphoric acid to pH 6.0. The mobile phase was filtered by using a 0.45 µm membrane filter.

0.05 M disodiumhydrogen phosphate (pH 5.3): 0.7098 g disodiumhydrogen phosphate were added into purified water and the volume was adjusted to 100 mL. The pH was adjusted to 5.3 by using 85 % (V/V) phosphoric acid. The solution was filtered by using a 0.22 µm membrane filter. The solution was used to mix with samples in order to prevent isomerisation of etoposide during analysis.

Giemsa stain solution: 0.75 mg of Giemsa powder were mixed with 50 mL of glycerine and placed at 60 °C for 2 h. 50 mL of methanol was added before use.

Crystal violet stain solution: 0.20 g of crystal violet powder were mixed with 2 mL ethanol. The volume was adjusted to 100 mL with purified water.

Stain solution for the colony forming assay: Stain solution was composed of Giemsa solution and crystal violet solution in a ratio 1:1 (V/V).

MTT solution: 100 mg of MTT powder were added into purified water and the volume was adjusted to 20 mL. The solution was protected from light with aluminium foil.

3.2.4 HPLC analysis for the determination of etoposide in cell culture medium

Etoposide concentrations in cell culture medium were measured by HPLC with UV detection.

HPLC system components

Pump	HPLC pump 125	Beckman Coulter, Fullerton, USA
Sample operation system	Autosampler 507 with 100 μ L sample loop	Beckman Coulter, Fullerton, USA
Column	Nucleosil™ 100-5 RP- C18, 5 μ m, 150 x 4.6 mm	Macherey-Nagel, Germany
Detector	Gold™ 168 UV detector	Beckman Coulter, Fullerton, USA
Integration software	Gold™ 32 Karat, version 3.0	Beckman Coulter, Fullerton, USA

Sample preparation and analysis

100 μ L of medium samples were mixed with 300 μ L acetonitrile and 15 μ L of 0.05 M disodiumhydrogen phosphate pH 5.3 and then centrifuged at 10000 g for 10 minutes. 350 μ L of the supernatant were evaporated to dryness and the residue was dissolved with 120 μ L of the mobile phase which consisted of methanol and phosphate buffer pH 5.3 in a ratio 52:48 (V/V). 50 μ L of the respective mixture were injected onto the HPLC system. The flow rate was set at 0.7 mL/min and the UV detector at 210 nm.

Stability of etoposide in cell culture medium

Etoposide stability in cell culture medium (Dulbecco's Modified Eagle Medium (DMEM™) with GlutaMax™) under incubation conditions was investigated. A solution of etoposide 10 μ g/mL in culture medium (DMEM™ with GlutaMax™) was prepared and placed in the incubator for 72 h. Samples were collected at 0, 1, 2, 4, 8, 12, 24 and 48 and 72 h respectively, and analysed with HPLC.

3.2.5 Cell line

The medulloblastoma cell line (D-425med) was obtained from Prof. Pietsch, Institute of Neuropathology, University of Bonn. The cells were cryopreserved with nitrogen gas in cell culture medium containing 10 % dimethylsulfoxide (DMSO) and kept under liquid nitrogen. The cells were thawed by using the water bath at 37 °C and immediately propagated in the medium. The cells were then kept in an incubator under a humidified atmosphere of 5 % CO₂ at 37 °C. The cells were harvested in the exponential growth phase and detached from culture flasks by flushing with culture medium. All experiments were done by using cells of the 16th passage in order to avoid variations among different passages which could affect the results.

3.2.6 MTT assay

Principle

The cytotoxic activity of etoposide was studied by using MTT assay. MTT (3-(4, 5-dimethylthiazol-2-yl)-2, 5-diphenyltetrazolium bromide) is a water-soluble yellow dye substance. The mitochondrial dehydrogenase from viable cells cleaves the tetrazolium ring of the pale yellow MTT and forms violet formazan crystals as shown in Fig. 6. This reduction product is water-insoluble. The violet formazan crystals are largely impermeable to cell membrane which leads to their accumulation inside the healthy cells. For measurement, the formazan crystals are dissolved by a mixture of 50 mL isopropanol and 165 µL of 1 N HCl. The number of surviving cells is directly proportional to the concentration of the formazan product formed as determined by a simple colorimetric assay. A multiwell scanning spectrophotometer was used for quantification.

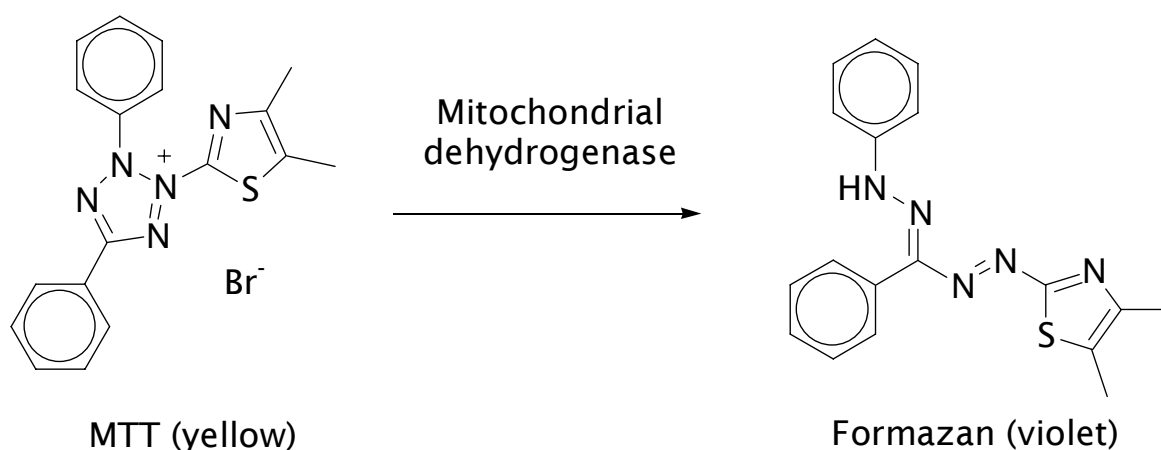


Figure 6. Reaction of MTT in mitochondria of living cells

Determination of a suitable initial cell number

The initial number of cells for plating is different for each type of tumour cells. An initial experiment was conducted to ensure that the well surfaces did not become over-confluent by the medulloblastoma cells at the end of the 72 h incubation period.

The suitable initial number of the D-425med cells for MTT assay (3 days incubation) were determined as follow. The cells were incubated in a T-flask with a surface area of 25 cm² until they formed a monolayer. The medium was removed and the cells were detached from the T-flask by slightly flushing with 10 mL of fresh medium. The number of cells was measured by using the CasyTM1 cell counter and recorded as the respective cell suspension concentration (cells/mL). 20 % (2 mL) of this suspension was further incubated in a T-flask with the same surface area (25 cm²). If the seeded cells (20 % of the monolayer) needed around three days to form a new monolayer then 20 % of the cell number were regarded as the suitable initial number for plating. If the seeded cells (20 % of the monolayer) needed around 4 - 5 days to form a new monolayer then the suitable initial number of the cells for plating should be more than 30 % of the cell number in the monolayer phase. If the seeded cells (20 % of the monolayer) needed only around 1-2 day to form a new monolayer then the suitable initial number of the cells for plating should be below 20 % of the cell number in the monolayer phase.

Determination of the EC_{50} of etoposide

Solutions of $10^{-8.0}$, $10^{-7.0}$, $10^{-6.0}$, $10^{-5.0}$, $10^{-4.5}$, $10^{-4.0}$, and $10^{-3.75}$ M etoposide were obtained by 10-fold serial dilutions with medium. The cells were suspended in cultured medium using an initial cell concentration of 3.31×10^5 cells/mL. 90 μ L aliquots of the cell suspension were dispensed into 96 well plates and kept at least 10 h in a humidified incubator with 5 % CO_2 at 37 °C. 10 μ L of each etoposide solution were added into the wells preparing each concentration in twelve-plicate. The first row of the multi-well plate was used as a blank control to which 10 μ L of etoposide-free cultured medium were added. Then the medulloblastoma cells were incubated with etoposide until 72 h in the incubator. At the end of the incubation time, 20 μ L of a MTT (5 mg/mL) solution were added to each well containing cells. The culture plate was further incubated around 1 h until the formazan crystals appeared. Then the crystals were dissolved with 150 μ L of a mixture of 50 mL isopropanol and 165 μ L of 1 N HCl. The 96-well culture plate was left at least 2 h in the refrigerator. Then the colour from formazan was measured by using the Polarstar™-Galaxy photometer and wavelengths of 595 and 690 nm. The absorption values at 595 nm were corrected by the respective absorption values at 690 nm, in order to subtract the effect of the interfering background such as cell components and protein. Data analysis was performed by using the GraphPad Prism™ program, version 4.0 (GraphPad Software Inc., San Diego, USA). Absorption of formazan was plotted against etoposide concentration on a semi-log scale. The EC_{50} value which is the etoposide concentration required to kill 50 % of the cells was estimated by nonlinear regression.

3.2.7 Colony forming assay

Effect of concentration and duration of exposure

The colony forming assay was used to investigate the dependence of etoposide antiproliferative activity on concentration and duration of exposure. Cells in exponential growth were seeded into a 6-well plate

(400 cells in 4 mL medium per well). Then the cells were kept overnight in the incubator in order to let them adhere to the surface of the culture plate. Etoposide solutions were prepared in medium with different concentrations 20 times higher than the final concentrations. 1 mL of each etoposide solution was added into each well of the cell suspension in order to obtain final etoposide concentrations of $2 \times 10^{-8.0}$, $2 \times 10^{-7.0}$, $2 \times 10^{-6.8}$, $2 \times 10^{-6.75}$, $2 \times 10^{-6.65}$, $2 \times 10^{-6.4}$, $2 \times 10^{-6.25}$, $2 \times 10^{-6.1}$, $2 \times 10^{-6.0}$, $2 \times 10^{-5.0}$ M for incubation time 12 h, concentrations of $1 \times 10^{-8.0}$, $1 \times 10^{-7.0}$, $1 \times 10^{-6.8}$, $1 \times 10^{-6.75}$, $1 \times 10^{-6.65}$, $1 \times 10^{-6.4}$, $1 \times 10^{-6.25}$, $1 \times 10^{-6.1}$, $1 \times 10^{-6.0}$, $1 \times 10^{-5.0}$ M for incubation time 24 h and concentrations of $1/5 \times 10^{-8.0}$, $1/5 \times 10^{-7.0}$, $1/5 \times 10^{-6.8}$, $1/5 \times 10^{-6.75}$, $1/5 \times 10^{-6.65}$, $1/5 \times 10^{-6.4}$, $1/5 \times 10^{-6.25}$, $1/5 \times 10^{-6.1}$, $1/5 \times 10^{-6.0}$, $1/5 \times 10^{-5.0}$ M for incubation time 120 h. Each concentration was investigated in triplicate. The cells incubated in etoposide-free medium were used as controls. Fresh medium containing etoposide was supplied daily for the exposure of 120 h to circumvent possible instability of etoposide. At the end of the exposure time, the cells were washed twice in PBS and kept in a freshly prepared etoposide-free medium. On day 8, colonies were washed with cold PBS, fixed with methanol and then stained with stain solution (Giemsa colour + crystal violet, s. 3.2.3). The colonies were counted by eye under microscopic examination. Each colony was composed of at least 40 cells.

The numbers of colonies in the drug-treated plates were expressed as a percentage of the control plates, which were given the value of 100 %. The mean \pm SD of colony counts from replicate experiments ($n = 3$) were calculated, and survival curves were plotted by using the GraphPad Prism™ program on a semi-logarithmic scale with the percentage remaining colonies against drug concentration. The antiproliferative effect of etoposide concentration and incubation duration were expressed as EC_{50} and AUC_{50} values. The EC_{50} was the etoposide concentration required to inhibit colony formation by 50 %. The AUC_{50} was the total drug exposure (duration x concentration) required to inhibit colony formation by 50 %.

Simulation of concentration-time profiles

The colony forming assay was used to investigate the dependence of the antiproliferative effect of etoposide on drug schedule by using an *in vitro* dilution model. The medulloblastoma cells were seeded into a 6-well plate (400 cells in 4 mL medium per well) and kept overnight in the incubator in order to let them adhere to the surface. The cells were exposed to the etoposide concentrations which simulated mean concentration-time profiles in CSF after intraventricularly administered etoposide 0.25 mg/12 h and 0.5 mg/24 h.

The concentration-time profiles were generated by a stepwise dilution method. On day 1, at 0 h, 1 mL of different concentrated etoposide solutions in medium were added into the wells to obtain the desired concentrations. At each pre-determined time-point of the simulated concentration-time profiles, culture medium was withdrawn and replaced by etoposide-free medium. The withdrawn and replaced volume of medium for each time-point was calculated by equation 23.

$$V_{drawn/replaced} = \frac{(C_i - C_{i+1}) \cdot V_{total}}{C_i} \quad (\text{eq.23})$$

Where:

$$\begin{aligned} V_{drawn/replaced} &= \text{withdrawn / replaced volume [mL]} \\ C_i &= \text{Concentration at time } i \text{ [h]} \\ C_{i+1} &= \text{Pre-determined concentration at the} \\ &\quad \text{next time-point (after time } i) \text{ [h]} \\ V_{total} &= \text{Total volume (5 mL)} \end{aligned}$$

The complete stepwise dilution protocols are shown in Appendix B3. At the last time-points (at every 12 or 24 h) of each profile, fresh etoposide solution was added into the system in order to simulate the next administration of etoposide *in vivo*. The medium was not completely removed in order to prevent the cells from stress due to a short-term lack of medium. Therefore, only 1.5 mL of culture medium were drawn and

replaced with 1.5 mL of different concentrated etoposide solutions which were prepared in medium to obtain the pre-determined concentrations. The concentrations of the etoposide solutions are presented in Appendix B3. After the incubation time (5 days), cells were washed twice in PBS and kept in freshly prepared etoposide-free medium.

On day 8, colonies were stained with stain solution (Giemsa colour + crystal violet, s. 3.2.3) and counted by eye under microscopic examination. Each colony was composed of at least 40 cells. The numbers of colonies in the drug-treated plates were expressed as percentage of the control plates, which were given the value of 100 %. The percentage remaining colonies were plotted against total drug exposure (AUC) by using Microsoft Excel™ and compared between the two dosage regimens.

4. Results

4.1 HPLC analysis of etoposide in CSF

Etoposide concentrations in CSF were determined by using HPLC with electrochemical detection. As the method was already fully validated at the Free University of Berlin, a partial validation was performed. All validation experiments were conducted in 0.9% NaCl as in this matrix results were comparable to CSF (s. 3.1.3). The validation results as shown below demonstrated that the HPLC method was suitable for measuring the concentrations of etoposide in CSF.

4.1.1 Selectivity

Typical blank chromatograms of CSF, buffer/NaCl, a spiked etoposide chromatogram, and a chromatogram of a patient's CSF sample are shown in Fig. 7, 8, 9 and 10, respectively. Retention time of etoposide ranged from 6.7 to 7.0 minutes. There was no interference from endogenous substances of pooled CSF, buffer and NaCl at this range of the retention time. The results indicate that the HPLC analysis method is selective for determining etoposide concentrations in CSF.

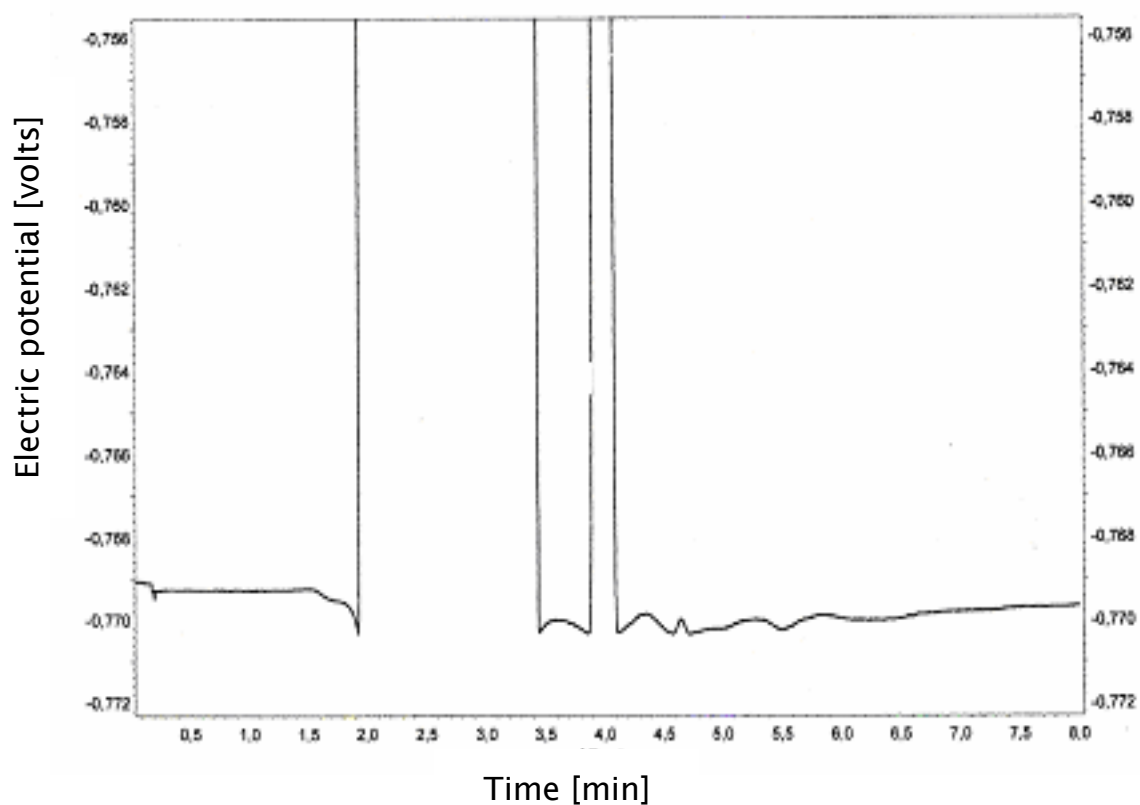


Figure 7. Representative blank HPLC chromatogram of pooled CSF without etoposide

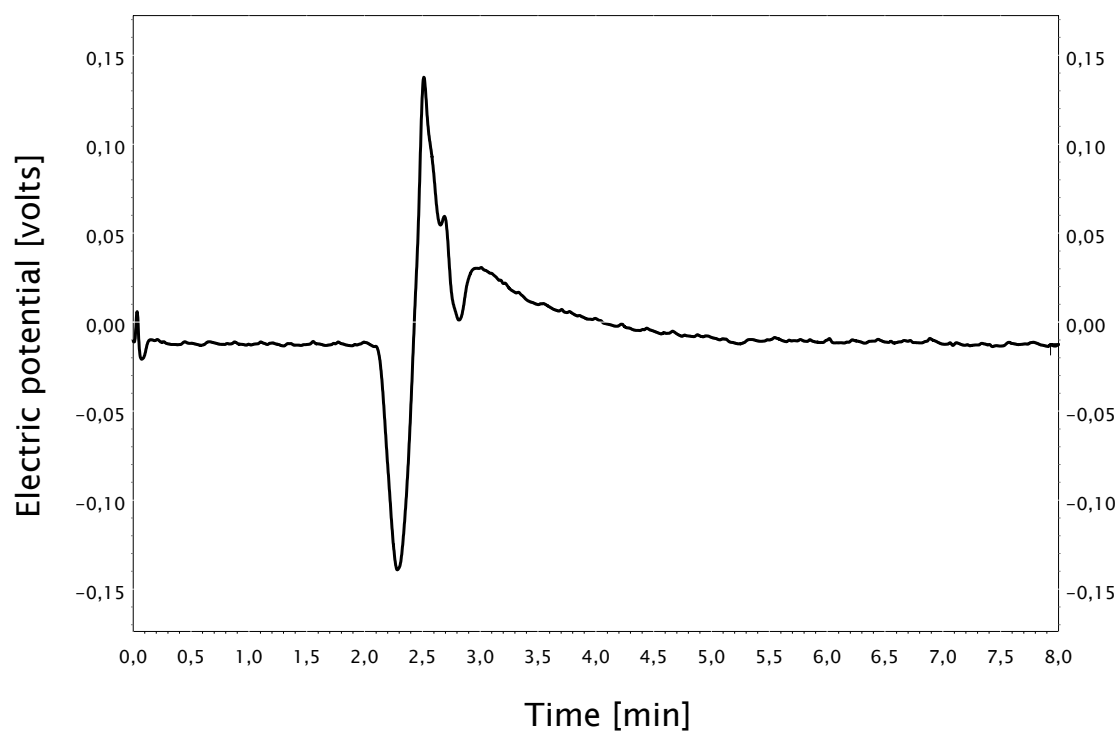


Figure 8. Representative blank HPLC chromatogram of 0.02 M phosphate buffer mixed with 0.9% NaCl (1:2 V/V)

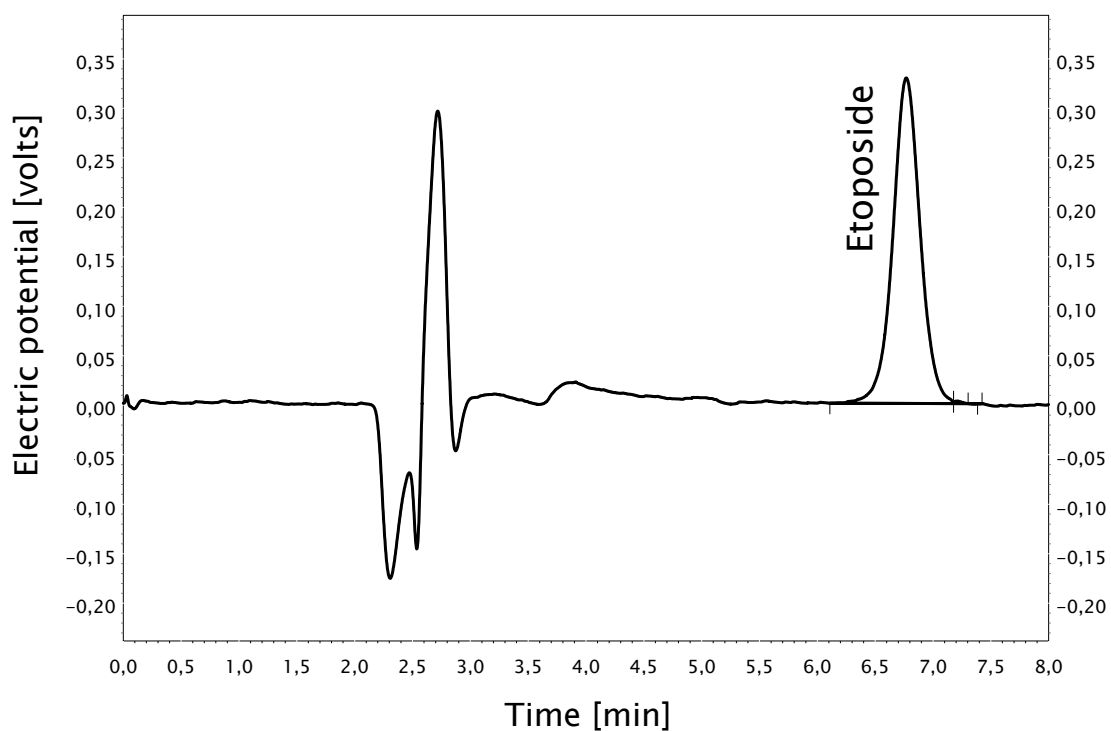


Figure 9. Representative HPLC chromatogram of spiked etoposide 0.80 $\mu\text{g/mL}$ in 0.02 M phosphate buffer mixed with 0.9% NaCl (1:2 V/V)

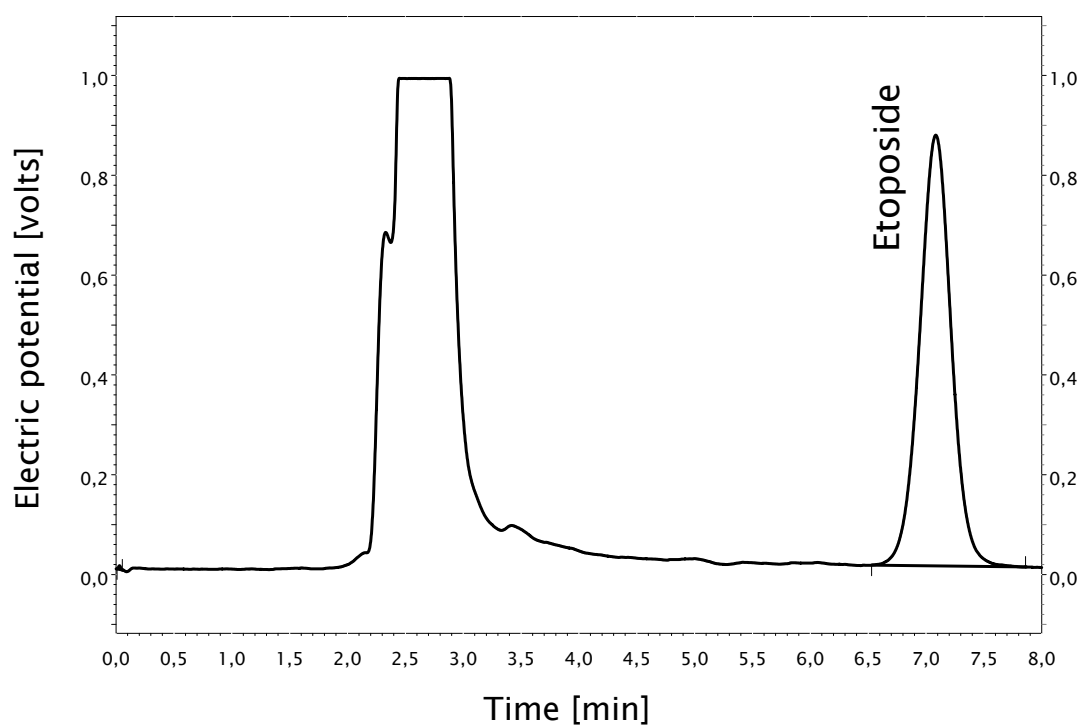


Figure 10. Representative HPLC chromatogram of etoposide in patient's CSF (determined concentration 1.18 $\mu\text{g/mL}$)

4.1.2 Linearity

Linearity was evaluated at five sensitivities of the electrochemical detector with five different concentration ranges. Each calibration curve contained six calibrators. Linearity was determined by plotting a standard curve using peak height versus the corresponding etoposide concentration in the sample. A linear regression least squares analysis was performed in order to determine the slope, intercept and correlation coefficient of the standard curve. The calibration curves were fitted using a weighting factor of $1/x$. The results are shown in Tab. 5. The coefficients of correlation on six different days were higher than 0.99 except at sensitivity 50 nA.

Table 5. Coefficients of correlation of calibration curves at different sensitivities (n = 6)

Sensitivity	Concentration range [µg/mL]	Correlation coefficient (r)
50 nA	0.05 – 0.20	0.9513 – 0.9967
2 µA	2.50 – 6.88	0.9981 – 0.9998
5 µA	6.25 – 17.50	0.9909 – 0.9980
10 µA	15.00 – 35.00	0.9957 – 0.9998
20 µA	30.00 – 100.00	0.9928 – 0.9961

4.1.3 Accuracy

Within-day accuracy

Within-day accuracy of the assay was calculated by comparing the measured concentration of spiked etoposide samples with the corresponding nominal concentration. Two concentrations of etoposide were measured at the sensitivities 50 nA and 20 µA in six replications within the same days. The accuracy was expressed as % RE. The within-day accuracy results are shown in Tab. 6. All the values obtained were within the limits regarded as acceptable for analysis of biological samples⁷⁴.

Table 6. Within-day accuracy of etoposide (n = 6)

Sensitivity	Concentration [μg/mL]	% RE
50 nA	0.10	(-2.67) - (+7.77)
	0.18	(-5.85) - (+14.31)
20 μA	40.00	(-12.93) - (-2.03)
	80.00	(-1.33) - (+0.76)

Between-day accuracy

Between-day accuracy of the assay was also calculated by comparing the measured concentration of spiked etoposide samples with the corresponding nominal concentration. Two concentrations of etoposide were measured for each sensitivity (50 nA, 2 μA, 5 μA, 10 μA, and 20 μA) once per day on subsequent six days. The accuracy was expressed as % RE. The between-day accuracy results are shown in Tab. 7. All the values obtained were within the limits regarded as acceptable for analysis of biological samples⁷⁴.

Table 7. Between-day accuracy of etoposide (n = 6)

Sensitivity	Concentration [μg/mL]	% RE
50 nA	0.10	(-13.69) - (+12.76)
	0.18	(-12.00) - (+3.34)
2 μA	2.50	(-3.60) - (+5.20)
	5.00	(-2.40) - (+2.40)
5 μA	7.50	(-10.27) - (+1.47)
	10.00	(-0.70) - (+7.50)
10 μA	20.00	(+0.70) - (+4.70)
	32.50	(-10.28) - (+7.48)
20 μA	40.00	(-7.20) - (+4.65)
	80.00	(-4.76) - (+1.48)

4.1.4 Precision

Within-day precision

Within-day precision of the assay was determined as coefficient of variation. Two concentrations of spiked etoposide samples were measured at the sensitivities 50 nA and 20 μ A in six replications on the same days. The within-day precision results are shown in Tab. 8. All the values obtained are within the limits regarded as acceptable for analysis of biological samples⁷⁴.

Table 8. Within-day precision of etoposide (n = 6)

Sensitivity	Concentration [μ g/mL]	% CV
50 nA	0.10	3.70
	0.18	8.36
20 μ A	40.00	3.77
	80.00	0.76

Between-day precision

Between-day precision of the assay was also determined as coefficient of variation. Two different concentrations of etoposide were measured for each sensitivity (50 nA, 2 μ A, 5 μ A, 10 μ A and 20 μ A) in six replications on six different days. The between-day precision results are shown in Tab. 9. All the values obtained are within limits regarded as acceptable for analysis of biological samples⁷⁴.

Table 9. Between-day precision of etoposide (n = 6)

Sensitivity	Concentration [µg/mL]	% CV
50 nA	0.10	13.83
	0.18	6.04
2 µA	2.50	3.77
	5.00	2.13
5 µA	7.50	4.59
	10.00	2.66
10 µA	20.00	1.58
	32.50	6.04
20 µA	40.00	4.06
	80.00	5.30

4.2 Pharmacokinetics of etoposide in CSF after intraventricular administration

4.2.1 Concentration-time profiles

Fig. 11, 12 and 13 show mean CSF concentration-time profiles following etoposide ivc administration of three different dosage regimens (0.25 mg/12 h, 0.50 mg/24 h and 1.0 mg/24 h, respectively) on five consecutive days. Fig. 14 shows the mean concentration-time profiles of etoposide in CSF following all dosage regimens. There was no drug accumulation in CSF after repeated ivc administration of etoposide during one cycle.

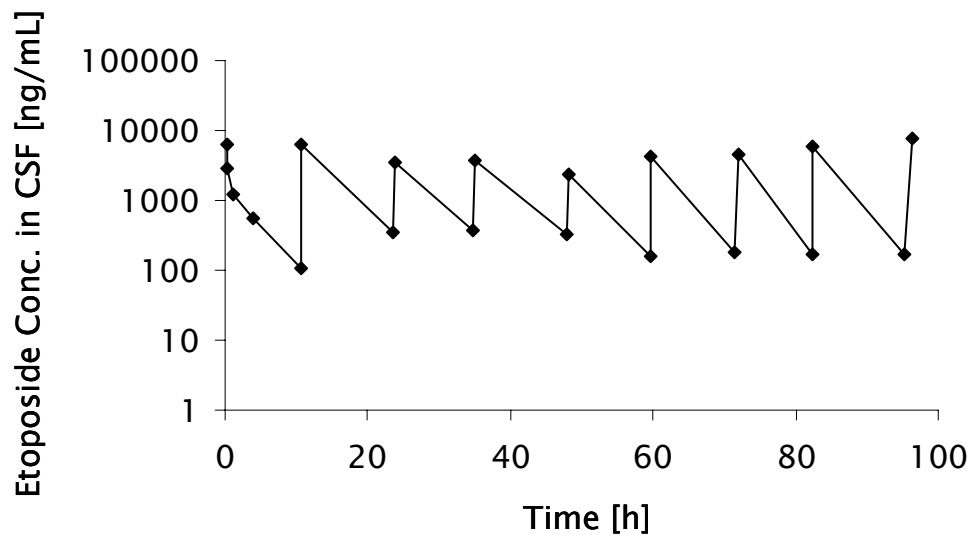


Figure 11. Mean CSF concentration-time profile following ivc administration of etoposide 0.25 mg/12 h on five consecutive days (2 patients, 8 cycles)

The diagram does not show standard deviations because data were obtained from only two patients.

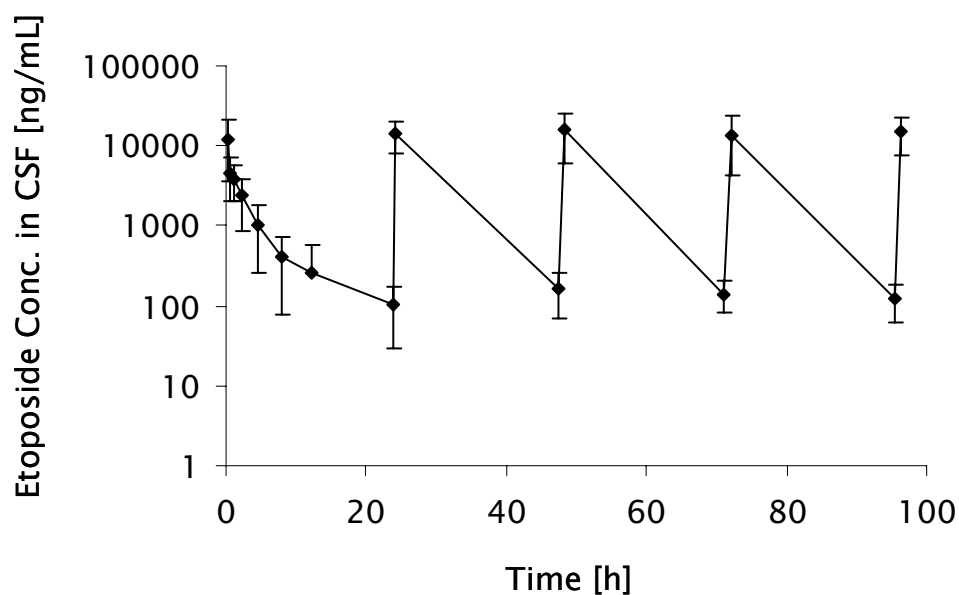


Figure 12. CSF concentration-time profile (mean \pm SD) following ivc administration of etoposide 0.50 mg/24 h on five consecutive days (8 patients, 41 cycles)

Standard deviation is not shown when lower value was below zero.

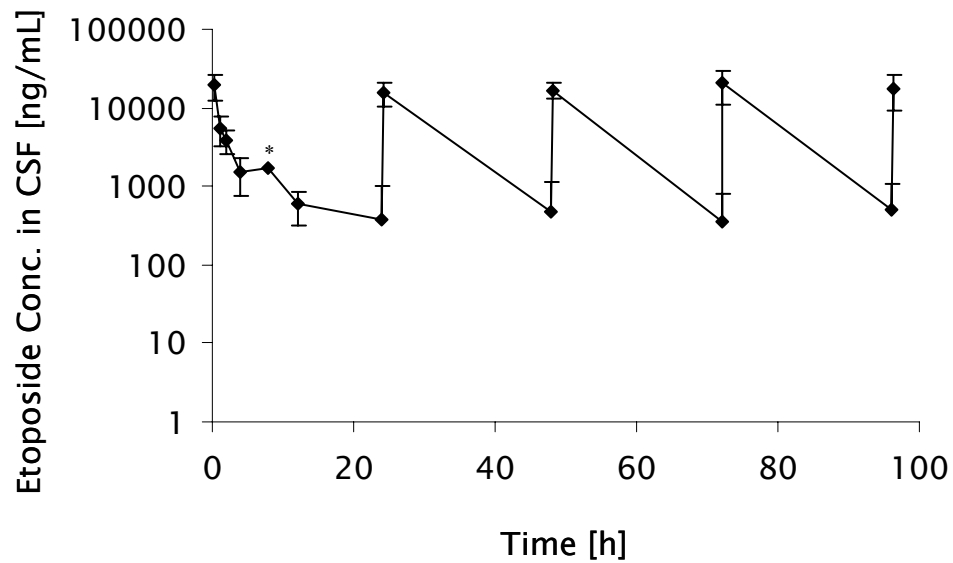


Figure 13. CSF concentration-time profile (mean \pm SD) following ivc administration of etoposide 1.0 mg/24 h on five consecutive days (14 patients, 73 cycles)

Standard deviations (*) were not shown because data were obtained from only one patient.

Standard deviations were not shown when lower values were below zero.

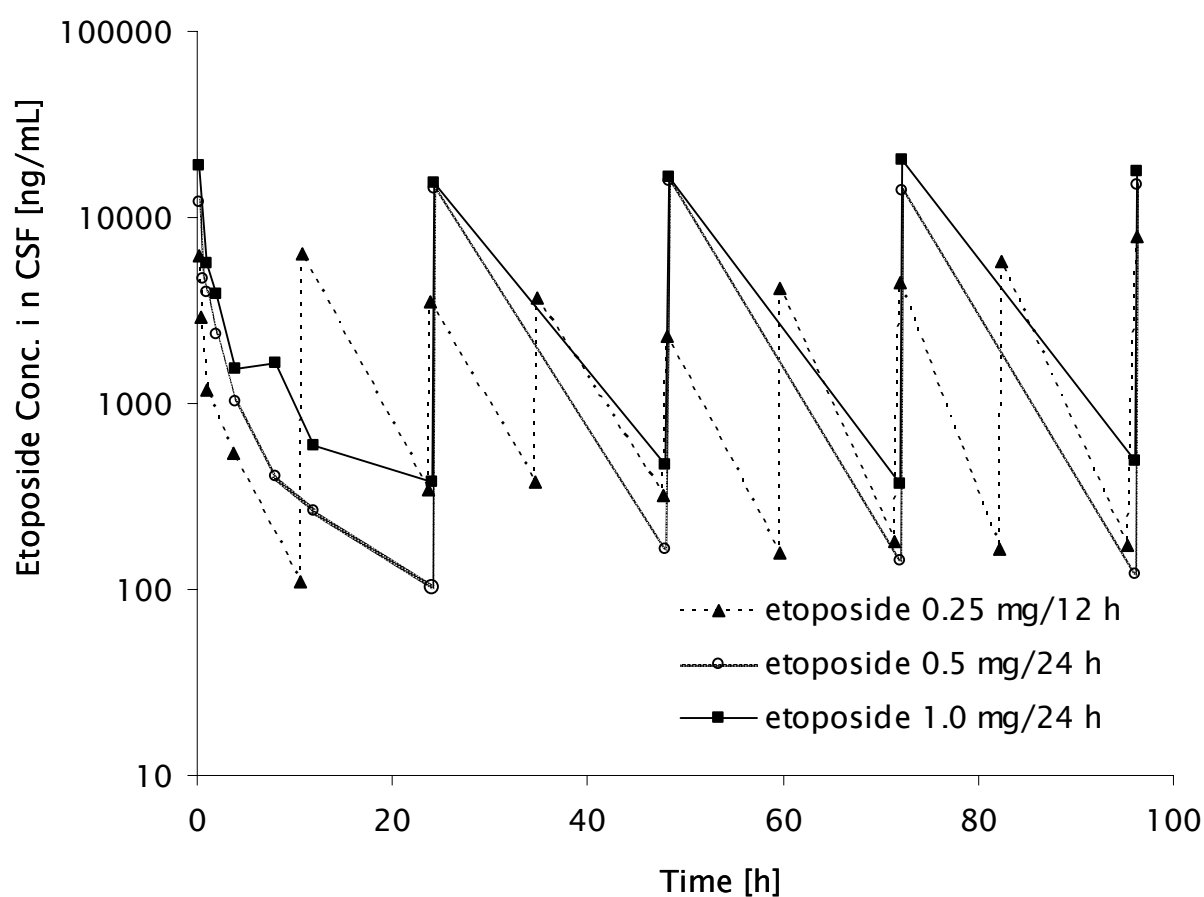


Figure 14. Mean concentration-time profiles of etoposide in CSF after ivc administration of three different dosage regimens

4.2.2 Generation of population parameters

First, the population values for the model parameters V_c , λ_z , r_c and λ_1 were estimated from data of seven patients undergoing full sampling as described in 3.1.9. The results are summarised in Tab. 10. The concentration-time profiles of these patients are shown in Appendix A2.

Table 10. Individual model parameters for Bayesian curve fitting

Patient	Cycle	Dosage regimen	V_c [L]	λ_z [h ⁻¹]	r_c	λ_1 [h ⁻¹]
1	9	1 mg/24 h	0.0358	0.1215	0.0523	1.7438
11	1	1 mg/24 h	0.0407	0.0948	0.0231	0.7468
15	1	1 mg/24 h	0.0674	0.0707	0.0999	0.6168
4	1	0.5 mg/24 h	0.1509	0.0965	0.0899	1.3370
5	1	0.5 mg/24 h	0.0893	0.1083	0.0415	0.6461
8	1	0.5 mg/24 h	0.0201	0.1272	0.2081	2.2527
9	1	0.5 mg/24 h	0.0619	0.1080	0.1702	0.4039

By using the Mann-Whitney U test, no statistical difference was found between the individual model parameters obtained from etoposide 0.5 mg/24 h and those obtained from etoposide 1.0 mg/24 h as shown in Tab. 11. Thus, the population parameters were obtained from both dosage regimens as mean and SD values of the individual model parameters from the seven patients as shown in Tab. 12.

Table 11. Comparison of parameters between the two dosage regimens (etoposide 0.5 mg/24 h and 1.0 mg/24 h) by using the Mann-Whitney U test

Model parameter	Statistical significance (p value)
V_c [L]	0.629
λ_z [h ⁻¹]	0.229
r_c	0.114
λ_1 [h ⁻¹]	0.857

Table 12. Population parameters used for Bayesian curve fitting

Model parameter	Mean	SD	CV [%]
V_c [L]	0.0666	0.0436	65.5382
λ_z [h^{-1}]	0.1039	0.0188	18.1358
r_c	0.0979	0.0687	70.1753
λ_1 [h^{-1}]	1.1067	0.6889	62.2505

4.2.3 Individual Bayesian curve fitting

Fig. 15, 16 and 17 show examples of CSF concentration-time profiles of etoposide 0.25 mg/12 h, 0.50 mg/24 h and 1.0 mg/24 h evaluated with SipharWinTM by using a two-compartment model and Bayesian curve fitting.

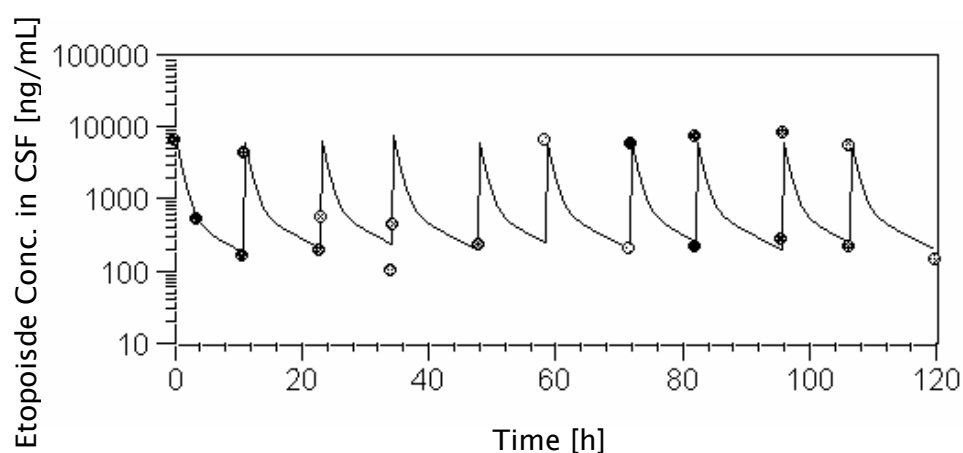


Figure 15. CSF concentration-time profile of a representative patient who received etoposide 0.25 mg/12 h obtained by Bayesian curve fitting

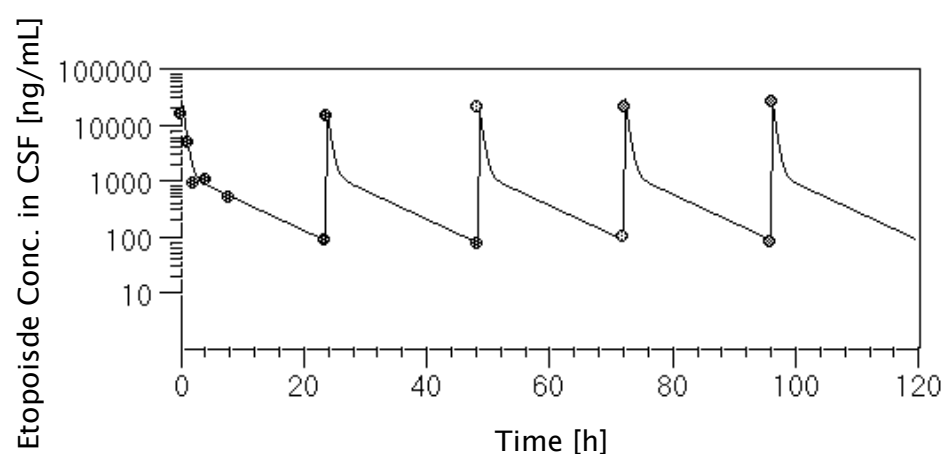


Figure 16. CSF concentration-time profile of a representative patient who received etoposide 0.50 mg/24 h obtained by Bayesian curve fitting

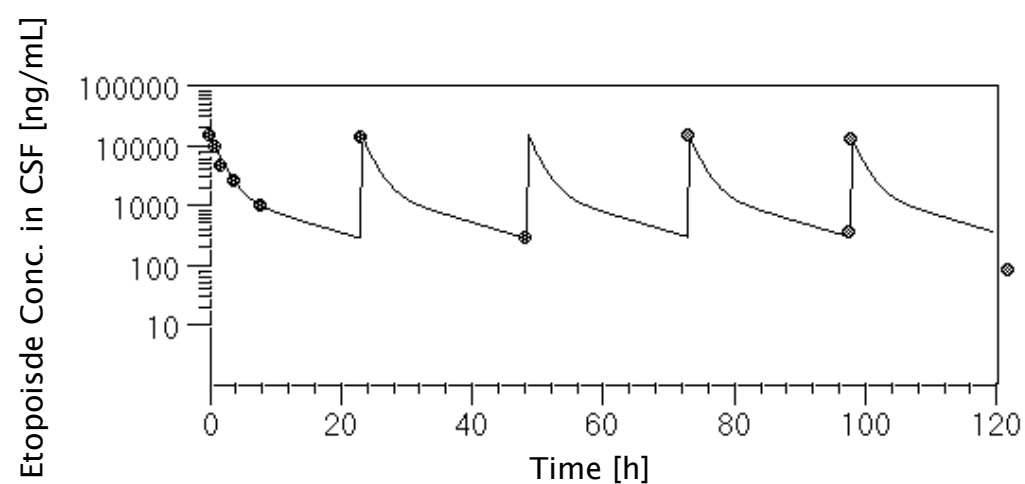


Figure 17. CSF concentration-time profile of a representative patient who received etoposide 1.0 mg/24 h obtained by Bayesian curve fitting

4.2.4 Pharmacokinetic parameters in CSF

Individual pharmacokinetic parameters of etoposide 0.25 mg/12 h, 0.50 mg/24 h and 1.0 mg/24 h are shown in Tab. 13 - 15, respectively. Etoposide pharmacokinetic parameters from all dosage regimens are summarised as means \pm SD in Tab. 16 by excluding one patient receiving etoposide 0.25 mg/12 h who had a hydrocephalus complication (s. 4.2.6). Individual pharmacokinetic data for each cycle are presented in Appendix A3. C_{\min} , C_{\max} and total area under the concentration-time curve in one cycle (AUC_{total}) of etoposide 1 mg/24 h were approximately two-fold higher than those observed after etoposide 0.5 mg/24 h indicating that CSF concentrations increase proportionally with etoposide dose. Because of the shorter dosage intervals mean C_{\min} after etoposide 0.25 mg/12 h was higher than that obtained after etoposide 0.5 mg/24 h. Tab. 13 - 16 show the large coefficients of variation of pharmacokinetic parameters of etoposide at any given dose in CSF indicating a high inter- and intraindividual variability in CSF disposition of etoposide after ivc administration.

4.2.5 Effect of dosage regimen on pharmacokinetic parameters

Fig. 18, 19 and 20 show the pharmacokinetic parameters $t_{1/2z}$, V_{ss} and CL as box plots. Median values of pharmacokinetic parameters after all dosage regimens were similar. Furthermore, no statistically significant differences of pharmacokinetic parameters among the three different dosage regimens were found by using the Kruskal-Wallis test (s. Tab. 16). This result indicates that etoposide pharmacokinetics in CSF is dose- and schedule- independent in the dose range studied.

Table 13. Individual pharmacokinetic parameters of etoposide in CSF (intraindividual mean \pm SD; % CV in brackets) after ivc administration of 0.25 mg/12 h

Patient	1	2 *	3 **
No. of cycles	4	1	3
AUC _{total} [$\mu\text{g} \times \text{h/mL}$]	115.29 \pm 6.52 (5.66)	139.70	111.45 \pm 62.66 (56.22)
CL [mL/min]	0.36 \pm 0.02 (5.45)	0.30	0.45 \pm 0.21 (46.96)
V _{ss} [L]	0.10 \pm 0.02 (15.93)	0.13	0.24 \pm 0.19 (77.02)
C _{min} [$\mu\text{g/mL}$]	0.17 \pm 0.03 (17.88)	0.37	0.37 \pm 0.16 (41.85)
C _{max} [$\mu\text{g/mL}$]	6.15 \pm 1.06 (17.23)	3.61	0.72 \pm 0.42 (58.35)
t _{1/2λ_1} [h ⁻¹]	0.74 \pm 0.07 (9.76)	0.54	0.53 \pm 0.12 (22.82)
t _{1/2z} [h ⁻¹]	6.56 \pm 0.06 (0.85)	7.21	7.83 \pm 1.35 (17.23)

* The SD is not shown because the patient received only one cycle.

** The patient exhibited a hydrocephalus (s. 4.2.6).

Table 14. Individual pharmacokinetic parameters of etoposide in CSF (intraindividual mean \pm SD; % CV in brackets) after ivc administration of 0.5 mg/24 h

Patient	1	4 *	5 *	6
No. of cycles	5	1	1	16
AUC _{total} [$\mu\text{g} \times \text{h/mL}$]	119.71 \pm 32.42 (27.08)	54.03	34.11	258.34 \pm 130.87 (22.21)
CL [mL/min]	0.37 \pm 0.11 (29.46)	0.77	1.22	0.21 \pm 0.12 (22.19)
V _{ss} [L]	0.12 \pm 0.04 (30.54)	0.18	0.38	0.06 \pm 0.05 (0.31)
C _{min} [$\mu\text{g/mL}$]	0.11 \pm 0.03 (27.89)	0.02	0.03	0.10 \pm 0.06 (13.55)
C _{max} [$\mu\text{g/mL}$]	10.38 \pm 2.26 (21.76)	3.08	2.56	27.52 \pm 15.04 (0.84)
t _{1/2λ_1} [h ⁻¹]	0.70 \pm 0.07 (10.32)	0.81	0.47	0.66 \pm 0.06 (2.73)
t _{1/2z} [h ⁻¹]	6.72 \pm 0.11 (1.60)	6.47	6.64	6.53 \pm 0.09 (1.43)

* The SD is not shown because the patients received only one or two cycles.

Table 14.-continued

Patient	7*	8*	9	10
No. of cycles	2	2	8	6
AUC _{total} [µg x h/mL]	157.53	170.97	143.30 ± 22.28 (15.55)	196.46 ± 50.36 (25.63)
CL [mL/min]	0.27	0.25	0.30 ± 0.05 (16.57)	0.23 ± 0.06 (27.14)
V _{ss} [L]	0.07	0.10	0.12 ± 0.03 (28.28)	0.08 ± 0.02 (25.28)
C _{min} [µg/mL]	0.06	0.21	0.18 ± 0.04 (21.10)	0.16 ± 0.10 (58.28)
C _{max} [µg/mL]	17.24	9.65	8.28 ± 2.96 (35.72)	16.40 ± 3.66 (22.33)
t _{1/2λ₁} [h ⁻¹]	0.69	0.79	0.99 ± 0.45 (45.81)	0.65 ± 0.02 (3.12)
t _{1/2z} [h ⁻¹]	6.46	6.96	7.24 ± 1.25 (17.33)	7.03 ± 0.81 (11.55)

* The SD is not shown because the patients received only one or two cycles.

Table 15. Individual pharmacokinetic parameters of etoposide in CSF (intraindividual mean \pm SD; % CV in brackets) after ivc administration of 1.0 mg/24 h

Patient	1	11	12*	13
No. of cycles	6	6	1	27
AUC _{total} [$\mu\text{g} \times \text{h/mL}$]	199.34 \pm 75.12 (37.68)	176.26 \pm 39.62 (22.48)	286.98	201.95 \pm 56.88 (28.16)
CL [mL/min]	0.49 \pm 0.23 (47.70)	0.50 \pm 0.15 (30.15)	0.29	0.44 \pm 0.12 (27.43)
V _{ss} [L]	0.15 \pm 0.08 (51.38)	0.14 \pm 0.04 (28.60)	0.11	0.14 \pm 0.04 (28.23)
C _{min} [$\mu\text{g/mL}$]	0.13 \pm 0.05 (38.58)	0.15 \pm 0.08 (51.43)	0.25	0.20 \pm 0.27 (134.16)
C _{max} [$\mu\text{g/mL}$]	18.41 \pm 4.34 (23.56)	27.42 \pm 11.92 (43.48)	23.46	18.33 \pm 4.96 (27.05)
t _{1/2λ_1} [h ⁻¹]	0.67 \pm 0.08 (11.30)	0.67 \pm 0.10 (14.39)	0.67	0.66 \pm 0.02 (2.49)
t _{1/2z} [h ⁻¹]	6.49 \pm 0.21 (3.24)	6.88 \pm 0.54 (7.87)	7.00	6.62 \pm 0.09 (1.38)

* The SD is not shown because the patients received only one or two cycles.

Table 15.-continued

Patient	14	15	16*	17*	18*
No. of cycles	4	3	1	2	1
AUC _{total} [µg x h/mL]	515.53 ± 109.89 (21.32)	250.20 ± 92.34 (36.90)	160.99	201.91	118.72
CL [mL/min]	0.17 ± 0.03 (17.70)	0.37 ± 0.14 (37.96)	0.52	0.41	0.70
V _{ss} [L]	0.12 ± 0.02 (12.42)	0.20 ± 0.10 (50.92)	0.12	0.16	0.22
C _{min} [µg/mL]	1.41 ± 0.47 (33.20)	0.66 ± 0.14 (21.51)	0.06	0.20	0.03
C _{max} [µg/mL]	23.13 ± 1.99 (8.61)	15.78 ± 8.81 (55.84)	21.44	12.76	n.a.
t _{1/2λ₁} [h ⁻¹]	0.49 ± 0.03 (5.70)	0.55 ± 0.06 (11.78)	0.64	0.67	0.63
t _{1/2z} [h ⁻¹]	10.13 ± 0.57 (5.62)	8.07 ± 0.87 (10.73)	6.39	7.05	6.58

* The SD is not shown because the patients received only one or two cycles.

n.a. = not available

Table 15.-continued

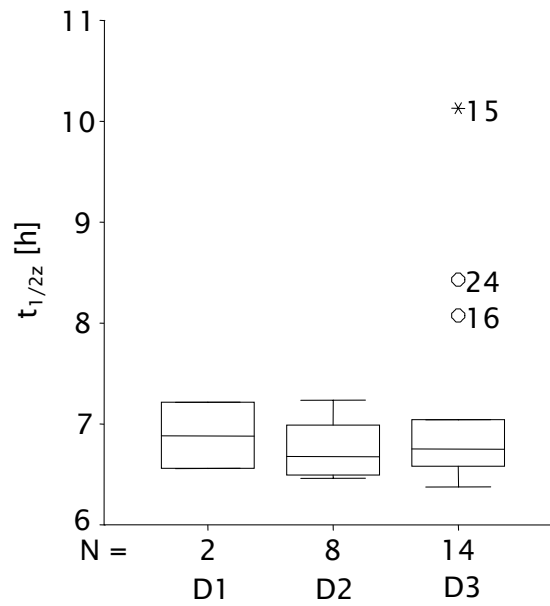
Patient	19*	20	21	22*	23
No. of cycles	2	3	6	2	9
AUC _{total} [μg x h/mL]	155.42	143.31±45.81 (31.97)	147.27±66.64 (45.25)	215.28	360.93±142.30 (39.42)
CL [mL/min]	0.56	0.63±0.25 (39.00)	0.67±0.28 (41.94)	0.39	0.27±0.11 (42.27)
V _{ss} [L]	0.18	0.18±0.08 (45.86)	0.22±0.11 (49.56)	0.15	0.13±0.02 (14.58)
C _{min} [μg/mL]	0.04	0.07±0.01 (8.62)	0.09±0.02 (24.27)	0.34	1.04±0.80 (76.68)
C _{max} [μg/mL]	16.77	15.20±0.60 (3.97)	13.27±6.64 (50.01)	16.89	20.63±2.87 (13.93)
t _{1/2λ₁} [h ⁻¹]	0.65	0.75±0.19 (25.27)	0.62±0.07 (10.70)	0.63	0.56±0.07 (12.91)
t _{1/2z} [h ⁻¹]	6.60	6.38±0.19 (2.95)	6.63±0.10 (1.49)	6.91	8.43±1.55 (18.35)

* The SD is not shown because the patients received only one or two cycles.

Table 16. Mean pharmacokinetic parameters (\pm SD; % CV in brackets) of etoposide in CSF after intraventricular administration of three different dosage regimens

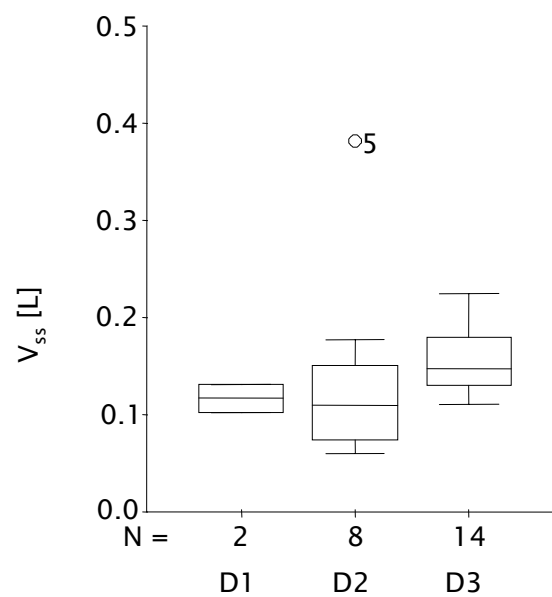
	0.25 mg / 12 h *	0.50 mg / 24 h	1.0 mg / 24 h	p value Kruskal- Wallis test
No. of patients	2	8	14	
No. of cycles	5	41	73	
AUC_{total} [$\mu\text{g} \times \text{h/mL}$]	127.50	141.81 ± 73.15 (51.59)	223.86 ± 105.42 (47.09)	0.038
CL [mL/min]	0.33	0.45 ± 0.36 (79.96)	0.45 ± 0.16 (34.02)	0.168
V_{ss} [L]	0.11	0.14 ± 0.11 (75.66)	0.16 ± 0.04 (23.62)	0.095
C_{min} [$\mu\text{g/mL}$]	0.27	0.11 ± 0.07 (69.54)	0.33 ± 0.42 (22.98)	0.198
C_{max} [$\mu\text{g/mL}$]	4.89	11.89 ± 8.27 (64.35)	18.73 ± 4.30 (124.60)	0.020
$t_{1/2\lambda_1}$ [h ⁻¹]	0.64	0.72 ± 0.15 (20.58)	0.63 ± 0.06 (10.04)	0.180
$t_{1/2z}$ [h ⁻¹]	6.88	6.76 ± 0.29 (4.28)	7.15 ± 1.05 (14.66)	0.906

*The SD is not shown because the mean value was calculated from only two patients.



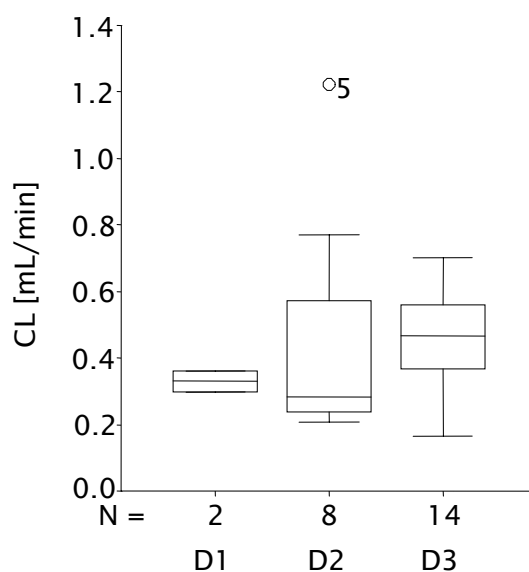
D1: Etoposide 0.25 mg/12 h; D2: Etoposide 0.50 mg/24 h; D3: Etoposide 1.0 mg/24 h

Figure 18. Box plot of elimination half-lives after three different dosage regimens of ivc etoposide



D1: Etoposide 0.25 mg/12 h; D2: Etoposide 0.50 mg/24 h; D3: Etoposide 1.0 mg/24 h

Figure 19. Box plot of volumes of distribution after three different dosage regimens of ivc etoposide



D1: Etoposide 0.25 mg/12 h; D2: Etoposide 0.50 mg/24 h; D3: Etoposide 1.0 mg/24 h

Figure 20. Box plot of clearances after three different dosage regimens of ivc etoposide

4.2.6 Case report of a patient with hydrocephalus

The effect of a hydrocephalus complication on the CSF disposition of etoposide was studied in three cycles in one patient. The pharmacokinetic parameters of this patient are summarised in Tab. 17. The V_{ss} (0.24 ± 0.19 L) in this patient was higher than those found in other patients (0.11 ± 0.02 L) who received etoposide with the same dosage regimen (0.25 mg/12 h). The difference between C_{max} and C_{min} was small in this patient.

Table 17. Pharmacokinetic parameters of one patient with hydrocephalus during ivc administration of etoposide 0.25 mg/12 h

Pharmacokinetic parameter	Mean \pm SD (n = 3)
C_{\max} [$\mu\text{g/mL}$]	0.72 ± 0.42
C_{\min} [$\mu\text{g/mL}$]	0.37 ± 0.16
$\text{AUC}_{\text{total}}$ [$\mu\text{g} \times \text{h/mL}$]	111.45 ± 62.66
CL [mL/min]	0.45 ± 0.21
V_{ss} [L]	0.24 ± 0.19
$t_{1/2z}$ [h]	7.83 ± 1.35

4.2.7 Distribution of etoposide inside the CSF

In order to study the distribution of etoposide inside the CSF compartment, CSF samples (n = 12) from four patients were taken simultaneously from an Ommaya reservoir (OMR) and by lumbar puncture four hours after etoposide ivc administration via the OMR. Etoposide concentrations of CSF samples collected from the OMR were similar to etoposide concentrations of samples collected by lumbar puncture (s. Tab. 18 and Fig. 21). By using paired t-test, no significant difference ($p = 0.988$) of etoposide concentrations in CSF was found between the two groups. The results indicate that etoposide is well distributed in the CSF compartment four hours after ivc administration via the OMR.

Table 18. Etoposide concentrations in CSF samples drawn from an OMR and by lumbar puncture (LP) four hours after etoposide ivc administration via OMR

Patient no. / Cycle	Etoposide concentration [µg/mL]	
	OMR	LP
0.25 mg/12 h		
Patient 1 / Cycle 5	0.54	0.47
Patient 1 / Cycle C	0.51	0.61
Patient 1 / Cycle 3	0.42	0.58
Patient 3 / Cycle 2	0.21	0.24
0.5 mg/24 h		
Patient 8 / Cycle 1	2.77	2.34
Patient 8 / Cycle 2	1.58	0.81
Patient 1 / Cycle 1	0.61	0.84
Patient 1 / Cycle 2	0.94	0.73
1.0 mg/24 h		
Patient 1 / Cycle 6	0.82	1.28
Patient 1 / Cycle 8	1.06	0.80
Patient 11 / Cycle 1	1.51	1.67
Patient 11 / Cycle 2	0.94	1.57

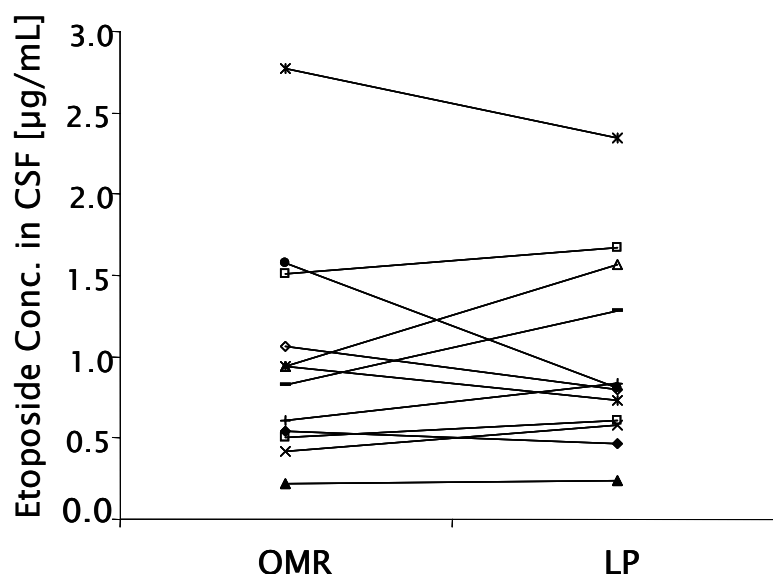


Figure 21. Comparison of etoposide concentrations in CSF samples drawn from an OMR and by lumbar puncture (LP) four hours after ivc administration via an OMR (n = 12 from 4 patients)

4.3 Stability of etoposide in cell culture medium

Stability of etoposide in cell culture medium (DMEM™ with GlutaMax™) was investigated as basis of the planned *in vitro* experiments. Etoposide 30 µg/mL in culture medium was incubated at 37 °C for up to 72 h. Samples were collected at 0, 1, 2, 4, 8, 12, 24, 31, 48, and 72 h, respectively. Etoposide concentrations in medium were measured by HPLC with UV detection. The results in Tab. 19 show that the concentrations of etoposide remain for 48 h above 90 % of the initial concentration. At 72 h, the concentration of etoposide in DMEM™ with GlutaMax™ under cell incubator conditions was only about 80 % of the initial concentration.

Table 19. Etoposide stability under cell incubator conditions (initial concentration was set to 100 %)

Time [h]	% remaining etoposide
1	106.61
2	99.21
4	109.86
8	107.90
12	104.98
24	103.27
31	97.46
48	94.51
72	80.77

4.4 Cytotoxic activity of etoposide in medulloblastoma cells

First, the optimal initial number of D-425med medulloblastoma cells for seeding was determined for the MTT assay on a 96-well culture plate. The cells were incubated in a T-flask with a surface area 25 cm² until they formed a monolayer. 20 % of the cells of the monolayer were further incubated in a T-flask with the same surface area (25 cm²). The cells needed around five days to form a monolayer again in the T-flask. As described in 3.2.6, 30 % of the cell number from the monolayer phase were hence regarded as the suitable initial seeding number for D-425med cells on 96-well plate. Afterwards, the absolute number of initial cells for seeding was calculated. The number of cells used to form the first monolayer in the T-flask 25 cm³ (100 %) was 7.88×10^5 cells/mL. Therefore, the equivalent number of cells for 96-well plate with a surface area of 35 cm² would be 1.10×10^6 cells/mL. As 30 % was determined as optimal for seeding, the suitable initial number of D-425med cells for the MTT

assay in 96-well plates was hence 3.31×10^5 cells/mL.

Then, the EC_{50} of etoposide for D-425med cells was determined by using the MTT assay. The D-425med cells of the 16th passage were incubated with etoposide in a concentration range of 10^{-8} to $10^{-3.75}$ M for 72 h. The results are shown in Fig. 22. The EC_{50} of etoposide in D-425med cells was found to be 0.25 ± 0.02 μ g/mL or $4.26 \times 10^{-7} \pm 0.32 \times 10^{-7}$ M, respectively. Individual data of the MTT assay are shown in Appendix B1.

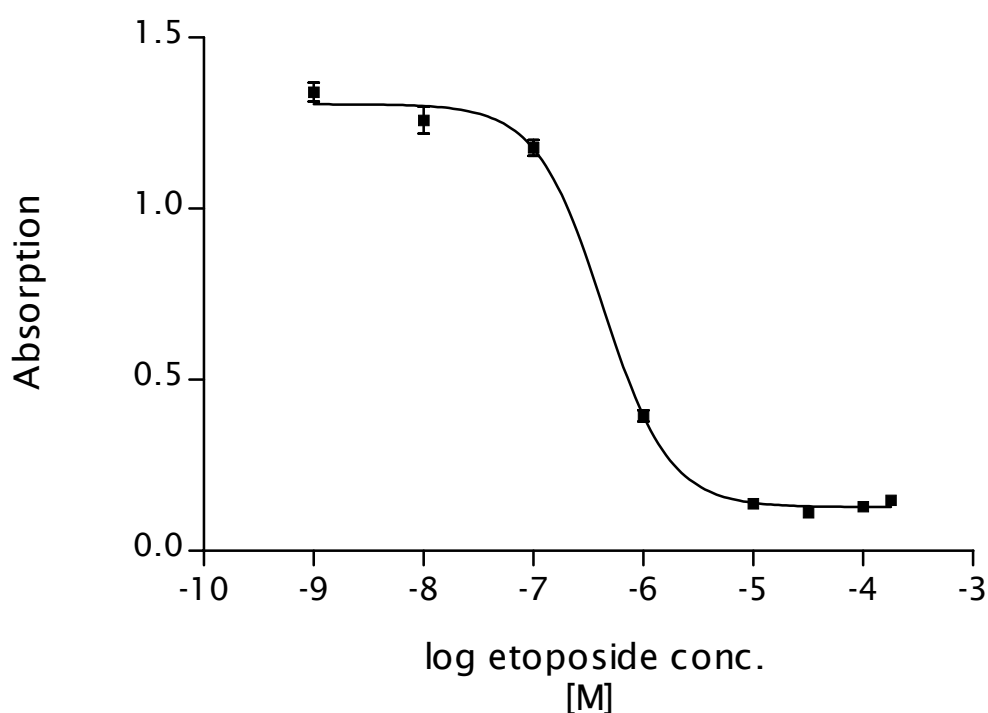


Figure 22. Concentration-effect relationship of etoposide in D-425med cells determined by using the MTT assay (n = 12)

4.5 Antiproliferative activity of etoposide in medulloblastoma cells

4.5.1 Effect of concentration and duration of exposure

For the colony forming assay, D-425med cells were incubated with different etoposide concentrations but the total drug exposures (AUC, concentration x time) were kept constant. Etoposide concentrations ranged from 2×10^{-8} to 2×10^{-5} M for an incubation period of 12 h, from 1×10^{-8} to 1×10^{-5} M for an incubation period of 24 h and from $1/5 \times 10^{-8}$ to $1/5 \times 10^{-5}$ M for an incubation period of 120 h.

The results are shown in Tab.20 and Fig. 23. The EC_{50} of etoposide at an incubation time of 12 h was around two-fold higher than those obtained from incubation times 24 h and 120 h. The AUC_{50} was comparable among the three groups. These results indicate that the growth of medulloblastoma cell colonies mainly depends on exposure rather than concentration only. The individual data of colony forming assay were shown in Appendix B2.

Table 20. EC_{50} and AUC_{50} of etoposide in medulloblastoma cells (D-425med) determined by using the colony forming assay (mean \pm SD; n = 3)

Incubation time [h]	EC_{50} [$\mu\text{g/mL}$]	AUC_{50} [$\mu\text{g} \times \text{h/mL}$]
12	0.46 ± 0.07	5.54 ± 0.84
24	0.24 ± 0.03	5.67 ± 0.71
120	0.20 ± 0.03	4.75 ± 0.84

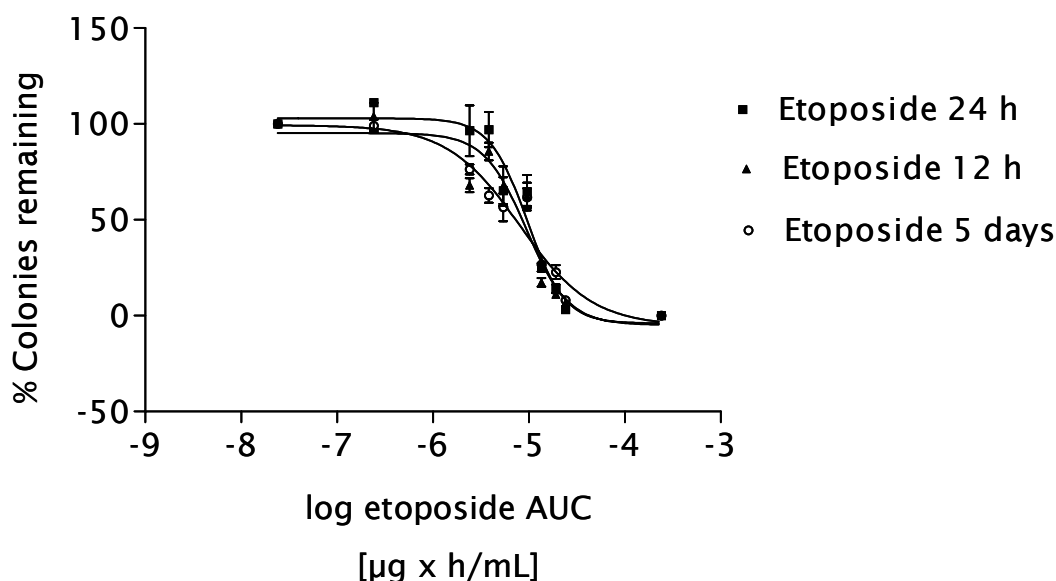


Figure 23. Effect of etoposide exposure on growth rate of medulloblastoma cells (D-425med) by using the colony forming assay (n = 3)

4.5.2 Effect of dosage regimen

The effect of two dosage regimens (0.25 mg/12 h and 0.50 mg/24 h) on etoposide antiproliferative activity was investigated by using an *in vitro* dilution model. The two dosage regimens were simulated *in vitro*.

The medulloblastoma cells were incubated with etoposide concentration-time profiles which were obtained from the pharmacokinetic study. Mean concentration-time profiles from both dosage regimens are shown in Tab. 21. To simulate etoposide concentration-time profiles, the concentrations of etoposide were adjusted by stepwise dilution at 0.25, 0.50, 1, 2, 4, 8, 12 h for etoposide 0.25 mg/12 h and at 0.25, 0.50, 1, 2, 4, 8, 12, 16, 20, 24 h for etoposide 0.50 mg/24 h. In the clinical study, etoposide was given to patients on five consecutive days, hence the cells were incubated with 10 repeated concentration-time profiles for twice daily administration (etoposide 0.25 mg/12 h) and 5 for once daily administration (etoposide 0.50 mg/24 h). On day 6, the cells were incubated for further 12 h with etoposide concentrations, reflecting the AUC from the last measurable concentration to infinity.

In order to characterise the pharmacokinetic disposition, two-compartment models were fitted to the mean concentration-time profiles of the patients after both dosage regimens as shown in Tab. 21. The obtained model equations (eq. 15) were used to simulate etoposide concentrations at each pre-determined time-point (s. 3.1.9). The simulated concentration-time profiles of etoposide 0.25 mg/12 h and etoposide 0.50 mg/24 h are shown in Tab. 22 and 23.

Table 21. Mean concentration-time profiles of etoposide 0.25 mg/12 h and 0.5 mg/24 h obtained from the clinical study

Etoposide 0.25 mg/12 h		Etoposide 0.50 mg/24 h	
Time [h]	Conc. [$\mu\text{g/mL}$]	Time [h]	Conc. [$\mu\text{g/mL}$]
0.25	6.27	0.25	12.16
0.42	2.90	0.50	4.67
1.00	1.18	1.11	3.93
3.79	0.54	2.27	2.36
12.00	0.11	4.53	1.04
12.25	6.41	8.05	0.40
24.00	0.34	12.22	0.26
24.25	3.52	24.00	0.10
36.00	0.38	24.25	14.28
36.25	3.67	48.00	0.17
48.00	0.32	48.25	15.58
48.25	2.30	72.00	0.14
60.00	0.16	72.25	13.80
60.25	4.11	96.00	0.12
72.00	0.18	96.25	14.93
72.25	4.45		
84.00	0.16		
84.25	5.80		
96.00	0.17		
96.25	7.81		

Table 22. Simulated concentration-time profile after 10 administrations of etoposide 0.25 mg/12 h

Time [h]	Etoposide concentration [µg/mL]										
Admin.	1	2	3	4	5	6	7	8	9	10	Mean
0.25	4.82	5.00	5.05	5.07	5.07	5.07	5.07	5.07	5.07	5.07	5.04
0.50	3.78	3.95	4.00	4.02	4.02	4.02	4.02	4.02	4.02	4.02	3.99
1	2.38	2.55	2.60	2.61	2.62	2.62	2.62	2.62	2.62	2.62	2.58
2	1.11	1.26	1.30	1.31	1.32	1.32	1.32	1.32	1.32	1.32	1.29
4	0.48	0.61	0.64	0.65	0.66	0.66	0.66	0.66	0.66	0.66	0.63
8	0.28	0.36	0.38	0.39	0.39	0.39	0.39	0.39	0.39	0.39	0.38
12	0.18	0.24	0.25	0.26	0.26	0.26	0.26	0.26	0.26	0.26	0.25

Admin. = Administration

Table 23. Simulated concentration-time profile after 5 administrations of etoposide 0.5 mg/12 h

Time [h]	Etoposide concentration [μg/mL]					
Admin.	1	2	3	4	5	Mean
0.25	11.88	12.00	12.01	12.01	12.01	11.98
0.50	9.34	9.46	9.46	9.47	9.47	9.44
1	5.91	6.02	6.03	6.03	6.03	6.00
2	2.70	2.80	2.81	2.81	2.81	2.79
4	1.11	1.18	1.19	1.19	1.19	1.17
8	0.62	0.67	0.68	0.68	0.68	0.66
12	0.41	0.44	0.45	0.45	0.45	0.44
16	0.27	0.29	0.30	0.30	0.30	0.29
20	0.18	0.20	0.20	0.20	0.20	0.19
24	0.12	0.13	0.13	0.13	0.13	0.13

Admin. = Administration

In the next step, the expected AUC_{total} was calculated from the simulated concentration-time profiles by the trapezoidal rule and compared with the AUC_{50} determined in 4.5.1. The AUC_{total} was found to be $127.50 \mu\text{g} \times \text{h/mL}$ for etoposide $0.25 \text{ mg}/12 \text{ h}$ and $141.81 \mu\text{g} \times \text{h/mL}$ for etoposide $0.5 \text{ mg}/24 \text{ h}$, respectively. These values were much higher than the AUC_{50} values ($4.75 \mu\text{g} \times \text{h/mL}$) for an incubation period of 120 h indicating that the simulated regimens would have been too toxic for the cells. Therefore, each concentration of the simulated mean concentration-time profiles was reduced by the factors 5, 10, and 15, respectively. The actually used concentration-time profiles with reduction factors 5, 10 and 15 are shown in Appendix B3. The AUC_{total} values for the *in vitro* study were calculated from the concentration-time profiles by using the trapezoidal rule and shown in Tab. 24.

Table 24. AUC_{total} values of actually used etoposide concentration-time profiles

Etoposide dosage regimen	AUC_{total} obtained	AUC_{total} obtained	AUC_{total} obtained
	with reduction	with reduction	with reduction
	factor 15	factor 10	factor 5
	$[\mu\text{g} \times \text{h/mL}]$	$[\mu\text{g} \times \text{h/mL}]$	$[\mu\text{g} \times \text{h/mL}]$
$0.25 \text{ mg}/12 \text{ h}$	5.60	11.20	16.80
$0.50 \text{ mg}/12 \text{ h}$	6.73	13.45	20.18

The results of this experiment are shown in Tab. 25 and 26. The percentage of colonies remaining was decreased when total drug exposures from both dosage regimens increased. A comparison of the percentage of colonies remaining between the two dosage regimens at the same total drug exposure (AUC) is shown in Fig. 24. More colonies remained after incubation with the once daily regimen compared to the twice daily regimen at the same exposure to etoposide. These data indicate that administration of etoposide $0.25 \text{ mg}/12 \text{ h}$ on five consecutive days etoposide may result in a higher antiproliferative activity than

administration of etoposide 0.50 mg/24 h both on five consecutive days. The individual data of this experiment are shown in Appendix B4.

Table 25. Remaining colonies of D-425med cells after exposure to the twice daily dosage regimen for five days

Total drug exposure [$\mu\text{g} \times \text{h/mL}$]	% colonies remaining (n = 3)				
	1	2	3	Mean	SD
5.60	73.17	75.41	69.31	72.63	3.09
11.20	81.67	57.14	40.96	59.92	20.49
16.80	25.23	45.83	38.35	36.47	10.43

Table 26. Remaining colonies of D-425med cells after exposure to the once daily dosage regimen for five days

Total drug exposure [$\mu\text{g} \times \text{h/mL}$]	% colonies remaining (n = 3)				
	1	2	3	Mean	SD
6.73	111.54	92.17	101.20	101.64	9.69
13.45	69.51	59.26	52.06	60.28	8.72
20.18	40.87	34.00	41.67	38.85	4.22

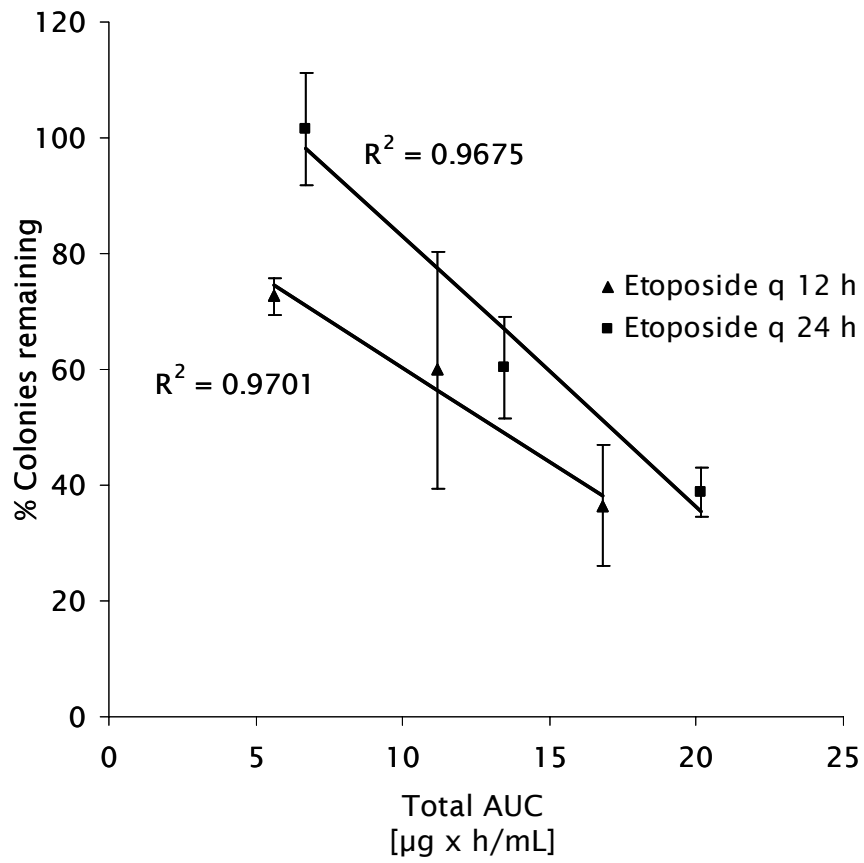


Figure 24. Antiproliferative activity of etoposide on D-425med cells after incubation with a once daily and twice daily regimen over five days (n = 3)

5. Discussion

5.1 Intraventricular administration of etoposide

The rationale for the administration of chemotherapy by the intra-CSF route is based on its ability to circumvent the blood-brain barrier, achieve high drug concentrations and drug exposure at the principle tumour site and minimize systemic drug exposure and systemic toxicity^{40,44,54}. Several disadvantages were found with intralumbar drug administration⁴⁴. Hence ivc drug administration is an interesting alternative for intra-CSF therapy. The advantages of ivc administration are less pain and inconvenience associated with frequent multiple administration, the feasibility of frequent multiple-dosing schedules, favourable pharmacokinetics with more homogeneous drug distribution within the CSF compartment, and the possibility of CSF sampling through the OMR with its catheter tip placed in the lateral ventricle^{40,44}. This technique enabled us to measure drug concentrations in CSF already shortly after ivc administration.

Several factors have led to the decision to develop etoposide as an agent for ivc administration. First, as a topoisomerase II inhibitor, etoposide has a different mechanism of antitumour activity from other agents used for intra-CSF therapy such as cytarabine and methotrexate which are classified as antimetabolites. Therefore, etoposide offers the potential of activity against tumours which are either initially unresponsive to antimetabolites or have acquired resistance to them. Second, etoposide is active against various tumour cells especially medulloblastoma and PNET. Third, it was previously demonstrated that intra-CSF administration of etoposide is feasible and safe. Moreover, etoposide is known to have a high protein binding in plasma (up to 97 %) which can impair the action of etoposide on tumour cells after systemic administration^{67,68}. Therefore, it was supposed that etoposide ivc administration can provide higher unbound etoposide levels in CNS because of the low protein concentrations in CSF. Under physiological conditions the protein concentrations in cerebrospinal fluid are less than one percent of the protein content in plasma⁸⁶.

5.2 Pharmacokinetics of etoposide in CSF after ivc administration

The pharmacokinetic data of etoposide in CSF were evaluated using Bayesian curve fitting which has some advantages such as estimation of pharmacokinetic parameters after sparse sampling. This means that the patients were less disturbed by sample collection. Moreover, it can minimise the problem of frequent sampling which may interfere with CSF dynamics and disturb the distribution of the intraventricularly administered drug. The pharmacokinetics of etoposide in CSF after ivc administration can be described with a linear two-compartment model as published in a previous report from Fleischhack et al.⁷⁰. The biphasic pattern might be the result of different processes such as diffusion along the concentration gradient from CSF to brain tissue or blood vessels, uptake of drug by receptor-mediated transport into the CNS, and elimination of drug by CSF bulk flow^{40,87,88}

5.2.1 Peak and trough concentrations

Mean C_{\max} , C_{\min} and AUC of etoposide in CSF increased proportionally with etoposide dose indicating that the disposition of etoposide within the CSF depends on processes that are not saturated in the dose range of the study. Mean C_{\max} (4.89 - 18.73 $\mu\text{g/mL}$) values from all dosage regimens were around 50 to 200 times higher than those obtained after high-dose systemic therapy confirming the advantage of regional therapy. Thus, ivc administration of etoposide allows a CSF exposure to etoposide that could never be achieved with systemic administration. Mean C_{\min} (0.11 - 0.33 $\mu\text{g/mL}$) values from our study were above the minimum cytotoxic concentration of etoposide to neuroblastoma cells from the study of Hill et al.¹² which reported that the concentration of etoposide required to reduce survival of the human neuroblastoma cell line CHP100 to 70 % was 0.08 $\mu\text{g/mL}$. Tomlinson et al.¹¹ reported concentrations of etoposide required to reduce survival of medulloblastoma cells to 63 % ranging from 0.11 to 2.24 $\mu\text{g/mL}$ (corresponding to 0.19 - 3.81 μM). The time of

exposure to etoposide in most *in vitro* studies in medulloblastoma and neuroblastoma cells was only up to 24 h^{11,12} whereas the typical clinical treatment is intravenous administration of etoposide for 3 - 5 consecutive days or orally for 14 - 21 consecutive days^{16,17,23}. Because the minimum cytotoxic concentrations depend not only on the tumour cell type but also on the incubation time, we designed an *in vitro* study which was supposed to simulate the incubation time and concentration-time profiles of the *in vivo* situation. The EC₅₀ values of etoposide reflecting growth inhibition of medulloblastoma cells (D-425med) by 50 % after five days of incubation was 0.20 µg/mL in our study. The C_{min} values after all dosage regimens of etoposide were close to or above this concentration. Comparing the mean C_{max} and C_{min} values with the EC₅₀ values from our *in vitro* studies, it can be assumed that all three dosage regimens lead to concentrations of etoposide in the CSF that are sufficiently high to achieve antitumour activity.

5.2.2 Distribution of etoposide in the CSF

The t_{1/2λ₁} in CSF ranged from 0.63 to 0.72 h indicating rapid distribution of etoposide in the CSF. Moreover, etoposide seems to equilibrate well in the CSF compartment after ivc administration because there was no difference in etoposide concentration between samples obtained from the OMR and by lumbar puncture four hours after ivc administration. Drugs which are administered through the OMR are carried in the same direction as the CSF bulk flow⁴⁴. This might be a reason for the good distribution of etoposide in the CSF compartment after ivc administration. However, the small V_{ss} of etoposide (about 150 mL) indicates that etoposide distributes mainly inside the CSF compartment which exhibits a total volume between 80 and 150 mL⁸⁹. This result is in agreement with Blasberg et al.⁹⁰ who reported that after intrathecal drug therapy of hydroxyurea, methotrexate, thiotepa, 1, 3-bis (2-chloroethyl)-1-nitrosourea (BCNU) and cytarabine in the rhesus monkey, drug diffusion was limited. The drugs only differed into brain parenchyma or subarachnoid tumour nodules by 2 - 3 mm. Basically, the

distribution of drugs from the intrathecal space depends on the physicochemical properties of the drug and the unbound fraction. Lipophilic drugs readily enter the spinal cord where they are absorbed systemically, whereas hydrophilic drugs tend to remain in the CSF. However, only the lipid-soluble molecules with a molecular weight lower than 500 Dalton can pass across the BBB⁸⁸. Molecular weight of etoposide is greater than 500 Dalton. This might be one possible reason why etoposide is mostly distributed in the CSF compartment, even though etoposide is a lipophilic drug and exhibits low protein binding in CSF.

5.2.3 Elimination of etoposide from the CSF

The $t_{1/2z}$ of etoposide in CSF ranged from 6.76 to 7.15 h indicating that etoposide is slowly eliminated from the CSF. Normally, drug clearance from the CSF can occur by CSF bulk flow to the arachnoid villi of the superior sagittal sinus and spinal epidural veins, active transport at the choroid plexus and extrachoroidal sites, diffusion into the central nervous system extracellular fluid and capillaries, and uptake or metabolism by central nervous system cells⁹¹. CSF bulk flow is usually of 0.30 – 0.52 mL/min⁹² which is comparable to the mean CL of etoposide from CSF of 0.33 - 0.45 mL/min. Therefore, it is likely that etoposide is eliminated mainly through CSF bulk flow. The variability of $t_{1/2z}$ and CL might be explained by the different ability to produce and excrete CSF as well as different CSF volumes among the patients. Our results showed no etoposide accumulation after repeated administration of etoposide on five consecutive days. Therefore, the risk of reaching potentially toxic concentrations is low.

5.2.4 Effect of disease state

The large variability of pharmacokinetic parameters of etoposide that we observed after all studied dosing regimens might be a consequence of the disease state of the patient, differences in individual CSF volume or different production, and excretion rate of the CSF. The effect of a

hydrocephalus on the pharmacokinetic disposition of etoposide in CSF was monitored in three cycles of one patient at the age of 0.92 years. This patient suffered from a medulloblastoma with leptomeningeal metastases. This tumour was resistant to first-line therapy, complicated by a hydrocephalus occlusus and the necessity of a ventricular-peritoneal shunt. Comparing the V_{ss} in this patient to the V_{ss} of the other two patients who received etoposide in the same dosage regimen, the V_{ss} of this patient was larger than those found in the other two patients. Therefore, it can be assumed that the large V_{ss} in this patient was the effect of the hydrocephalus. The C_{max} of this patient was considerably lower compared to the C_{max} values of the other two patients due to the larger V_{ss} .

5.2.5 Comparison with other intra-CSF administered agents

At present, methotrexate, cytarabine and thiotepa are widely used for intra-CSF therapy. Other cytotoxic agents such as mafosfamide, topotecan, diaziquone, temozolomide and etoposide have been studied for intra-CSF therapy. Tab. 27 summarises the pharmacokinetic parameters of these agents in CSF after intra-CSF administration available so far. Nimustine, mercaptopurine, mafosfamide, and diaziquone exhibit very short half-lives whereas topotecan, cytarabine, etoposide, and methotrexate show longer half-lives between 3 – 13 hours. The longest half-life was reported for liposomal cytarabine.

Table 27. Pharmacokinetic parameters of anticancer agents in CSF after intra-CSF administration

Agent	Dose [mg]	Adm.	No. of pts.	CL [mL/min]	V _{ss} [L]	t _{½z} [h]
Nimustine ⁹³	10-20	ivc	3	n.a.	n.a.	0.2-1.1
Diaziquone ⁵²	1, 2	ivc	6	0.37 (0.10-0.93)	n.a.	1.3 (0.8-2.6)
Mercaptopurine ⁴⁵	5, 10	ivc	7	0.63	n.a.	1.4
Mafosfamide ⁵⁸	1-5	ivc, LP	11	0.50 (0.19-1.10)	n.a.	1.2 (0.7-2.6)
Topotecan ⁵⁴	0.2-0.7	ivc, LP	9	0.3 (0.23-0.35)	0.04-0.05	2.6 (2.4-2.9)
Cytarabine ^{45,93}	30	ivc	7	n.a.	0.55	3.4 (2.5-4.4)
	15-30	ivc	3	n.a.	n.a.	(1.8-6.2)
Etoposide*	0.5-1	ivc	22	0.33-0.45	0.11-0.16	6.8-7.2
Methotrexate ^{45,93}	10-20	ivc	3	n.a.	n.a.	2.2-13.5
	0.5	ivc	1	n.a.	n.a.	6.6
	6.25 mg/m ²	ivc	5	n.a.	n.a.	8
	6	ivc	12	n.a.	0.03	5.7 (3.3-20)
	12 mg/m ²	ivc	16	n.a.	n.a.	7.1
	15 mg/m ²	ivc	n.a.	n.a.	n.a.	10.5
Liposomal Cytarabine ⁵⁵	50	ivc, LP	2	n.a.	n.a.	55-57

* = Data from our study; Adm. = Administration; n.a. = not available; pts. = patients

5.2.6 Clinical consequences

The pharmacokinetic data of intraventricularly administered etoposide displayed dose-independent pharmacokinetics in the CSF. The AUC increases proportionally with dose indicating linear pharmacokinetics. Linear pharmacokinetics is an important prerequisite for the safe use of this new mode of administration.

Intraventricular chemotherapy is primarily directed against cells dispersed within or lining the CSF compartment rather than against malignant cells within the brain parenchyma. Main factors for its consideration are the distribution of the drug within the CSF, the extent of drug clearance from the CSF and the time course of action⁹⁴. Considering these factors along with our pharmacokinetic data, ivc etoposide seem to be suitable for treating tumours or metastases which are located in or close to the CSF space to prevent further seeding into the leptomeninges.

Moreover, our data might be used to simulate concentration-time profiles following other regimens in order to optimise ivc therapy of etoposide. A prospective, randomized multi-institutional phase II clinical trial of intraventricularly administered etoposide is currently conducted to assess the clinical response and the quality of life.

5.3 In vitro pharmacodynamics of etoposide in medulloblastoma cells

Conventionally, in *in vitro* experiments the tumour cells are exposed to constant concentrations of cytotoxic agents. In fact, in the *in vivo* situation the tumour cells are not exposed to constant concentrations but to a specific concentration-time profile which is determined by pharmacokinetic processes. One aim of our *in vitro* experiments was to study the effect of the dosage regimen on medulloblastoma cells. The concentration-time profiles were simulated using data from the clinical study.

5.3.1 Suitability of the colony forming assay

The colony forming assay was used to determine the effect of concentration, duration of exposure and dosage regimen on etoposide antiproliferative activity. The colony forming assay is a direct measure of cell survival and proliferation. It is a reproducible method, easy to set up, and inexpensive. Moreover, the colony forming assay can be used to measure the antiproliferative activity without "dead-cell condition" which is needed in the MTT test. Disadvantages are that it is time-consuming and labour-intensive. Usually, the stepwise dilution can lead to cell loss and reduce the number of colony forming units especially when cells are suspended in culture medium. Thus, it can interfere with the measured antiproliferative effect caused by etoposide. However, in our study tumour cells were fixed to the surface of the culture plate. Therefore, the probability to lose tumour cells along with the dilution step is low compared to the suspension model. A limitation of our experimental conditions is that the form of the cells differs from the form under *in vivo* conditions where cells are in spheroid form (solid tumour) or floating in the CSF compartment^{95,96}.

5.3.2 Effect of concentration and duration of exposure on antiproliferative activity

The results obtained in this study demonstrated that the antiproliferative activity of etoposide on medulloblastoma cells depends on concentration and duration of exposure of the drug. This observation is in agreement with previous reports^{13,18-22}. The concentration-dependence of antiproliferative activity of etoposide would support the concept of high-dose therapy which maximises total drug exposure. However, this strategy would produce more systemic toxicity such as myelosuppression which is the dose-limiting toxicity of etoposide. At the same time, our results showed that the etoposide antiproliferative activity also depends on the duration of exposure. As the duration of exposure increases, the dose required to produce maximum antiproliferative activity decreases. Our

results are in accordance with *in vivo* studies which showed the advantage of schedules with longer drug exposure in tumour patients^{16,17,23}. The clinical trial from Slevin et al.¹⁶ showed that the response rate of etoposide 100 mg/m² given on five consecutive days is clearly superior to the response rate of etoposide 500 mg/m² administered as 24 h continuous infusion. Both *in vitro* and *in vivo* results support and confirm the benefit of a prolonged therapy regimen which offers a therapeutic advantage in terms of both efficacy and toxicity. *In vitro* results from Liu et al.¹³ also showed that at the same total drug exposure, etoposide cytotoxic activity increased relatively with duration of exposure. He recognised also the importance of etoposide concentration. If etoposide concentration was below an effective threshold, the cytotoxic activity in schedules of more protracted duration showed a gradual reduction. Therefore, it is necessary to find out the suitable duration of exposure and the sufficient total drug exposure or the threshold of etoposide concentration for each type of tumour cell.

5.3.3 Effect of dosage regimen

One of the objectives of this study was to investigate the effect of dosage regimen on the antiproliferative activity of etoposide. The results show that a twice daily regimen of etoposide exhibits a higher antiproliferative activity than a once daily regimen. In the pharmacokinetic study in brain tumour patients both dosage regimens (0.25 mg/12 h and 0.50 mg/24 h) led to a comparable total drug exposure, but after the twice daily regimen drug concentration was longer above the EC₅₀ than after the once daily regimen. From the *in vitro* experiments it can be concluded that prolonged maintenance of low etoposide concentrations is more important for obtaining a response than high peak concentrations. This supports the so called concentration times time (C x T) strategy, i.e. repeating low doses of etoposide over a relatively short period of time.

An explanation of these experimental observations is that etoposide is classified as cell cycle phase-specific cytotoxic agent. Main target of

etoposide is DNA topoisomerase II. It induces the formation of DNA topoisomerase II cleavable complexes which results in DNA single- and double- strand breaks. This action takes place in two specific phases. The first one is the phase between the last division and the start of DNA replication (the S phase) and the second phase is the replication of DNA (the G₂ phase)¹. The effect of etoposide on the DNA topoisomerase II complex is reversible when the cells have been incubated with inappropriate time or insufficient concentrations which may be non- or sub-lethal to the cells. This means that a longer exposure to a threshold concentration of etoposide would affect more cells as a larger fraction of cells completes a full cell cycle.

In conclusion, etoposide 0.25 mg/12 h may be the best dosage regimen of the regimens studied because of a higher antiproliferative efficacy. Moreover, toxicity is probably comparable to the regimen 0.50 mg/24 h because of a similar drug exposure. These findings should be confirmed in a randomised, controlled clinical trial.

6. Summary

Intraventricular (ivc) administration of etoposide was introduced to solve one of the major problems in treating central nervous system tumours, namely the limited distribution of cytotoxic drugs across the blood-brain barrier. Well characterised relationships between pharmacokinetics and pharmacodynamics facilitate the clinical development of optimal dosage regimens.

Pharmacokinetic disposition of etoposide in cerebrospinal fluid was investigated in 22 patients (119 cycles) after intraventricular administration of three different dosage regimens (0.25 mg/12 h, 0.5 mg/24 h and 1.0 mg/24 h) through an Ommaya reservoir. CSF concentrations of etoposide were determined by reversed-phase high-performance liquid chromatography (HPLC) with electrochemical detection. The pharmacokinetic parameters were estimated by using a two-compartment model and Bayesian curve fitting. The maximum concentration (C_{\max}) of etoposide in CSF was observed 15 minutes after ivc administration. Mean C_{\max} and area under the curve of etoposide in CSF increased proportionally with etoposide dose. After repeated ivc administration of etoposide on five consecutive days no drug accumulation in CSF was observed. The pharmacokinetics of etoposide in the CSF was found to be dose- and schedule-independent in the dose range studied as no statistically significant differences were found in terminal elimination half-life ($t_{1/2\alpha}$), volume of distribution (V_{ss}) and clearance (CL) among the three dosage regimens. One patient with a hydrocephalus exhibited a larger V_{ss} . The distribution of etoposide inside the CSF compartment was investigated by simultaneous collection of CSF samples via Ommaya reservoir (OMR) and lumbar puncture (LP) four hours after an ivc administration. Etoposide concentrations did not differ between both sites indicating homogeneous distribution of etoposide in the CSF after ivc administration.

In order to characterise the pharmacodynamics of etoposide in

medulloblastoma cells, the effect of concentration and total drug exposure on antiproliferative activity was investigated in D-425med cells by using the colony forming assay. The cells were incubated with different etoposide concentrations but the total drug exposures (AUC, concentration x duration of exposure) were kept constant. The percent colonies remaining decreased when etoposide concentration was increased. The EC_{50} of etoposide after an incubation time of 12 h was around two times higher than that obtained after the incubation times 24 h and 120 h. However, the AUC_{50} (duration x concentration) was comparable among the three groups. The results indicate that the antiproliferative activity of etoposide on medulloblastoma cells mainly depends on total drug exposure. Moreover, the effects of two different dosing schedules (once daily and twice daily on five consecutive days) on the medulloblastoma cells were investigated by using an *in vitro* dilution model. At the same total exposure, fewer colonies remained after exposure with simulated concentration-time profiles of etoposide given every 12 h compared to the regimen with etoposide administration every 24 h. The *in vitro* pharmacodynamic investigation revealed that at the same drug exposure (AUC), the twice daily administration was more effective than the once daily administration.

In conclusion, the clinical results indicate linear pharmacokinetics of intraventricularly administered etoposide in the CSF which is an important prerequisite for the safe use of this new mode of administration. The *in vitro* results suggest that a more frequent administration of etoposide is favourable as it can produce a higher antiproliferative activity with the same drug exposure.

7. References

- [1] Giri A, Narasu L. Production of podophyllotoxin from podophyllum hexandrum: a potential natural product for clinically useful anticancer drugs. *Cytotechnology* 2000; 34: 17-26.
- [2] Henwood JM, Brogden RN. Etoposide. A review of its pharmacodynamic and pharmacokinetic properties, and therapeutic potential in combination chemotherapy of cancer. *Drugs* 1990; 39: 438-490.
- [3] GRY-Pharma GmbH. Ökonomie in der Onkologie. Eto-Gry 20 mg/ml - Standardinformation für Krankenhausapotheker, 2001.
- [4] Joel S. The clinical pharmacology of etoposide: an update. *Cancer Treat Rev* 1996; 22: 179-221.
- [5] O'Dwyer PJ, Leyland-Jones B, Alonso MT et al. Etoposide (VP-16-213). Current status of an active anticancer drug. *N Engl J Med* 1985; 312: 692-700.
- [6] Slevin ML. The clinical pharmacology of etoposide. *Cancer* 1991; 67(1 Suppl): 319-329.
- [7] Holden JA. DNA topoisomerases as anticancer drug targets: from the laboratory to the clinic. *Curr Med Chem Anti -Canc Agents* 2001; 1: 1-25.
- [8] Hainsworth JD, Greco FA. Etoposide: twenty years later. *Ann Oncol* 1995; 6: 325-341.
- [9] Chabner BA, Ryan DP, Ares PL et al. Antineoplastic Agents. In: Hardman JG, Limbird LE, Gilman AG, editors: Goodman & Gilman's The pharmacological basis of therapeutics. 10th ed., The McGraw-Hill company, Inc., USA, 2001; 1421-1422.

- [10] Meresse P, Dechaux E, Monneret C et al. Etoposide: discovery and medicinal chemistry. *Curr Med Chem* 2004; 11: 2443-2466.
- [11] Tomlinson FH, Lihou MG, Smith PJ. Comparison of in vitro activity of epipodophyllotoxins with other chemotherapeutic agents in human medulloblastomas. *Br J Cancer* 1991; 64: 1051-1059.
- [12] Hill BT, Whelan RD. Assessments of the sensitivities of cultured human neuroblastoma cells to anti-tumour drugs. *Pediatr Res* 1981; 15: 1117-1122.
- [13] Liu WM, Joel SP. The schedule-dependent effects of etoposide in leukaemic cell lines: a function of concentration and duration. *Cancer Chemother Pharmacol* 2003; 51: 291-296.
- [14] Wolff SN, Grosh WW, Prater K et al. In vitro pharmacodynamic evaluation of VP-16-213 and implications for chemotherapy. *Cancer Chemother Pharmacol* 1987; 19: 246-249.
- [15] Hande KR. The importance of drug scheduling in cancer chemotherapy: Etoposide as an Example. *Oncologist* 1996; 1: 234-239.
- [16] Slevin ML, Clark PI, Joel SP et al. A randomized trial to evaluate the effect of schedule on the activity of etoposide in small-cell lung cancer. *J Clin Oncol* 1989; 7: 1333-1340.
- [17] Clark PI, Cottier B. The activity of 10-, 14-, and 21-day schedules of single-agent etoposide in previously untreated patients with extensive small cell lung cancer. *Semin Oncol* 1992; 19(6 Suppl 14): 36-39.
- [18] Kanzawa F, Matsushima Y, Chiang CD et al. Comparative studies of pulse and continuous exposure in human tumor clonogenic assay. *J Pharmacobiodyn* 1987; 10: 449-451.
- [19] Kimura T. In vitro schedule dependency in the treatment of topoisomerase I and II inhibitor. *Osaka City Med J* 2001; 47: 33-41.

- [20] Ludwig R, Alberts DS, Miller TP et al. Evaluation of anticancer drug schedule dependency using an in vitro human tumor clonogenic assay. *Cancer Chemother Pharmacol* 1984; 12: 135-141.
- [21] Matsushima Y, Kanzawa F, Hoshi A et al. Time-schedule dependency of the inhibiting activity of various anticancer drugs in the clonogenic assay. *Cancer Chemother Pharmacol* 1985; 14: 104-107.
- [22] Ohishi Y, Fujiwara K, Kohno I. Effect of the exposure dose of etoposide on the cell growth and cell kinetics of human ovarian cancer cells. *Cancer Chemother Pharmacol* 1996; 38: 141-146.
- [23] Clark PI, Slevin ML, Joel SP et al. A randomized trial of two etoposide schedules in small-cell lung cancer: the influence of pharmacokinetics on efficacy and toxicity. *J Clin Oncol* 1994; 12: 1427-1435.
- [24] Aisner J, Lee EJ. Etoposide. Current and future status. *Cancer* 1991; 67(1 Suppl): 215-219.
- [25] Belani CP, Doyle LA, Aisner J. Etoposide: current status and future perspectives in the management of malignant neoplasms. *Cancer Chemother Pharmacol* 1994; 34(Suppl): S118-S126.
- [26] Hande KR. Clinical applications of anticancer drugs targeted to topoisomerase II. *Biochim Biophys Acta* 1998; 1400: 173-184.
- [27] Packer RJ. Brain tumors in children. *Arch Neurol* 1999; 56: 421-425.
- [28] Pollack IF. Brain tumors in children. *N Engl J Med* 1994; 331: 1500-1507.
- [29] Albright AL. Pediatric brain tumors. *CA Cancer J Clin* 1993; 43: 272-288.
- [30] Jenkin D, Greenberg M, Hoffman H et al. Brain tumors in children: long-term survival after radiation treatment. *Int J Radiat Oncol Biol Phys* 1995; 31: 445-451.

- [31] Packer RJ, Finlay JL. Chemotherapy for Childhood Medulloblastoma and Primitive Neuroectodermal Tumors. *Oncologist* 1996; 1: 381-393.
- [32] Duffner PK, Horowitz ME, Krischer JP et al. Postoperative chemotherapy and delayed radiation in children less than three years of age with malignant brain tumors. *N Engl J Med* 1993; 328: 1725-1731.
- [33] Packer RJ, Goldwein J, Nicholson HS et al. Treatment of children with medulloblastomas with reduced-dose craniospinal radiation therapy and adjuvant chemotherapy: A Children's Cancer Group Study. *J Clin Oncol* 1999; 17: 2127-2136.
- [34] Schmandt S, Kuhl J. Chemotherapy as prophylaxis and treatment of meningosis in children less than 3 years of age with medulloblastoma. *J Neurooncol* 1998; 38: 187-192.
- [35] Packer RJ, Sutton LN, Elterman R et al. Outcome for children with medulloblastoma treated with radiation and cisplatin, CCNU, and vincristine chemotherapy. *J Neurosurg* 1994; 81: 690-698.
- [36] Evans AE, Jenkin RD, Sposto R et al. The treatment of medulloblastoma. Results of a prospective randomized trial of radiation therapy with and without CCNU, vincristine, and prednisone. *J Neurosurg* 1990; 72: 572-582.
- [37] Packer RJ. Chemotherapy for medulloblastoma/primitive neuroectodermal tumors of the posterior fossa. *Ann Neurol* 1990; 28: 823-828.
- [38] Tait DM, Thornton-Jones H, Bloom HJ et al. Adjuvant chemotherapy for medulloblastoma: the first multi-centre control trial of the International Society of Paediatric Oncology (SIOP I). *Eur J Cancer* 1990; 26: 464-469.
- [39] Castro MG, Cowen R, Williamson IK et al. Current and future strategies

- for the treatment of malignant brain tumors. *Pharmacol Ther* 2003; 98: 71-108.
- [40] Misra A, Ganesh S, Shahiwala A et al. Drug delivery to the central nervous system: a review. *J Pharm Pharm Sci* 2003; 6: 252-273.
- [41] Berweiler U, Krone A, Tonn JC. Reservoir systems for intraventricular chemotherapy. *J Neurooncol* 1998; 38: 141-143.
- [42] Chamberlain MC, Kormanik PA, Barba D. Complications associated with intraventricular chemotherapy in patients with leptomeningeal metastases. *J Neurosurg* 1997; 87: 694-699.
- [43] Balis FM, Poplack DG. Central nervous system pharmacology of antileukemic drugs. *Am J Pediatr Hematol Oncol* 1989; 11: 74-86.
- [44] Blaney SM, Balis FM, Poplack DG. Pharmacologic approaches to the treatment of meningeal malignancy. *Oncology (Huntingt)* 1991; 5: 107-116.
- [45] Fleischhack G, Jaehde U, Bode U. Pharmacokinetics following intraventricular administration of chemotherapy in patients with neoplastic meningitis. *Clin Pharmacokinet* 2005; 44: 1-31.
- [46] Vezmar S, Becker A, Bode U et al. Biochemical and clinical aspects of methotrexate neurotoxicity. *Chemotherapy* 2003; 49: 92-104.
- [47] Berg SL, Poplack DG. Treatment of Meningeal Malignancy. *Oncologist* 1996; 1: 56-61.
- [48] Strong JM, Collins JM, Lester C et al. Pharmacokinetics of intraventricular and intravenous N,N',N"-triethylenethiophosphoramide (thiotepa) in rhesus monkeys and humans. *Cancer Res* 1986; 46: 6101-6104.
- [49] Heideman RL, Cole DE, Balis F et al. Phase I and pharmacokinetic evaluation of thiotepa in the cerebrospinal fluid and plasma of

- pediatric patients: evidence for dose-dependent plasma clearance of thiotepa. *Cancer Res* 1989; 49: 736-741.
- [50] Slavc I, Schuller E, Czech T et al. Intrathecal mafosfamide therapy for pediatric brain tumors with meningeal dissemination. *J Neurooncol* 1998; 38: 213-218.
- [51] Slavc I, Schuller E, Falger J et al. Feasibility of long-term intraventricular therapy with mafosfamide (n = 26) and etoposide (n = 11): experience in 26 children with disseminated malignant brain tumors. *J Neurooncol* 2003; 64: 239-247.
- [52] Berg SL, Balis FM, Zimm S et al. Phase I/II trial and pharmacokinetics of intrathecal diaziquone in refractory meningeal malignancies. *J Clin Oncol* 1992; 10: 143-148.
- [53] Bergman I, Barmada MA, Heller G et al. Treatment of neoplastic meningeal xenografts by intraventricular administration of an antiganglioside monoclonal antibody, 3F8. *Int J Cancer* 1999; 82: 538-548.
- [54] Blaney SM, Heideman R, Berg S et al. Phase I clinical trial of intrathecal topotecan in patients with neoplastic meningitis. *J Clin Oncol* 2003; 21: 143-147.
- [55] Bomgaars L, Geyer JR, Franklin J et al. Phase I trial of intrathecal liposomal cytarabine in children with neoplastic meningitis. *J Clin Oncol* 2004; 22: 3916-3921.
- [56] Nakagawa H, Yamada M, Fukushima M et al. Intrathecal 5-fluoro-2'-deoxyuridine (FdUrd) for the treatment of solid tumor neoplastic meningitis: an in vivo study. *Cancer Chemother Pharmacol* 1999; 43: 247-256.
- [57] Sampson JH, Archer GE, Villavicencio AT et al. Treatment of neoplastic meningitis with intrathecal temozolomide. *Clin Cancer Res* 1999; 5:

1183-1188.

- [58] Blaney SM, Balis FM, Berg S et al. Intrathecal mafosfamide: a preclinical pharmacology and phase I trial. *J Clin Oncol* 2005; 23: 1555-1563.
- [59] Glantz MJ, Jaeckle KA, Chamberlain MC et al. A randomized controlled trial comparing intrathecal sustained-release cytarabine (DepoCyt) to intrathecal methotrexate in patients with neoplastic meningitis from solid tumors. *Clin Cancer Res* 1999; 5: 3394-3402.
- [60] Blaney SM, Poplack DG. New cytotoxic drugs for intrathecal administration. *J Neurooncol* 1998; 38: 219-223.
- [61] Savaraj N, Lu K, Feun LG et al. Comparison of CNS penetration, tissue distribution, and pharmacology of VP 16-213 by intracarotid and intravenous administration in dogs. *Cancer Invest* 1987; 5: 11-16.
- [62] Zentrum für Kinderheilkunde, Abteilung Pädiatrische Hämatologie und Onkologie, Universität Bonn. HIT-REZ-97 Multizentrische, kooperative Therapiestudie zur Behandlung von Kindern und Jugendlichen mit therapieresistenten oder rezidierten primitiv neuroektodermalen Hirntumoren. Therapieprotokoll in der Fassung vom 01.05.1999.
- [63] Kiya K, Uozumi T, Ogasawara H et al. Penetration of etoposide into human malignant brain tumors after intravenous and oral administration. *Cancer Chemother Pharmacol* 1992; 29: 339-342.
- [64] Relling MV, Mahmoud HH, Pui CH et al. Etoposide achieves potentially cytotoxic concentrations in CSF of children with acute lymphoblastic leukemia. *J Clin Oncol* 1996; 14: 399-404.
- [65] Hande KR, Wedlund PJ, Noone RM et al. Pharmacokinetics of high-dose etoposide (VP-16-213) administered to cancer patients. *Cancer Res* 1984; 44: 379-382.
- [66] Postmus PE, Holthuis JJ, Haaxma-Reiche H et al. Penetration of VP 16-213 into cerebrospinal fluid after high-dose intravenous

- administration. *J Clin Oncol* 1984; 2: 215-220.
- [67] Liu B, Earl HM, Poole CJ et al. Etoposide protein binding in cancer patients. *Cancer Chemother Pharmacol* 1995; 36: 506-512.
- [68] Clark PI. Clinical pharmacology and schedule dependency of the podophyllotoxin derivatives. *Semin Oncol* 1992; 19(Suppl 6): 20-27.
- [69] van der Gaast A, Sonneveld P, Mans DR et al. Intrathecal administration of etoposide in the treatment of malignant meningitis: feasibility and pharmacokinetic data. *Cancer Chemother Pharmacol* 1992; 29: 335-337.
- [70] Fleischhack G, Reif S, Hasan C et al. Feasibility of intraventricular administration of etoposide in patients with metastatic brain tumours. *Br J Cancer* 2001; 84: 1453-1459.
- [71] Henke G. Pharmakokinetik von Etoposid im Liquor nach intraventrikulärer Applikation: Vergleich verschiedener Dosierungsschemata. Diplomarbeit, Rheinische Friedrich-Wilhelms-Universität Bonn, 2001.
- [72] Reif S. Ansätze zur Optimierung der Chemotherapie mit Etoposid auf der Grundlage pharmakokinetischer Untersuchungen. Dissertation. Freie Universität Berlin, 2002.
- [73] Reif S, Kingreen D, Kloft C et al. Bioequivalence investigation of high-dose etoposide and etoposide phosphate in lymphoma patients. *Cancer Chemother Pharmacol* 2001; 48: 134-140.
- [74] Gastl G, Berdel W, Edler L et al. SOP 12: Validation of Bioanalytical Methods. In: Standard Operating Procedures for clinical trials of the CESAR Central European Society for Anticancer Drug Research-EWIV. *Onkologie* 2003; 26 (suppl 6): 52-55.
- [75] US Department of Health and Human Services and Food and Drug Administration. Guidance for Industry: Bioanalytical Method Validation,

2001.

- [76] Zentrum für Kinderheilkunde, Abteilung Pädiatrische Hämatologie und Onkologie, Universität Bonn. Intraventrikuläre Therapie mit Etoposid im Rahmen individueller Heilversuche. Therapieprotokoll in der Fassung vom 01.03.2003.
- [77] World Health Organization (WHO). WHO handbook for reporting results of cancer treatment. WHO Offset Publication 1979; 38: 1-41.
- [78] Benda GI, Hiller JL, Reynolds JW. Benzyl alcohol toxicity: impact on neurologic handicaps among surviving very low birth weight infants. *Pediatrics* 1986; 77: 507-512.
- [79] Hall CM, Milligan DW, Berrington J. Probable adverse reaction to a pharmaceutical excipient. *Arch Dis Child Fetal Neonatal Ed* 2004; 89: F184.
- [80] Jardine DS, Rogers K. Relationship of benzyl alcohol to kernicterus, intraventricular hemorrhage, and mortality in preterm infants. *Pediatrics* 1989; 83: 153-160.
- [81] Pharmacia. Fachinformationen zu Etoposid-ETO CS 100 mg, 500 mg, 1998.
- [82] Bristol Arzneimittel GmbH. Vepesid®. Standard-Information für Krankenhaus-Apotheker, 1995.
- [83] Gastl G, Berdel W, Edler L et al. SOP 13: Pharmacokinetic Data Analysis. In: Standard Operating Procedures for clinical trials of the CESAR Central European Society for Anticancer Drug Research-EWIV. *Onkologie* 2003; 26 (suppl 6): 56-59.
- [84] Jaehde U. Klinische Pharmakokinetik. In: Jaehde U, Radziwill R, Mühlebach S, Schunack W, editors: Lehrbuch der Klinischen Pharmazie. 2nd ed., Wissenschaftliche Verlagsgesellschaft mbH, Stuttgart, Germany 2003; 67-85.

- [85] Derendorf H. Grundlagen der Pharmakokinetik. In: Derendorf H, Gramatté T, Schäfer HG, editors: *Pharmakokinetik, einföhrung in die theorie und relevanz für die arzneimittel therapie*. 2nd ed., Wissenschaftliche Verlagsgesellschaft mbH, Stuttgart, Germany 2002; 16-99.
- [86] Bonati M, Kanto J, Tognoni G. Clinical pharmacokinetics of cerebrospinal fluid. *Clin Pharmacokinet* 1982; 7: 312-335.
- [87] Lee G, Dallas S, Hong M et al. Drug transporters in the central nervous system: brain barriers and brain parenchyma considerations. *Pharmacol Rev* 2001; 53: 569-596.
- [88] Pardridge WM. Drug delivery to the brain. *J Cereb Blood Flow Metab* 1997; 17: 713-731.
- [89] Nilsson C, Axelsson ML, Owman C. Role of the cerebrospinal fluid in volume transmission involving the choroid plexus. In: Fuxe K, Agnati LF, editors: *Volume transmission in the brain*. 1st ed., Raven Press Ltd., New York 1991;307-315.
- [90] Blasberg RG, Patlak C, Fenstermacher JD. Intrathecal chemotherapy: brain tissue profiles after ventriculocisternal perfusion. *J Pharmacol Exp Ther* 1975; 195: 73-83.
- [91] Chiro GD, Hammock MK, Bleyer WA. Spinal descent of cerebrospinal fluid in man. *Neurology* 1976; 26: 1-8.
- [92] Bering EA, Jr. The cerebrospinal fluid and the extracellular fluid of the brain. Introductory remarks. *Fed Proc* 1974; 33: 2061-2066.
- [93] Morikawa N, Mori T, Kawashima H et al. Pharmacokinetics of nimustine, methotrexate, and cytosine arabinoside during cerebrospinal fluid perfusion chemotherapy in patients with disseminated brain tumors. *Eur J Clin Pharmacol* 1998; 54: 415-420.
- [94] Blasberg RG. Pharmacodynamics and the blood-brain barrier. *Natl*

Cancer Inst Monogr 1977; 46: 19-27.

- [95] Durand RE, Vanderbyl SL. Schedule dependence for cisplatin and etoposide multifraction treatments of spheroids. *J Natl Cancer Inst* 1990; 82: 1841-1845.
- [96] Carlsson J, Nederman T. Tumour spheroid technology in cancer therapy research. *Eur J Cancer Clin Oncol* 1989; 25: 1127-1133.

8. Appendix

Appendix A

A1: Patient characteristics

A2: Individual concentration-time profiles of patients which were used to generate population parameters.

A3: Individual etoposide pharmacokinetic parameters for each cycle

Appendix B

B1: Individual data of the MTT assay

B2: Individual data of the colony forming assay (effect of concentration and duration of exposure)

B3: Simulated concentration-time profiles of etoposide (0.25 mg/12 h and 0.50 mg/24 h) derived by compartmental data analysis using $W = 1/y^2$

B4: Individual data of the colony forming assay (effect of dosage regimen)

Appendix A1

Patient characteristics

Characteristics of patients (0.25 mg/12 h)

Pt	G	No. of cycles	Age [years]	W [kg]	H [cm]	BSA [m ²]	Diagnosis
1	F	4	18	68	162	1.70	2 nd relapse of medulloblastoma and spinal metastases
2	M	1	4	15	96	0.65	1 st relapse of acute lymphoblastic leukaemia with CNS manifestation
3	F	3	0.92	13	72	0.51	Medulloblastoma with leptomeningeal metastases, resistant to first-line therapy, complicated by hydrocephalus occlusus and need of a ventricular-peritoneal shunt

Pt = patient, G = gender, W = weight, H = height, BSA = body surface area

Characteristics of patients (0.5 mg/24 h)

Pt	G	No. of cycles	Age [years]	W [kg]	H [cm]	BSA [m ²]	Diagnosis
1	F	5	18	68	162	1.70	2 nd relapse of medulloblastoma and spinal metastases
4	M	1	11	33	143	1.13	Malignant ependymoma, 3 rd cervical spinal local relapse
5	F	1	32	77	153	1.83	1 st relapse of medulloblastoma of fossa posterior and three cerebral metastases
6	F	12	3	10	89	0.50	Pineoblastoma with meningeal metastases, residual tumour in cauda equina after first-line therapy
7	F	2	21	50	168	1.54	Intraspinal malignant peripheral nerve sheath tumour with meningeal metastases
8	M	2	7	29	118	0.96	Relapse of medulloblastoma with leptomeningeal metastases, cluster of tumor cells in the ventricular and lumbar CSF
9	F	8	25	61	173	1.72	3 rd relapse of medulloblastoma of fossa posterior with spinal thoracal metastases
10	M	6	15	46	178	1.56	Relapse of medulloblastoma locally and in the 4 th ventricle, bone metastases

Pt = patient, G = gender, W = weight, H = height, BSA = body surface area

Characteristics of patients (1.0 mg/24 h)

Pt	G	No. of cycles	Age [years]	W [kg]	H [cm]	BSA [m ²]	Diagnosis
1	F	6	18	68	162	1.70	2 nd relapse of medulloblastoma with spinal metastases
11	M	6	31	76	180	1.95	2 nd local relapse of medulloblastoma with spinal metastases
12	M	1	12	n.a.	n.a.	n.a.	1 st relapse of desmoplastic medulloblastoma
13	M	27	6	27	114	0.92	1 st relapse of medulloblastoma with spinal metastases
14	M	4	7	22	120	0.86	1 st relapse of anaplastic ependymoma
15	F	3	10	32	125	1.05	Multiple relapse of plexus carcinoma
16	M	1	19	55	172	1.62	PNET in pineal region, 2 nd local relapse with meningeosis, CSF with tumour cells
17	F	2	7	36	137	1.17	1 st relapse of medulloblastoma with three lesions in the right lateral ventricle, CSF with tumour cells
18	M	1	5	14	101	0.64	1 st local relapse of medulloblastoma, residual tumour in the 4 th ventricle
19	F	2	3	n.a.	n.a.	n.a.	1 st spinal relapse of medulloblastoma

Pt = patient, G = gender, W = weight, H = height, BSA = body surface area, n.a. = not available

Characteristics of patients (1.0 mg/24 h, continued)

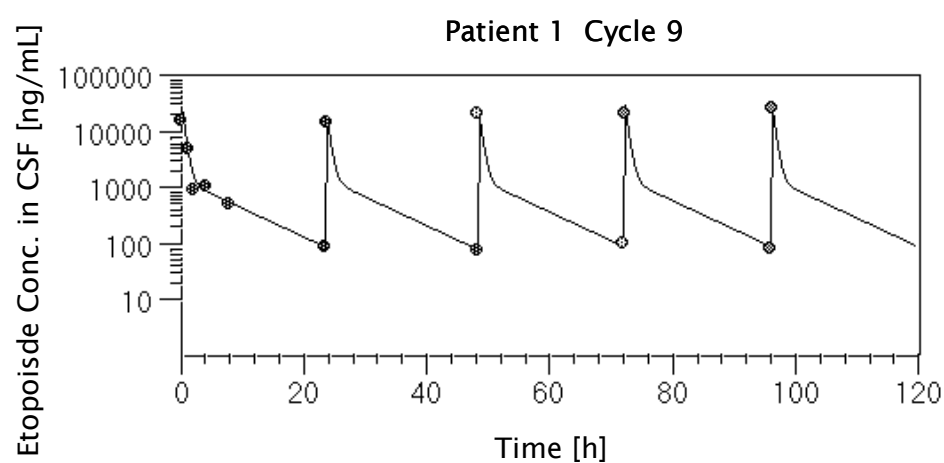
Pt	G	No. of cycles	Age [years]	W [kg]	H [cm]	BSA [m ²]	Diagnosis
20	F	3	13	58	164	1.62	Medulloblastoma, resistant to first-line therapy, metastases in the 3 rd ventricle, ventricular CSF with tumour cells
21	F	6	5	n.a.	n.a.	n.a.	Medulloblastoma, residual vital tumour after first-line therapy
22	M	2	10	n.a.	n.a.	n.a.	1 st relapse of medulloblastoma with meningeosis
23	M	9	12	35	141	1.17	1 st relapse of medulloblastoma, metastases in the cerebellum, meningeosis, spinal metastases

Pt = patient, G = gender, W = weight, H = height, BSA = body surface area, n.a. = not available

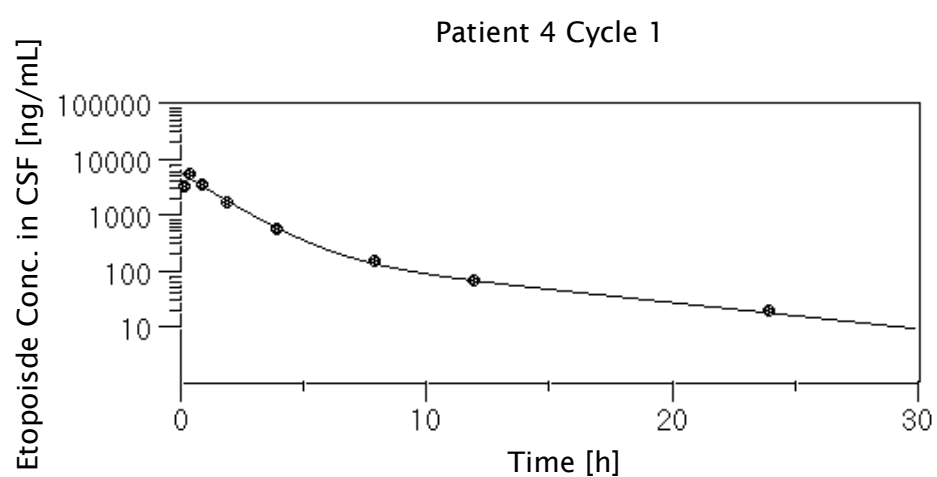
Appendix A2

Individual concentration-time profiles of patients
which were used to generate population parameters

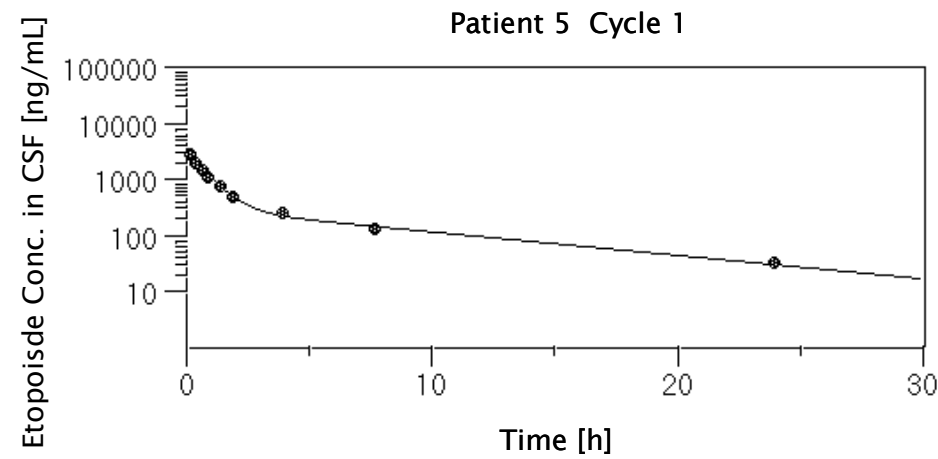
CSF concentration-time profile of patient 1 (cycle 9) following ivc administration of etoposide 1 mg/24 h



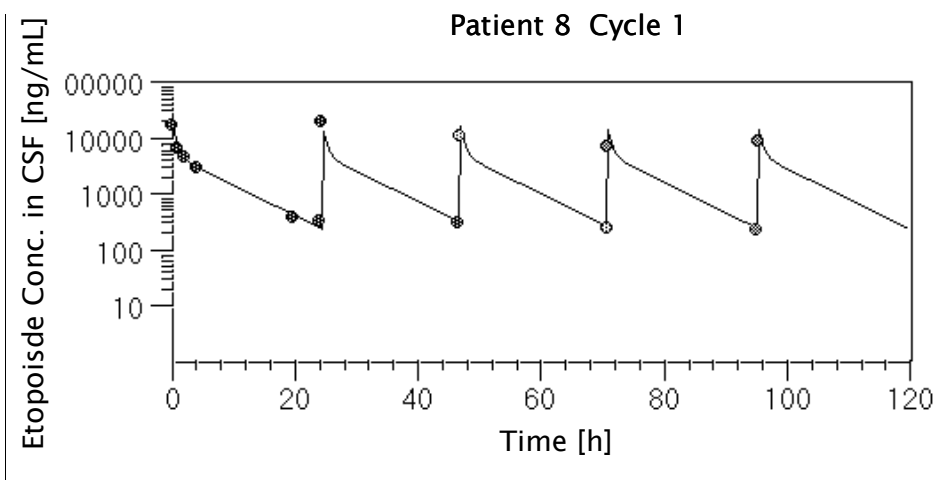
CSF concentration-time profile of patient 4 (cycle 1) following ivc administration of etoposide 0.5 mg/24 h



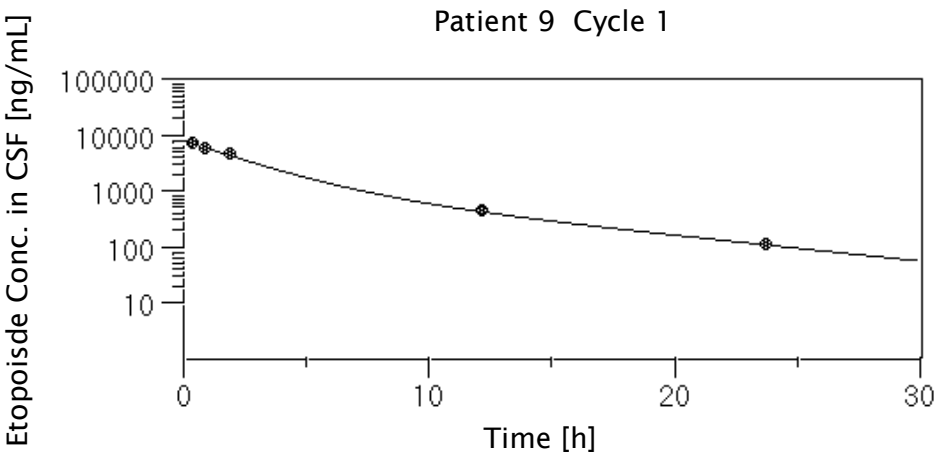
CSF concentration-time profile of patient 5 (cycle 1) following ivc administration of etoposide 0.5 mg/24 h



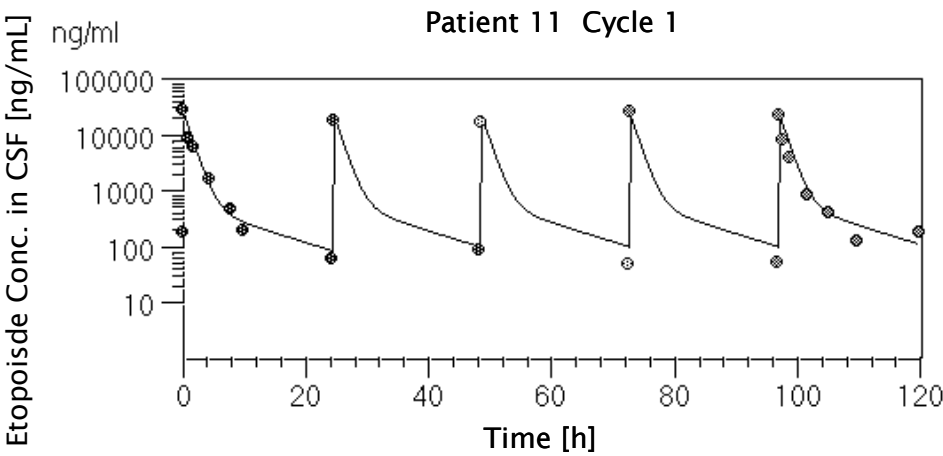
CSF concentration-time profile of patient 8 (cycle 1) following ivc administration of etoposide 0.5 mg/24 h



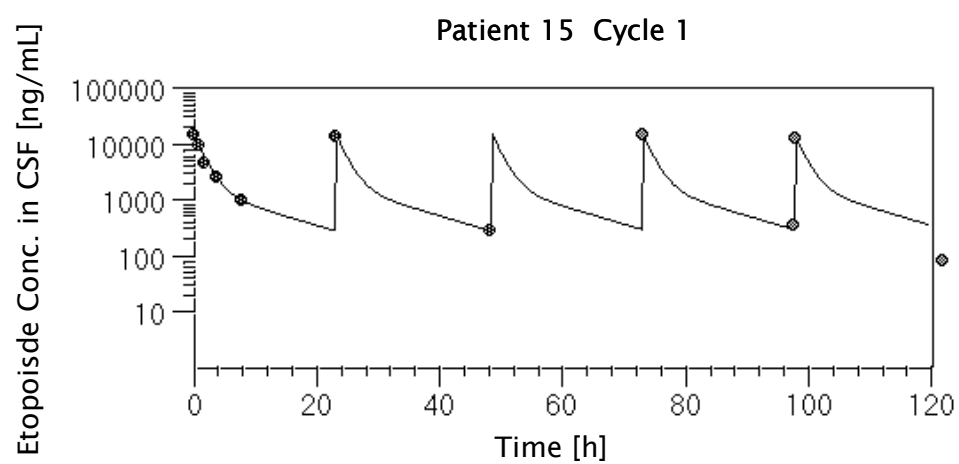
CSF concentration-time profile of patient 9 (cycle 1) following ivc administration of etoposide 0.5 mg/24 h



CSF concentration-time profile of patient 11 (cycle 1) following ivc administration of etoposide 1 mg/24 h



CSF concentration-time profile of patient 15 (cycle 1) following ivc administration of etoposide 1 mg/24 h



Appendix A3

Individual etoposide pharmacokinetic parameters for each cycle

Individual etoposide pharmacokinetic parameters in each cycle (0.25 mg/12 h)

Pt	No. of cycles	AUC _{total} [μg x h/mL]	CL [mL/min]	V _{ss} [L]	C _{min} [μg/mL]	C _{max} [μg/mL]	t _{1/2λ₁} [h ⁻¹]	t _{1/2z} [h ⁻¹]
1	3	124.87	0.33	0.08	0.13	5.24	0.81	6.52
1	4	110.21	0.38	0.12	0.20	5.63	0.68	6.61
1	5	112.97	0.37	0.09	0.15	7.65	0.80	6.50
1	C	113.13	0.37	0.11	0.18	6.07	0.68	6.60
2	1	139.70	0.30	0.13	0.37	3.61	0.54	7.21
3	1	64.13	0.65	0.45	0.43	0.99	0.39	9.39
3	2	87.72	0.48	0.18	0.20	0.24	0.60	6.96
3	3	182.51	0.23	0.09	0.49	0.94	0.61	7.16

Individual etoposide pharmacokinetic parameters in each cycle (0.5 mg/24 h)

Pt	No. of cycles	AUC _{total} [µg x h/mL]	CL [mL/min]	V _{ss} [L]	C _{min} [µg/mL]	C _{max} [µg/mL]	t _{1/2λ₁} [h ⁻¹]	t _{1/2z} [h ⁻¹]
1	1	96.57	0.43	0.13	0.08	10.33	0.66	6.58
1	2	121.20	0.34	0.12	0.13	9.85	0.78	6.82
1	7	78.64	0.53	0.18	0.08	7.37	0.63	6.73
1	A	153.49	0.27	0.09	0.13	13.69	0.67	6.65
1	B	148.67	0.28	0.10	0.15	10.64	0.78	6.83
4	1	54.03	0.77	0.18	0.02	3.08	0.81	6.47
5	1	34.11	1.22	0.38	0.03	2.56	0.47	6.64
6	1	187.35	0.22	0.07	0.05	17.40	0.67	6.56
6	2	158.35	0.26	0.04	0.05	18.55	0.76	6.46
6	3	210.25	0.20	0.06	0.04	19.83	0.67	6.53
6	4	137.12	0.30	0.10	0.08	12.05	0.67	6.61
6	5	193.70	0.22	0.06	0.06	17.59	0.68	6.53
6	6	175.30	0.24	0.08	0.05	13.24	0.67	6.62
6	9	255.91	0.16	0.02	0.06	43.83	0.46	6.52
6	10	481.42	0.09	0.02	0.25	55.98	0.68	6.39
6	11	372.31	0.11	0.03	0.11	31.88	0.67	6.51
6	12	497.89	0.08	0.02	0.16	53.01	0.67	6.40
6	13	234.59	0.18	0.06	0.15	20.42	0.66	6.59
6	14	358.17	0.12	0.03	0.12	31.40	0.67	6.47
6	15	197.42	0.21	0.06	0.06	17.90	0.67	6.55
6	16	443.56	0.09	0.03	0.17	45.23	0.67	6.43
6	17	160.19	0.26	0.08	0.09	14.57	0.68	6.56
6	18	69.98	0.60	0.20	0.09	n.a.	0.63	6.72
7	1	182.27	0.23	0.07	0.06	17.14	0.68	6.53
7	2	132.79	0.31	0.07	0.07	17.34	0.70	6.40
8	1	201.07	0.21	0.09	0.26	11.89	0.91	7.17
8	2	140.86	0.30	0.11	0.15	7.41	0.67	6.74

n.a. = not available

Individual etoposide pharmacokinetic parameters in each cycle
(0.5 mg/24 h, continued)

Pt	No. of cycles	AUC _{total} [μg × h/mL]	CL [mL/min]	V _{ss} [L]	C _{min} [μg/mL]	C _{max} [μg/mL]	t _{1/2λ₁} [h ⁻¹]	t _{1/2z} [h ⁻¹]
9	1	152.60	0.27	0.09	0.11	n.a.	1.70	6.49
9	2	150.93	0.28	0.09	0.15	n.a.	0.78	6.74
9	3	106.34	0.39	0.19	n.a.	5.54	1.42	9.98
9	4	145.07	0.29	0.13	0.20	7.05	1.19	7.68
9	5	143.03	0.29	0.13	0.18	7.51	1.15	7.45
9	6	120.72	0.35	0.16	0.18	5.65	0.71	7.32
9	7	181.27	0.23	0.09	0.19	11.67	0.49	6.04
9	8	146.45	0.29	0.11	0.22	12.24	0.45	6.22
10	4	198.69	0.21	0.07	n.a.	17.36	0.66	6.74
10	5	224.32	0.19	0.06	n.a.	19.64	0.66	6.67
10	6	136.90	0.31	0.11	0.24	10.59	0.64	6.92
10	7	268.42	0.16	0.08	0.24	18.36	0.62	8.66
10	8	208.96	0.20	0.06	0.12	19.23	0.67	6.58
10	9	141.51	0.30	0.09	0.05	13.24	0.67	6.58

n.a. = not available

Individual etoposide pharmacokinetic parameters in each cycle
(1.0 mg/24 h)

Pt	No. of cycles	AUC _{total} [μg × h/mL]	CL [mL/min]	V _{ss} [L]	C _{min} [μg/mL]	C _{max} [μg/mL]	t _{1/2λ₁} [h ⁻¹]	t _{1/2z} [h ⁻¹]
1	6	206.63	0.40	0.12	0.13	22.08	0.63	6.59
1	8	95.17	0.88	0.27	0.08	12.17	0.60	6.50
1	9	284.20	0.29	0.07	0.08	18.87	0.79	6.07
1	10	227.64	0.37	0.12	0.20	17.82	0.71	6.62
1	11	258.95	0.32	0.10	0.18	24.10	0.67	6.61
1	12	123.48	0.68	0.22	0.11	15.44	0.60	6.53
11	1	159.88	0.52	0.11	0.08	21.52	0.81	7.48
11	2	207.19	0.40	0.12	0.25	31.68	0.52	7.65
11	3	203.01	0.41	0.12	0.23	18.95	0.67	6.66
11	4	105.08	0.79	0.21	0.07	16.14	0.64	6.48
11	5	177.19	0.47	0.14	0.15	48.84	0.72	6.53
11	6	205.24	0.41	0.11	0.11	27.41	0.69	6.46
12	1	286.98	0.29	0.11	0.25	23.46	0.67	7.00
13	1	233.30	0.36	0.12	0.25	20.03	0.65	6.73
13	2	161.96	0.52	0.16	0.07	14.66	0.66	6.58
13	3	161.26	0.52	0.17	0.13	14.12	0.65	6.64
13	4	156.59	0.53	0.17	0.10	14.14	0.65	6.61
13	5	252.53	0.33	0.11	0.24	20.92	0.65	6.73
13	6	130.26	0.64	0.18	0.10	14.64	0.64	6.49
13	7	133.90	0.62	0.20	0.08	12.16	0.64	6.59
13	8	188.26	0.44	0.14	0.08	17.23	0.67	6.56
13	9	153.93	0.54	0.17	0.12	13.71	0.65	6.59
13	10	256.55	0.33	0.10	0.16	23.18	0.68	6.57
13	11	144.84	0.58	0.19	0.11	13.10	0.64	6.63
13	12	187.22	0.45	0.14	0.13	17.13	0.67	6.57
13	13	208.74	0.40	0.15	0.29	16.03	0.63	6.90
13	14	309.08	0.27	0.09	0.21	26.51	0.67	6.62

n.a. = not available

Individual etoposide pharmacokinetic parameters in each cycle
(1.0 mg/24 h, continued)

Pt	No. of cycles	AUC _{total} [μg × h/mL]	CL [mL/min]	V _{ss} [L]	C _{min} [μg/mL]	C _{max} [μg/mL]	t _{1/2λ₁} [h ⁻¹]	t _{1/2z} [h ⁻¹]
13	15	256.77	0.33	0.09	0.11	24.05	0.69	6.48
13	16	266.39	0.31	0.09	0.18	24.78	0.68	6.55
13	17	217.52	0.38	0.12	0.16	19.70	0.67	6.56
13	18	251.72	0.33	0.10	0.20	22.63	0.67	6.60
13	19	256.73	0.33	0.10	0.14	22.73	0.67	6.59
13	20	333.98	0.25	0.08	0.24	30.88	0.68	6.55
13	21	226.72	0.37	0.11	0.13	20.67	0.68	6.54
13	22	192.63	0.43	0.14	1.49	20.00	0.66	6.61
13	23	116.85	0.71	0.23	0.09	10.67	0.62	6.62
13	24	146.67	0.57	0.18	0.11	13.34	0.65	6.60
13	25	154.83	0.54	0.19	0.16	16.59	0.65	6.82
13	26	166.41	0.50	0.17	0.16	14.59	0.65	6.67
13	27	187.08	0.45	0.14	0.10	16.86	0.66	6.61
14	1	456.92	0.18	0.13	1.71	22.71	0.49	9.66
14	2	678.44	0.12	0.10	0.72	25.54	0.45	10.95
14	3	483.63	0.17	0.12	1.71	23.53	0.51	9.87
14	4	443.15	0.19	0.14	1.50	20.73	0.51	10.02
15	1	345.47	0.24	0.10	0.52	25.61	0.62	7.08
15	2	244.03	0.34	0.20	0.81	13.13	0.53	8.68
15	3	161.11	0.52	0.30	0.66	8.59	0.50	8.46
16	1	160.99	0.52	0.12	0.06	21.44	0.64	6.39
17	1	207.02	0.40	0.16	0.23	13.27	0.69	7.08
17	2	196.80	0.42	0.17	0.18	12.26	0.65	7.01
18	1	118.72	0.70	0.22	0.03	n.a.	0.63	6.58
19	1	188.00	0.44	0.14	0.04	16.77	0.67	6.60
19	2	122.83	0.68	0.22	0.04	n.a.	0.63	6.61
20	1	166.91	0.50	0.16	0.07	14.78	0.66	6.59

n.a. = not available

Individual etoposide pharmacokinetic parameters in each cycle
(1.0 mg/24 h, continued)

Pt	No. of cycles	AUC _{total} [μg × h/mL]	CL [mL/min]	V _{ss} [L]	C _{min} [μg/mL]	C _{max} [μg/mL]	t _{1/2λ₁} [h ⁻¹]	t _{1/2z} [h ⁻¹]
20	2	172.50	0.48	0.11	0.08	15.63	0.97	6.31
20	3	90.51	0.92	0.27	0.07	n.a.	0.63	6.23
21	1	119.12	0.70	0.22	0.07	10.97	0.62	6.60
21	2	135.30	0.62	0.20	0.10	12.23	0.64	6.62
21	3	79.41	1.05	0.38	0.09	6.15	0.52	6.73
21	4	91.61	0.91	0.33	0.13	7.58	0.55	6.77
21	5	238.54	0.35	0.11	0.09	21.72	0.68	6.56
21	6	219.62	0.38	0.11	0.07	20.98	0.68	6.51
22	1	236.17	0.35	0.13	0.36	18.69	0.64	6.87
22	2	194.40	0.43	0.16	0.31	15.09	0.62	6.96
23	1	573.85	0.15	0.12	2.50	22.97	0.47	10.90
23	2	264.87	0.32	0.17	0.62	16.30	0.55	8.13
23	3	184.92	0.45	0.15	0.17	16.21	0.66	6.66
23	4	541.75	0.15	0.11	1.74	23.62	0.48	10.00
23	5	193.46	0.43	0.14	0.22	20.46	0.66	6.46
23	6	371.02	0.23	0.13	1.17	20.01	0.54	8.71
23	7	441.21	0.19	0.12	1.15	23.63	0.53	8.93
23	8	274.78	0.30	0.11	0.27	22.52	0.65	6.84
23	9	402.54	0.21	0.13	1.49	20.00	0.53	9.19

n.a. = not available

Appendix B1

Individual data of the MTT assay

Individual data of the MTT assay

Etoposide Conc. [M]	Absorption							
	10^{-9}	10^{-8}	10^{-7}	10^{-6}	10^{-5}	$10^{-4.5}$	10^{-4}	$10^{-3.75}$
1	1.27	1.47	1.30	0.41	0.09	0.11	0.16	0.15
2	1.15	1.41	1.31	0.29	0.14	0.12	0.14	0.14
3	1.32	1.11	1.11	0.44	0.13	0.11	0.13	0.18
4	1.41	1.42	1.21	0.46	0.14	0.16	0.13	0.15
5	1.41	1.24	1.15	0.44	0.17	0.12	0.14	0.15
6	1.37	1.28	1.19	0.37	0.17	0.11	0.13	0.14
7	1.45	1.31	1.09	0.38	0.13	0.07	0.11	0.14
8	1.39	*	1.20	0.48	0.14	0.11	0.12	0.14
9	1.44	1.13	1.08	0.41	0.14	0.12	0.12	0.14
10	1.29	1.10	*	0.33	0.15	0.10	0.10	0.17
11	1.40	1.17	1.13	0.33	0.12	0.11	0.13	0.14
12	1.21	1.21	1.19	0.38	0.15	0.11	0.15	0.14
Mean	1.34	1.26	1.18	0.39	0.14	0.11	0.13	0.15
SD	0.10	0.13	0.08	0.06	0.02	0.02	0.02	0.01

* Data were excluded because they were much different from other values and hence regarded as outliers.

Appendix B2

Individual data of the colony forming assay
(effect of concentration and duration of exposure)

Number of colonies remaining of D-425med incubated with etoposide for 12 h

Etoposide Conc. (M)	No. of colonies remaining			Mean
	1	2	3	
$2 \times 10^{-8.0}$	187	256	192	211.67
$2 \times 10^{-7.0}$	219	194	247	220.00
$2 \times 10^{-6.8}$	129	148	155	144.00
$2 \times 10^{-6.75}$	164	197	183	181.33
$2 \times 10^{-6.65}$	103	148	178	143.00
$2 \times 10^{-6.4}$	101	148	146	131.67
$2 \times 10^{-6.25}$	40	43	27	36.67
$2 \times 10^{-6.1}$	26	19	25	23.33
$2 \times 10^{-6.0}$	17	9	16	14.00
$2 \times 10^{-5.0}$	0	0	0	0

Percent colonies remaining of D-425med incubated with etoposide for 12 h

Etoposide Conc. (M)	% colonies remaining			Mean
	1	2	3	
$2 \times 10^{-8.0}$	100.00	100.00	100.00	100.00
$2 \times 10^{-7.0}$	103.46	91.65	116.69	103.94
$2 \times 10^{-6.8}$	60.94	69.92	73.23	68.03
$2 \times 10^{-6.75}$	77.48	93.07	86.46	85.67
$2 \times 10^{-6.65}$	48.66	69.92	84.09	67.56
$2 \times 10^{-6.4}$	47.72	69.92	68.98	62.20
$2 \times 10^{-6.25}$	18.90	20.31	12.76	17.32
$2 \times 10^{-6.1}$	12.28	8.98	11.81	11.20
$2 \times 10^{-6.0}$	8.03	4.25	7.56	6.61
$2 \times 10^{-5.0}$	0.00	0.00	0.00	0.00

Number of colonies remaining of D-425med incubated with etoposide for 24 h

Etoposide Conc. (M)	No. of colonies remaining			Mean
	1	2	3	
$10^{-8.0}$	191	252	247	230.00
$10^{-7.0}$	253	259	n.a.	256.00
$10^{-6.8}$	224	274	168	222.00
$10^{-6.75}$	265	208	197	223.33
$10^{-6.65}$	118	169	163	150.00
$10^{-6.4}$	187	139	121	149.00
$10^{-6.25}$	68	53	53	58.00
$10^{-6.1}$	37	38	22	32.33
$10^{-6.0}$	11	10	2	7.67
$10^{-5.0}$	0	0	0	0.00

n.a. = not available

Percent colonies remaining of D-425med incubated with etoposide for 24 h

Etoposide Conc. (M)	% colonies remaining			Mean
	1	2	3	
$10^{-8.0}$	100.00	100.00	100.00	100.00
$10^{-7.0}$	110.00	112.61	n.a.	111.30
$10^{-6.8}$	97.39	119.13	73.04	96.52
$10^{-6.75}$	115.22	90.43	85.65	97.10
$10^{-6.65}$	51.30	73.48	70.87	65.22
$10^{-6.4}$	81.30	60.43	52.61	64.78
$10^{-6.25}$	29.57	23.04	23.04	25.22
$10^{-6.1}$	16.09	16.52	9.57	14.06
$10^{-6.0}$	4.78	4.35	0.87	3.33
$10^{-5.0}$	0.00	0.00	0.00	0.00

Number of colonies remaining of D-425med incubated with etoposide for 120 h

Etoposide Conc. (M)	No. of colonies remaining			Mean
	1	2	3	
$1/5 \times 10^{-8.0}$	267	296	365	309.33
$1/5 \times 10^{-7.0}$	342	287	317	315.33
$1/5 \times 10^{-6.8}$	174	248	240	220.67
$1/5 \times 10^{-6.75}$	289	183	182	218.00
$1/5 \times 10^{-6.65}$	230	131	205	188.67
$1/5 \times 10^{-6.4}$	181	168	217	188.67
$1/5 \times 10^{-6.25}$	48	91	83	74.00
$1/5 \times 10^{-6.1}$	77	50	89	72.00
$1/5 \times 10^{-6.0}$	21	20	31	24.00
$1/5 \times 10^{-5.0}$	0	0	0	0.00

Percent colonies remaining of D-425med incubated with etoposide for 120 h

Etoposide Conc. (M)	% colonies remaining			Mean
	1	2	3	
$1/5 \times 10^{-8.0}$	100.00	100.00	100.00	100.00
$1/5 \times 10^{-7.0}$	110.56	92.78	102.48	101.94
$1/5 \times 10^{-6.8}$	56.25	80.17	77.59	71.34
$1/5 \times 10^{-6.75}$	93.43	59.16	58.84	70.47
$1/5 \times 10^{-6.65}$	74.35	42.35	66.27	60.99
$1/5 \times 10^{-6.4}$	58.51	54.31	70.15	60.99
$1/5 \times 10^{-6.25}$	15.52	29.42	26.83	23.92
$1/5 \times 10^{-6.1}$	24.89	16.16	28.77	23.28
$1/5 \times 10^{-6.0}$	6.79	6.47	10.02	7.76
$1/5 \times 10^{-5.0}$	0.00	0.00	0.00	0.00

Appendix B3

Simulated concentration-time profiles of etoposide

(0.25 mg/12 h and 0.50 mg/24 h)

derived by compartmental data analysis using $W = 1/y^2$

Simulated concentration-time profile of etoposide administered every 12 h with 15-fold dilution of CSF concentrations

At 0 h of day 1 (day time), 1 mL of etoposide 1260 ng/mL was added to 4 mL medium to obtain an etoposide concentration of 252 ng/mL

At 0 h of day 1 (night time) and day 2 - 5, 1.5 mL of broth solution was replaced by 1.5 mL of etoposide 804 ng/mL to obtain an etoposide concentration of 252 ng/mL

Time [h]	Theoretical concentration [ng/mL]	Calculated volume of withdrawn / replaced medium [μL]	Practical volume of withdrawn / replaced medium [μL]	Obtained concentration [ng/mL]
0.00 - 0.25	251.92	-	-	252.00
0.25 - 0.50	225.68	522.32	522	225.69
0.50 - 1.00	164.33	1359.32	1350	164.75
1.00 - 2.00	96.83	2061.50	2050	97.21
2.00 - 4.00	48.00	2530.94	2550	47.63
4.00 - 8.00	25.22	2352.80	2350	25.24
8.00 - 12.00	15.64	1902.26	1900	15.65
Only for day 6				
0.00 - 12.00	4.87	3444.98	3450	9.70

Simulated concentration-time profile of etoposide administered every 12 h with 10-fold dilution of CSF concentrations

At 0 h of day 1 (day time), 1 mL of etoposide 2520 ng/mL was added to 4 mL medium to obtain an etoposide concentration of 504 ng/mL

At 0 h of day 1 (night time) and day 2 - 5, 1.5 mL of broth solution was replaced by 1.5 mL of etoposide 1608 ng/mL to obtain an etoposide concentration of 504 ng/mL

Time [h]	Theoretical concentration [ng/mL]	Calculated volume of withdrawn / replaced medium [μL]	Practical volume of withdrawn / replaced medium [μL]	Obtained concentration [ng/mL]
0.00 - 0.25	503.84	-	-	504.00
0.25 - 0.50	451.35	522.32	522	451.38
0.50 - 1.00	328.67	1359.32	1350	329.51
1.00 - 2.00	193.65	2061.50	2050	194.41
2.00 - 4.00	96.00	2530.94	2550	95.26
4.00 - 8.00	50.44	2352.80	2350	50.49
8.00 - 12.00	31.28	1902.26	1900	31.30
Only for day 6				
0.00 - 12.00	9.74	3444.98	3450	9.70

Simulated concentration-time profile of etoposide administered every 12 h with 5-fold dilution of CSF concentrations

At 0 h of day 1 (day time), 1 mL of etoposide 3780 ng/mL was added to 4 mL medium to obtain an etoposide concentration of 756 ng/mL

At 0 h of day 1 (night time) and day 2 - 5, 1.5 mL of broth solution was replaced by 1.5 mL of etoposide 2410 ng/mL to obtain an etoposide concentration of 756 ng/mL

Time [h]	Theoretical concentration [ng/mL]	Calculated volume of withdrawn / replaced medium [μL]	Practical volume of withdrawn / replaced medium [μL]	Obtained concentration [ng/mL]
0.00 - 0.25	755.75	-	-	756.00
0.25 - 0.50	677.03	522.32	522	677.07
0.50 - 1.00	493.00	1359.32	1350	494.26
1.00 - 2.00	290.48	2061.50	2050	291.62
2.00 - 4.00	144.00	2530.94	2550	142.89
4.00 - 8.00	75.65	2352.80	2350	75.73
8.00 - 12.00	46.92	1902.26	1900	46.95
Only for day 6				
0.00 - 12.00	14.60	3444.98	3450	14.56

Simulated concentration-time profile of etoposide administered every 24 h with 15-fold dilution of CSF concentrations

At 0 h of day 1 (day time), 1 mL of etoposide 2995 ng/mL was added to 4 mL medium to obtain an etoposide concentration of 599 ng/mL

At 0 h of day 1 (night time) and day 2 - 5, 1.5 mL of broth solution was replaced by 1.5 mL of etoposide 1978 ng/mL to obtain an etoposide concentration of 599 ng/mL

Time [h]	Theoretical concentration [ng/mL]	Calculated volume of withdrawn / replaced medium [μL]	Practical volume of withdrawn / replaced medium [μL]	Obtained concentration [ng/mL]
0.00 - 0.25	599.21	-	-	599.00
0.25 - 0.50	535.59	529.34	529	535.63
0.50 - 1.00	386.07	1396.08	1400	385.65
1.00 - 2.00	219.78	2150.49	2150	219.82
2.00 - 4.00	99.05	2747.04	2750	98.92
4.00 - 8.00	45.94	2677.93	2650	46.49
8.00 - 12.00	27.55	2037.67	2000	27.90
12.00 - 16.00	18.23	1733.32	1750	18.13
16.00 - 20.00	12.08	1668.17	1650	12.15
20.00 - 24.00	8.01	1702.85	1700	8.02
Only for day 6				
0.00 - 12.00	3.48	2830.30	2850	3.45

Simulated concentration-time profile of etoposide administered every 24 h with 10-fold dilution of CSF concentrations

At 0 h of day 1 (day time), 1 mL of etoposide 5990 ng/mL was added to 4 mL medium to obtain an etoposide concentration of 1198 ng/mL

At 0 h of day 1 (night time) and day 2 - 5, 1.5 mL of broth solution was replaced by 1.5 mL of etoposide 3956 ng/mL to obtain an etoposide concentration of 1198 ng/mL

Time [h]	Theoretical concentration [ng/mL]	Calculated volume of withdrawn / replaced medium [μL]	Practical volume of withdrawn / replaced medium [μL]	Obtained concentration [ng/mL]
0.00 - 0.25	1198.41	-	-	599.00
0.25 - 0.50	1071.17	529.34	529	535.63
0.50 - 1.00	772.14	1396.08	1400	385.65
1.00 - 2.00	439.57	2150.49	2150	219.82
2.00 - 4.00	198.10	2747.04	2750	98.92
4.00 - 8.00	91.88	2677.93	2650	46.49
8.00 - 12.00	55.09	2037.67	2000	27.90
12.00 - 16.00	36.45	1733.32	1750	18.13
16.00 - 20.00	24.17	1668.17	1650	12.15
20.00 - 24.00	16.02	1702.85	1700	8.02
Only for day 6				
0.00 - 12.00	6.96	2830.30	2850	

Simulated concentration-time profile of etoposide administered every 24 h with 5-fold dilution of CSF concentrations

At 0 h of day 1 (day time), 1 mL of etoposide 8990 ng/mL was added to 4 mL medium to obtain an etoposide concentration of 1798 ng/mL

At 0 h of day 1 (night time) and day 2 - 5, 1.5 mL of broth solution was replaced by 1.5 mL of etoposide 5937 ng/mL to obtain an etoposide concentration of 1798 ng/mL

Time [h]	Theoretical concentration [ng/mL]	Calculated volume of withdrawn / replaced medium [μL]	Practical volume of withdrawn / replaced medium [μL]	Obtained concentration [ng/mL]
0.00 - 0.25	1797.62	-	-	1798.00
0.25 - 0.50	1606.76	531.82	532	1606.69
0.50 - 1.00	1158.21	1395.67	1400	1156.82
1.00 - 2.00	659.35	2150.16	2150	659.39
2.00 - 4.00	297.15	2746.78	2750	296.72
4.00 - 8.00	137.82	2677.67	2650	139.46
8.00 - 12.00	82.64	2037.33	2000	83.68
12.00 - 16.00	54.68	1732.94	1750	54.39
16.00 - 20.00	36.25	1667.79	1650	36.44
20.00 - 24.00	24.03	1702.48	1700	24.05
Only for day 6				
0.00 - 12.00	10.44	2830.05	2850	10.34

Appendix B4

Individual data of the colony forming assay
(effect of dosage regimen)

Number and percent colonies remaining of D-425med incubated with simulated CSF concentration-time profiles (every 12 h for five consecutive days); results of the respective control experiment are given in brackets)

AUC _{total}	No. of colonies			% colonies remaining			Mean
	1	2	3	1	2	3	
5.60	30 (41)	46 (61)	70 (101)	73.17	75.41	69.31	72.63
11.20	49 (60)	36 (63)	34 (83)	81.67	57.14	40.96	59.92
16.80	28 (111)	66 (144)	51 (133)	25.23	45.83	38.35	36.47

Number and percent colonies remaining of D-425med incubated with simulated CSF concentration-time profiles (every 24 h for five consecutive days); results of the respective control experiment are given in brackets)

AUC _{total}	No. of colonies			% colonies remaining			Mean
	1	2	3	1	2	3	
6.73	87 (78)	106 (115)	168 (166)	111.54	92.17	101.20	101.64
13.45	57 (82)	80 (135)	101 (194)	69.51	59.26	52.06	60.28
20.18	47 (115)	34 (100)	45 (108)	40.87	34.00	41.67	38.85